Note to the Reader

A few portions of this EPRI report, "Modeling Analysis of the Big Bend Regional Aerosol Visibility Observational (BRAVO) Study," are currently being revised. The final version of the EPRI report was not ready for inclusion in the Appendix of the Peer Review Draft of the BRAVO Study Final Report. This body of this draft of the BRAVO Study report does, however, already reflect the changes that are being made in the EPRI report, and therefore there are temporarily some minor inconsistencies between the two reports.

EPRI

Modeling Analysis of the Big Bend Regional Aerosol and Visibility Observational (BRAVO) Study

Technical Report

Modeling Analysis Of The Big Bend Regional Aerosol Visibility Observational (Bravo) Study

1009283

Final Report, February 2004

Cosponsors

American Electric Power
1616 Woodall Rodgers Freeway
Dallas, TX 75202

TXU
1601 Bryan Street
Dallas, TX 75201

Reliant
12301 Kurland Drive
Houston, TX 77034

City Public Services of San Antonio
145 Navarro at Villita
San Antonio, TX 78205

EPRI Project Manager
N. Kumar

EPRI • 3412 Hillview Avenue, Palo Alto, California 94304 • PO Box 10412, Palo Alto, California 94303 • USA
800.313.3774 • 650.855.2121 • askepri@epri.com • www.epri.com

DISCLAIMER OF WARRANTIES AND LIMITATION OF LIABILITIES

ORGANIZATION(S) THAT PREPARED THIS DOCUMENT

Atmospheric and Environmental Research, Inc.

EPRI

ORDERING INFORMATION

Requests for copies of this report should be directed to EPRI Orders and Conferences, 1355 Willow Way, Suite 278, Concord, CA 94520, (800) 313-3774, press 2 or internally x5379, (925) 609-9169, (925) 609-1310 (fax).

CITATIONS

This report was prepared by

Atmospheric and Environmental Research, Inc.
2682 Bishop Drive, Suite 120
San Ramon CA 94583

Principal Investigators
B. Pun
C. Seigneur
S. Wu

Electric Power Research Institute
3412 Hillview Ave.
Palo Alto, CA 94303

Principal Investigators
E. Knipping
N. Kumar

This report describes research sponsored by EPRI, American Electric Power, TXU, Reliant, and City Public Services of San Antonio.

The report is a corporate document that should be cited in the literature in the following manner:

Modeling Analysis of the Big Bend Regional Aerosol Visibility Observational (BRAVO) Study, EPRI, Palo Alto, CA: 2004. 1009283.

REPORT SUMMARY

Particulate sulfate compounds account for approximately half of the particulate matter (PM) during periods of poor visibility at Big Bend National Park (BBNP). Poor visibility is associated with two distinct meteorological regimes – one dominated by flow from Mexico during spring and summer months and another characterized by transport from regions northeast of BBNP during fall months. Accordingly, the monitoring component of BRAVO took place from July to October 1999. More than 30 sites were established to measure PM and its components, visibility conditions, and sulfur dioxide (SO_2) in Texas. In addition, four inert tracers were released from potential source areas and monitored throughout Texas to assess atmospheric transport patterns.

Objectives

First, to evaluate the performance of a state-of-the-science air quality model for the transport of inert tracers and for the formation, transport, and fate of PM; second, to estimate the potential contributions of several source areas to fine particulate sulfate in BBNP.

Approach

Investigators applied the Community Multiscale Air Quality (CMAQ) model, augmented with the Model for Aerosol Dynamics, Reaction, Ionization and Dissolution (MADRID), for simulation of the four-month BRAVO period. The modeling domain covered BBNP, Texas, neighboring states, northeastern Mexico, and the northwestern part of the Gulf of Mexico. Investigators obtained boundary conditions from a simulation conducted with the Regional Modeling System for Aerosols and Deposition (REMSAD) following calibration with observations. First, they simulated the inert tracers with CMAQ to assess the ability of the model to reproduce transport from individual sources to receptors over large distances (several hundreds of kilometers). Next, they simulated PM with CMAQ-MADRID. Following an evaluation of the performance of CMAQ-MADRID for PM concentrations and chemical composition, they applied the model to estimate the contributions of several source areas to the concentrations of particulate sulfate estimated by the model at the K-Bar site in BBNP.

Results

The evaluation of CMAQ performance for tracers showed that the model explained only 5 to 13% of the variance for all but one of the six tracers at K-Bar, BBNP. For the remaining tracer, the model explained 40% of the variance. With respect to the timing of tracers, CMAQ could be more apt in depicting regional-scale transport of distributed pollutants from multiple sources and more restricted in capturing transport from a single source to specific receptors. In general, fine sulfate particles are regionally distributed due to their long atmospheric lifetimes in the absence of wet deposition.

Since large uncertainties are associated with the use of CMAQ to conduct PM attribution for individual sources, source attribution for fine particulate sulfate is limited to large geographical source regions.

The evaluation of CMAQ-MADRID performance yielded normalized error and bias values of 48% and 13% for fine particulate sulfate at BBNP, respectively. The model explained slightly more than 50% of the observed variance in sulfate. However, when all BRAVO sites were considered, sulfate performance deteriorated because of significant overpredictions of sulfate in the eastern half of the domain. The distribution of sulfur between SO_2 and sulfate was predicted accurately on average at all sites, with about 60% of sulfur residing in the particulate phase. Normalized errors of other PM components at BBNP ranged from 51 to 96%.

Five source areas were considered for the sulfate source attribution: Mexico, Texas, the eastern United States, western United States (excluding Texas), and boundary conditions of the broader REMSAD domain (comprising nearly the entirety of the continental United States and Mexico). On average, during the four-month study period, Mexico accounted for 32%, Texas for 19%, the eastern U.S. for 38%, the western U.S. for 6%, and boundary conditions for 5% of the particulate sulfate concentrations at the K-Bar site in BBNP.

EPRI Perspective

The air quality model used in this report, CMAQ-MADRID, employs among the most scientifically rigorous treatments of PM available in atmospheric models. Over the four-month BRAVO Study period, CMAQ-MADRID yielded encouraging performance statistics (low bias and low error) on the ability of the model to reproduce fine particulate sulfate concentrations measured at BBNP. However, model performance for sulfate was not consistent throughout the modeling domain and exhibited significant daily and episodic variations. Model performance was influenced by compensating errors and regional biases. With respect to other aerosol components, e.g., organic mass and black (elemental) carbon, the model performed poorly over the entire study period. Modeling of the BRAVO Study was particularly challenging due to large uncertainties in Mexico's emissions and meteorological information. Despite this finding, PM models generally have not shown better performance at regional scales than that of CMAQ-MADRID during the BRAVO study.

The analysis of source-region attribution for particulate sulfate compounds during the BRAVO period is inextricably connected to model performance. Currently, there is no guidance to benchmark "acceptable" model performance for Eulerian PM models or to guide their use within source apportionment studies. Such guidance must be drafted in order to ensure their adequacy and appropriate use as part of future studies.

Keywords

Air Quality Modeling
Big Bend National Park
Particulate Matter (PM)
Regional Haze
Source Apportionment
Tracers

ACKNOWLEDGMENTS

Funding to AER was provided by EPRI under agreement EP-P2542/C1151 and by EPA through a subcontract from Air Resources Specialists No. 03-02-AER1. American Electric Power, City Public Services of San Antonio, Reliant, and TXU provided the supplemental funding to EPRI. N. N. Dharmrajan and Dick Robertson provided valuable comments during the course of this work. Jeff Vukovich, UNC, provided emission inputs. Mark Green, DRI, provided tracer emission and ambient monitoring data. Nelson Seaman, Pennsylvania State University, provided MM5 outputs. Mian Chin, NASA, provided GOCART outputs. Mike Barna, CIRA, provided REMSAD outputs. We would also like to thank the BRAVO team for many insightful discussions.

EXECUTIVE SUMMARY

The Big Bend Regional Aerosol and Visibility Observational (BRAVO) study is a multi-year monitoring and assessment study of the causes of regional haze in Big Bend National Park (BBNP). Poor visibility at BBNP is associated with two distinct meteorological regimes. During spring and early summer, when visibility is most impaired, the dominant flow is from Mexico. During fall, poor visibility is at times associated with transport from regions to the northeast of BBNP. The monitoring component of the BRAVO study took place in the summer and fall months of 1999. More than 30 sites were established to measure particulate matter (PM), PM components, haze, and sulfur dioxide (SO_2) in Texas. In addition, four inert tracers were released from several potential source areas and monitored throughout Texas to assess atmospheric transport patterns.

A two-phase air quality modeling strategy was developed for BRAVO, one of the first large-scale modeling studies for PM and regional haze. First, tracer simulations were conducted to evaluate transport processes in air quality models. Once model performance for transport was assessed by comparing tracer simulation results with measurements, chemical transport model simulations were performed to estimate the impact of different source regions to regional haze at BBNP. In accordance with the BRAVO Technical Committee, source attribution was limited to fine particulate sulfate. On average during the BRAVO Study period (July 1 – October 30, 1999), sulfate constituted the largest $PM_{2.5}$ mass fraction and contribution to haze of any single $PM_{2.5}$ component measured at BBNP, followed by organic compounds.

The Community Multiscale Air Quality (CMAQ) model and CMAQ-MADRID (Model for Aerosol Dynamics, Reaction, Ionization, and Dissolution) were applied to simulate inert tracers and particulate matter (PM) for the BRAVO Study. Focused model development efforts were undertaken to improve transport characteristics of the CMAQ model based on tracer observations. The Smagorinsky horizontal diffusion module was implemented to provide diffusion characteristics more commensurate with tracer plumes observed during BRAVO. (The Smagorinsky scheme led to slightly better model performance over initial fine resolution model simulations.) CMAQ was run with a 36-km horizontal resolution over the entire 4-month BRAVO period using version 2.1 of the Meteorology-Chemistry Interface Processor (MCIP). The modeling domain for the 36-km resolution simulations is shown in Figure E-1.

Figure E-1
Modeling domain of CMAQ-MADRID.

The collective dispersion algorithms of the CMAQ three-dimensional Eulerian air-quality model were tested by simulating the transport of inert tracers emitted from specific point sources to receptor sites. Four perfluorocarbon tracers were released from locations near the cities of Eagle Pass (adjacent to the Texas/Mexico border), San Antonio, and Houston, and from a site in Northeast Texas, respectively. From early July to mid September, "timing" tracers were released at intermittent periods from Eagle Pass in addition to the continuous tracer. Six BRAVO network stations measured tracer concentrations during the study. Tracer emissions were developed based on information obtained from the Desert Research Institute (DRI). Major transport pathways were inferred by inspecting the spatial distribution of tracers. Given the prevalence of southerly winds, air masses from Mexico frequently influenced the air quality at BBNP. In the second half of the BRAVO period, air masses from source areas in northeast Texas affected BBNP more frequently than during the first half of the BRAVO study.

Overall, CMAQ explained 5 to 13% of the variance (as estimated by the coefficient of determination, r^2) for all but one of the six tracers at K-Bar, BBNP (40% of the variance could be explained by CMAQ for the San Antonio tracer at K-Bar). No standard of performance currently exists for inert tracers. However, better performance results with respect to the timing of tracer arrivals at monitors indicated that the CMAQ modeling system could be more apt in depicting regional scale transport of more distributed pollutants from multiple sources and restricted in its ability of capturing transport from a single source to specific receptors.

In general, fine sulfate-containing aerosol particles are regionally distributed due to their long atmospheric lifetimes in the absence of wet deposition. However, it was recognized that significant uncertainties are associated with the use of CMAQ-MADRID to conduct PM attribution for individual sources, such as transport performance issues elucidated from tracer simulations. Therefore, source attribution for fine particulate sulfate based on the results of Eulerian models was limited to larger geographical source regions.

For the chemical transport model simulations, emissions for the 36-km resolution domain were generated based on inputs and control scripts provided by the University of North Carolina (UNC). Based on information from an Undersecretary of the Mexican Ministry of Energy, sulfur dioxide (SO_2) and fine sulfate emissions were increased by a factor of two for Mexican sources, with the exception of the Carbón power plant facility, within the CMAQ-MADRID domain. Boundary conditions for the chemistry run were extracted from the Regional Modeling System for Aerosols and Deposition (REMSAD), and respeciated for CMAQ-MADRID. Sulfur dioxide and fine particulate sulfate at the boundary were scaled to available measurements to minimize the propagation of errors from REMSAD into the CMAQ simulation via boundary conditions. Initial conditions were developed based on BRAVO measurements.

The statistical performance of CMAQ-MADRID for PM_{10}, $PM_{2.5}$, and $PM_{2.5}$ components at K-Bar, BBNP is summarized in Table E-1 for the 4-month BRAVO simulation. The best performance was obtained for sulfate, which was overpredicted with a normalized error of 55% and a fractional error of 46%. A correlation coefficient of 0.72 indicated that the model was able to explain more than 50% of the observed variance in sulfate. Similar levels of performance for sulfate were also obtained at other individual BBNP sites and the normalized error and bias averaged over the three BBNP sites were 48% and 13%, respectively. The distribution of sulfur between SO_2 and sulfate was predicted accurately on average at all sites; both the model and ambient data indicated that 61-62% of sulfur resided in the particulate phase. CMAQ-MADRID was able to represent the regional gas-particle conversion characteristics of sulfate, but on the basis of individual days and locations, significant scatter was observed between observations and simulated values.

Table E-1
Statistical model performance of CMAQ-MADRID for $PM_{2.5}$, sulfate, nitrate, ammonium, organic mass (OM) and black carbon (BC) at K-Bar. BBNP.

Statistical Metric (BIBE)	units	SO_4^{2-}	NO_3^-	NH_4^+	BC	OM	$PM_{2.5}$
Observed mean	$\mu g/m^3$	2.49	0.23	0.82	0.23	1.25	6.33
Predicted mean	$\mu g/m^3$	2.61	0.03	0.7	0.05	0.45	4.61
Coef. of determination (r^2)		0.52	0.01	0.47	0.13	0.1	0.23
Mean bias	$\mu g/m^3$	0.12	-0.19	-0.12	-0.18	-0.8	-1.72
Normalized bias		20%	-79%	7%	-76%	-59%	7%
Fractional bias		0%	-166%	-12%	-135%	-98%	-31%
Mean error	$\mu g/m^3$	1.08	0.21	0.35	0.18	0.81	3.09
Normalized error		55%	96%	51%	76%	62%	70%
Fractional error		46%	173%	48%	135%	100%	62%
Root mean square, RMS, error	$\mu g/m^3$	1.51	0.24	0.45	0.14	1.08	4.05
Valid Points		109	89	105	41	110	106

(1) A threshold of 0.1 $\mu g/m^3$ was applied for all species.

(2) CMAQ-MADRID modeling period corresponds to July 2 – October 28, 1999.

The model also performed well for ammonium, which tended to be associated with sulfate, rather than nitrate, at BBNP. The fact that ammonium was slightly underpredicted on average while sulfate was overpredicted indicated that the modeled degree of sulfate neutralization by ammonium deviated from the observed relationship. One possible reason was an underprediction of the ammonia emissions inventory.

When all BRAVO sites were considered (Table E-2), sulfate performance deteriorated. CMAQ-MADRID significantly overpredicted sulfate in the eastern part of the domain, even though the effects of overpredictions of SO_2 and sulfate by REMSAD, which was used to define the CMAQ boundary conditions, were corrected via calibration using ambient data.

Organic PM is composed of primary and secondary components. At BBNP, secondary organic aerosols of biogenic origin were found to constitute a large fraction of organic mass (OM) in the simulation. Underpredictions of organic PM could be attributed to sources of primary PM not currently accounted for in emissions inventories (e.g., biomass burning) or to uncertainties in the production of secondary PM. The correlation of predicted and observed PM organic material improved when all sites were considered, but consistent underpredictions were evident in the bias statistics.

Table E-2
Statistical model performance for $PM_{2.5}$, sulfate, OM and BC at all BRAVO sites.

Statistical Metric (BRAVO Network)	units	SO_4^{2-}	NO_3^{-} (3)	NH_4^{+} (3)	BC	OM	$PM_{2.5}$
Observed mean	$\mu g/m^3$	3.10	0.23	0.82	0.17	2.36	9.92
Predicted mean	$\mu g/m^3$	3.97	0.03	0.70	0.15	1.22	9.54
Coef. of determination (r^2)		0.47	0.01	0.47	0.03	0.61	0.21
Mean bias	$\mu g/m^3$	0.87	-0.19	-0.12	-0.03	-1.14	-0.39
Normalized bias		37%	-79%	7%	4%	-50%	16%
Fractional bias		8%	-166%	-12%	-34%	-78%	-15%
Mean error	$\mu g/m^3$	1.67	0.21	0.35	0.12	1.23	5.04
Normalized error		65%	96%	51%	73%	55%	65%
Fractional error		47%	173%	48%	81%	82%	56%
Root mean square, RMS, error	$\mu g/m^3$	2.65	0.24	0.45	0.2	1.55	7.06
Valid Points		3607	89	105	131	508	3169
Valid Stations		37	1	1	6	6	37

(1) A threshold of 0.1 $\mu g/m^3$ was applied for all species.

(2) CMAQ-MADRID modeling period corresponds to July 2 – October 28, 1999.

(3) The statistics (shown in grey) for ammonium and nitrate observations reflect measurement at only one station (K-Bar, Big Bend National Park) and may not reflect model performance over larger regions.

To conduct source attribution for sulfate in BBNP, the CMAQ-MADRID domain was divided into five source areas: Mexico, Texas, eastern U.S., western U.S. (excluding Texas) and boundary conditions of the broader REMSAD domain. The apportionment of sulfate at K-Bar, BBNP was calculated using sensitivity simulations in which SO_2 and primary sulfate emissions from each of those source areas were removed. Areas outside the CMAQ-MADRID domain were taken into account by apportioning the boundary conditions using REMSAD source apportionment results. The average apportionment over the 4-month period is presented in Table E-3. The contributions were calculated as a percentage of the average 4-month sulfate concentration at the K-Bar site. The results showed that Mexico accounted for 32% of the sulfate load, Texas 19%, eastern U.S. 38%, western U.S. 6% and boundary conditions 5%. On a 4-month basis, the SO_2/sulfate relationship was fairly linear since 97% of the total predicted sulfate load was accounted for by these individual contributions. Since Mexico tended to account for a larger fraction of sulfate on clean days, whereas Texas and the other in-domain areas contributed relatively more on hazy days, the average of daily contributions was considerably higher for Mexico (44%), and lower for the other source areas.

Table E-3
Summary of 4-month average source attribution of sulfate at K-Bar, BBNP.

	Mexico	Texas	Eastern U.S.	Western U.S.	BCs
Apportionment of the overall sulfate load (1)	32% (2)	19% (3)	38% (4)	6% (5)	5% (6)
Average daily sulfate apportionment(7)	44%	14%	26%	8%	8%

(1) 4-month average sulfate load in base case = 2.61 $\mu g/m^3$; observed mean sulfate = 2.49 $\mu g/m^3$; the difference between the total sulfate load and individual contributions results from non-linearities in the SO_2/sulfate chemistry and emission sources located over water.

(2) 4-month average contribution from Mexico = 0.81 $\mu g/m^3$.

(3) 4-month average contribution from Texas = 0.49 $\mu g/m^3$.

(4) 4-month average contribution from eastern U.S. = 0.96 $\mu g/m^3$.

(5) 4-month average contribution from western U.S. = 0.15 $\mu g/m^3$.

(6) 4-month average contribution from BC = 0.12 $\mu g/m^3$

(7) 4-month average value of the daily sulfate apportionments.

CONTENTS

LIST OF FIGURES

LIST OF TABLES

1
INTRODUCTION

1.1 BRAVO

The Big Bend Regional Aerosol and Visibility Observational (BRAVO) study is a multi-year monitoring and assessment study of the causes of regional haze in Big Bend National Park (BBNP). BBNP is located in southwestern Texas close to the U.S.-Mexico border, where the Rio Grande makes a large "U-turn". In addition to the Rio Grande, the 1252 square mile national park features also desert and mountain landscapes. BBNP was designated as a National Park in 1944 and a Biosphere Reserve in 1976 due to the diverse varieties of plant and animal species native to the area.

The BRAVO study (hereafter referred to as BRAVO) was performed in response to public reports of decreased visibility at BBNP and the construction of two coal-fired power plants in Mexico, approximately 125 miles southeast of BBNP. A preliminary study took place in 1996 in Texas and northern Mexico. BRAVO, a more comprehensive investigation, was recommended in the report of the preliminary study. Unfortunately, the U.S. and Mexico did not agree on the study design, and BRAVO only included monitoring sites in the United States. Multiple stake-holder groups were involved in BRAVO, including the U.S. Environmental Protection Agency (EPA), the U.S. National Park Service (NPS), the Texas Commission on Environmental Quality (TCEQ), EPRI, electric utility companies, and environmental groups.

Poor visibility at BBNP is associated with two distinct meteorological regimes. During spring and early summer, when visibility is most impaired, the dominant flow is from Mexico. During fall, poor visibility is at times associated with transport from regions to the northeast of BBNP. The monitoring component of BRAVO took place in the summer and fall months of 1999. More than 30 sites were established to measure particulate matter (PM), PM components, haze, and sulfur dioxide (SO_2) in Texas. In addition, four inert tracers were released from several potential source areas and monitored throughout Texas to assess atmospheric transport patterns. Figure 1-1 is a BRAVO map showing the tracer release locations and the PM sampling sites.

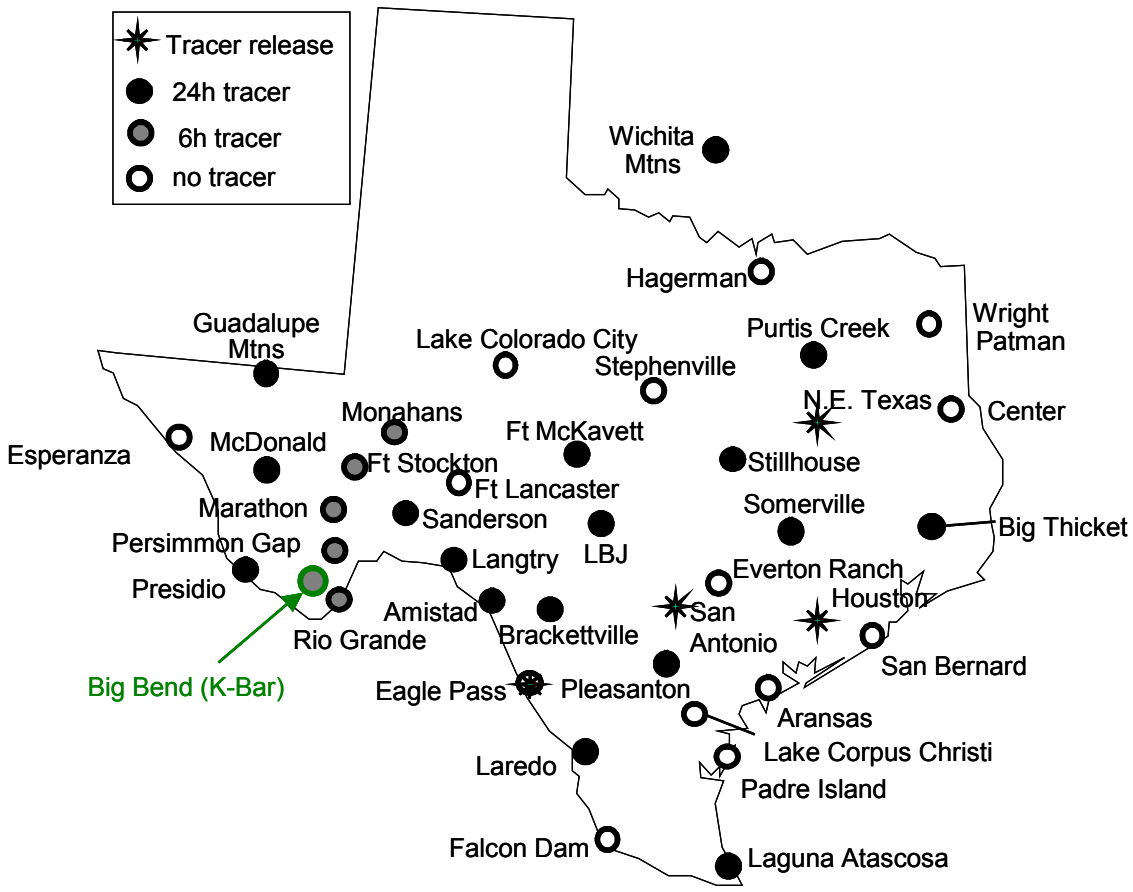

Figure 1-1
BRAVO Study tracer release locations and sampling sites.

The main objectives of the modeling component of BRAVO are to understand the long-range, trans-boundary transport of visibility-reducing particles from regional sources in the U.S. and Mexico and to quantify the contributions of specific source regions to visibility reductions at BBNP. To attain these goals, different types of models were used, ranging from relatively simple tracer methods and empirical orthogonal function analyses, to forward and back trajectory source apportionment techniques and air mass history analyses, to deterministic three-dimensional (3-D) Eulerian models. In accordance with the BRAVO Technical Committee, source attribution was limited to fine particulate sulfate. During BRAVO, sulfate on average constituted the largest mass fraction and contribution to haze of any single $PM_{2.5}$ component measured at BBNP, followed by organic compounds.

1.2 The Eulerian Modeling Component of BRAVO

Two Eulerian models were applied in BRAVO: the Regional Modeling System for Aerosols and Deposition (REMSAD) and the Community Multiscale Air Quality (CMAQ) model enhanced with the Model for Aerosol Dynamics, Reactions, Ionization, and Dissolution (MADRID), or simply CMAQ-MADRID. Modeling performed with CMAQ-MADRID is documented in this report. Section 2 provides a brief discussion of CMAQ-MADRID, followed by a discussion of the development of the modeling strategy. Details are also provided in Section 2 on the CMAQ-MADRID inputs, including the sources of raw data and the processing steps involved in generating relevant input files. Section 3 discusses the results of tracer simulations, which reflect the performance of the transport components of CMAQ. In Section 4, the CMAQ-MADRID base case simulation results are evaluated against available data and key findings regarding PM levels at BBNP are discussed. Results from sensitivity simulations conducted to provide source attribution estimates are discussed in Section 5. Finally, conclusions and recommendations are provided in Section 6.

Comments on an alternative modeling technique used by other participants of BRAVO, the Trajectory Mass Balance (TrMB) Method for Sulfate Source Apportionment, are presented in Appendix A.

A summary of analysis of emissions estimates for Mexico from different sources is provided in Appendix B.

2
MODELS AND METHODS

2.1 Brief Description of CMAQ-MADRID

The Community Multiscale Air Quality (CMAQ) model was used to perform simulations representative of ambient conditions during BRAVO. CMAQ (Byun and Ching, 1999) is a modular air quality model developed for simulating the fate and transport of atmospheric gases and particulate matter. CMAQ was employed to simulate the tracer release experiments using the following configuration options: Bott scheme for horizontal and vertical advection, the eddy diffusion scheme for vertical diffusion, and the Smagorinsky scheme for horizontal diffusion.

For chemical transport simulations, the CMAQ-MADRID (Model for Aerosol Dynamics, Reaction, Ionization, and Dissolution) model was applied to BRAVO. The MADRID atmospheric aerosol modules were implemented within the 2000 version of CMAQ and replaced the aerosol code of the EPA-distribution. Gas-phase chemistry was simulated using the regional acid deposition mechanism, version 2 (RADM 2) with the 4-product isoprene chemistry and aqueous processes were simulated using the RADM cloud module.

The MADRID modules were formulated after a comprehensive review of currently available data and algorithms for simulating processes that govern the chemical composition and size distribution of ambient particulate matter (EPRI, 2002; Zhang et al., 2004). Whereas the original CMAQ aerosol code tracks a modal representation of the particle size distribution, the MADRID modules track a discrete sectional representation of the particle size distribution. Several configuration options are available within MADRID to represent the particle size distribution, the physics of aerosol particles and the thermodynamics of their organic and inorganic aerosol constituents. The set of modules selected for the BRAVO application offers an optimal combination of numerical accuracy and computational efficiency. Two size sections represent fine ($PM_{2.5}$) and coarse particles, respectively. Each section is composed of ammonium, chloride, nitrate, sodium, sulfate, other (unclassified) inorganic species, water, elemental (black) carbon, primary organic compounds, and 38 surrogates of anthropogenic and biogenic secondary organic aerosol (SOA) compounds.

The thermodynamics of inorganic aerosol species is simulated by the ISORROPIA module (Nenes et al., 1999), modified in order to improve numerical stability via on-line calculation of activity coefficients. The RADM2 mechanism was extended when used with the MADRID modules to include detailed reactions of volatile organic compounds with atmospheric oxidants leading to the formation of low volatility products. In accordance with their vapor pressure, these semi-volatile organic compounds (SVOC) undergo reversible absorption between the gas phase and the particle phase resulting in the formation of secondary organic aerosol. The MADRID–1 option selected for this study uses an empirical approach, based on the results of smog chamber

experiments, for calculation of the SOA yields and the partitioning of SVOC into aerosol particles comprising of complex mixtures of primary and secondary organic compounds.

Coagulation processes were not modeled with CMAQ-MADRID. Observational data for PM and PM components during BRAVO were collected exclusively on a mass basis; the number concentrations of particles were not measured. Therefore, with no evaluation data available, simulation of coagulation was unnecessary since coagulation decreases the number of particles without any appreciable effects to the overall mass within the two particulate matter size bins. Furthermore, although the particle size distribution may significantly affect the scattering efficiency of ambient aerosols, at present the most common method to estimate light extinction, the IMPROVE equation, is based on the mass of specific $PM_{2.5}$ components and total coarse-particle mass ($PM_{2.5-10}$).

New sulfate particle formation was modeled using an approach based on relative rates of nucleation and condensation due to significant uncertainties in current algorithms that predict absolute nucleation rates. Condensational growth and shrinkage are not simulated in MADRID when two sections are used because effects of mass growth and shrinkage between the fine and coarse sections are negligible. Gas-particle mass transfer was modeled using a bulk equilibrium approach, with the material transferred being allocated to different size sections using weighing factors based on surface area.

Additional CMAQ modules were modified for compatibility with MADRID, including the gas-phase chemical mechanism (addition of SVOC) cloud processes and dry/wet deposition. Detailed descriptions of the CMAQ-MADRID modules are provided elsewhere (EPRI, 2002; Zhang et al., 2004).

2.2 Meteorological Inputs

Meteorological inputs are required by the chemical transport models, CMAQ and CMAQ-MADRID, and the emissions processor, the Sparse Matrix Operator Kernel Emissions (SMOKE) Modeling System (Houyoux et al., 2000). Meteorological simulations using the Fifth-Generation Mesoscale Model (MM5) (Anthes and Warner, 1978; Dudnia, 1993; Stauffer and Seaman, 1994; Seaman and Stauffer, 2003) were conducted at Pennsylvania State University for nested grids of 36-, 12-, and 4-km horizontal resolutions over the four-month BRAVO period. For CMAQ simulations, meteorological inputs were processed by the Meteorology-Chemistry Interface Processor (MCIP) (Byun et al., 1999) and involved collapsing 35 layers simulated in MM5 to 13 layers for the air-quality modeling applications.

2.3 Emissions Inputs

Four perfluorocarbon tracers – oPDCH, PDCB, PTCH, and iPPCH – were released from Eagle Pass, San Antonio, Houston, and Northeast Texas, respectively, during the BRAVO study. From early July to mid September, "timing" tracers were released at intermittent periods from Eagle Pass in addition to the continuous tracer. Tracer emissions were generated based on information from Pitchford et al. (2001). Plume rise was calculated based on meteorology files from MCIP and an algorithm consistent with the plume-rise algorithm in SMOKE.

The University of North Carolina (UNC) prepared emissions inputs for the four-month BRAVO campaign for REMSAD in latitude/longitude coordinates with a spatial resolution of 3/8 degree

longitude by 1/3 degree latitude, thereby approximating a 36-km grid (Vukovich, 2002). Emission files for CMAQ-MADRID simulations at a 36-km horizontal resolution on a Lambert projection were generated using SMOKE version 1.4b using the following procedures.

All input files and run scripts were obtained from UNC for BRAVO. The input files included raw inventories, temporal profiles, chemical speciation data, and spatial surrogate data. The run scripts controlled programs to generate point source, area source, mobile, and biogenic emissions for the United States, Mexico, and offshore sources. Various source types and source areas were then merged to produce a single three-dimensional emission file.

Lambert conformal spatial surrogate files were prepared for area/mobile sources and for biogenic emissions for 36-km resolution by spatially aggregating the previously developed 12-km resolution files (Vukovich, 2002). Procedures to generate emissions for four months were set up for CMAQ based on those used to produce REMSAD emissions. Most notably, the same "representative days" were used for the generation of mobile sources and area sources in the United States and for point and area sources offshore and in Mexico.

Extensive quality assurance checks were performed to ensure that the input files for CMAQ were consistent with those for REMSAD. These steps included visual inspection of spatial distributions, comparisons of the spatial distributions with REMSAD emissions, comparisons of diurnal profiles of emissions at selected locations, verifications of daily total emissions against weekly profiles of representative days, and spot check comparisons between CMAQ and REMSAD total emissions for Texas for individual days. Total emissions for the CMAQ 36-km domain are listed in Tables 2-1 through 2-5 for different source types and regions. These emissions were consistent with the CMAQ 12-km grid results presented in Vukovich (2002). Total emissions were slightly smaller in some states close to the border because the 36-km CMAQ domain was slightly smaller than the 12-km domain.

Table 2-1
Area/non-road source state emissions totals for the CMAQ 36-km grid

State	CO [tons/day]	NO_x [tons/day]	VOC [tons/day]	NH_3 [tons/day]	SO_2 [tons/day]	$PM_{2.5}$ [tons/day]	$PM_{2.5-10}$ [tons/day]
Arkansas	1,314.4	270.0	407.6	403.0	72.9	280.8	886.1
Colorado	63.7	15.2	19.3	38.5	1.9	23.2	84.9
Illinois	14.5	9.0	6.5	4.3	1.8	7.0	25.1
Kansas	370.8	200.7	140.6	258.9	22.0	147.4	561.1
Kentucky	9.1	7.8	3.7	4.4	1.3	3.2	9.8
Louisiana	1,629.7	904.9	492.0	180.9	331.7	280.6	517.6
Mississippi	804.9	163.0	238.3	107.7	91.0	170.1	473.4
Missouri	498.2	82.0	159.5	231.2	30.2	189.8	790.6
New Mexico	772.9	126.9	179.1	123.4	27.2	354.7	1,611.6
Oklahoma	994.2	269.3	343.0	564.1	41.2	398.8	1,719.4
Tennessee	404.4	336.5	158.1	18.4	35.7	55.0	129.8
Texas	6,051.9	1,299.8	1,928.8	1,354.3	187.2	1,429.3	5,801.8
Gulf of Mexico	69.3	273.9	34.1	0.0	0.0	0.0	0.0
Total	**12,997.8**	**3,958.8**	**4,110.6**	**3,288.9**	**844.0**	**3,339.7**	**12,611.1**

Table 2-2
Area/non-road and on-road mobile source Mexican state emissions totals for the CMAQ 36-km grid

State	CO [tons/day]	NO_x [tons/day]	VOC [tons/day]	NH_3 [tons/day]	SO_2 [tons/day]	$PM_{2.5}$ [tons/day]	$PM_{2.5-10}$ [tons/day]
Coahuila	1,330.7	83.5	286.7	33.4	48.1	43.6	104.7
Chihuahua	1,088.7	62.5	208.5	53.2	28.4	42.5	85.5
Durango	893.6	48.2	193.5	68.7	29.8	42.8	70.8
Nuevo Leon	3,234.7	189.2	455.8	40.1	104.4	170.4	226.7
San Luis Potosi	47.9	2.5	10.9	4.6	1.8	2.5	3.8
Sinaloa	159.0	7.3	50.0	28.8	9.7	12.6	12.5
Tamaulipas	1,460.2	79.9	253.1	83.1	28.9	59.7	114.6
Zacatecas	304.7	12.9	63.6	49.8	8.2	22.0	23.8
Total	**8,519.6**	**486.0**	**1,522.2**	**361.6**	**259.2**	**396.2**	**642.2**

Table 2-3
Mobile source state emissions totals for the CMAQ 36-km grid

State	CO [tons/day]	NO_x [tons/day]	VOC [tons/day]	NH_3 [tons/day]	SO_2 [tons/day]	$PM_{2.5}$ [tons/day]	$PM_{2.5-10}$ [tons/day]
Arkansas	1,724.5	296.2	194.0	7.6	11.3	7.8	2.1
Colorado	122.7	21.4	11.5	0.5	0.8	0.6	0.1
Illinois	55.1	13.4	5.8	0.3	0.5	0.3	0.1
Kansas	561.4	86.6	57.1	2.4	3.4	2.2	0.6
Kentucky	14.5	2.7	1.6	0.1	0.1	0.1	0.0
Louisiana	2,683.3	429.1	296.9	10.9	16.0	11.5	3.0
Mississippi	1,177.6	197.6	134.4	5.1	7.7	5.4	1.4
Missouri	686.0	154.2	80.5	4.3	6.5	3.9	1.1
New Mexico	1,456.2	213.9	142.5	5.5	8.2	5.6	1.5
Oklahoma	2,702.6	418.3	289.7	11.4	16.4	10.9	3.0
Tennessee	797.2	112.0	84.1	3.5	4.6	2.8	0.8
Texas	11,626.5	2,142.1	1,297.5	59.3	84.2	58.0	16.2
Total	**23,607.3**	**4,087.6**	**2,595.4**	**110.7**	**159.5**	**108.9**	**29.9**

Table 2-4
Point source state emissions totals for the CMAQ 36-km grid

State	CO [tons/day]	NO_x [tons/day]	VOC [tons/day]	NH_3 [tons/day]	SO_2 [tons/day]	$PM_{2.5}$ [tons/day]	$PM_{2.5-10}$ [tons/day]
Arkansas	173.2	137.9	74.3	3.3	148.3	24.4	12.8
Colorado	7.2	14.3	4.2	0.0	0.0	1.6	1.1
Illinois	0.8	25.9	0.5	0.0	53.3	1.0	2.3
Kansas	177.9	176.6	32.2	2.7	27.6	16.0	4.6
Kentucky	22.5	1.9	2.8	0.0	1.6	0.6	0.1
Louisiana	1,408.9	350.7	160.4	28.4	570.0	51.4	18.2
Mississippi	68.2	154.3	53.4	74.2	23.4	7.3	4.1
Missouri	251.5	34.3	90.7	29.1	214.1	32.1	51.8
New Mexico	123.2	297.5	49.0	0.2	130.2	6.8	2.9
Oklahoma	605.6	413.6	122.7	49.0	191.3	18.1	10.8
Tennessee	9.9	57.3	43.1	0.1	5.9	0.9	0.4
Texas	1,102.4	1,463.7	671.4	3.5	872.1	74.3	31.9
Gulf of Mexico	45.2	194.6	509.2	0.0	0.4	3.3	0.3
Total	**3,996.4**	**3,322.8**	**1,813.9**	**190.4**	**2,238.1**	**237.6**	**141.3**

Table 2-5
Point source Mexican state emissions totals for the CMAQ 36-km grid

State	CO [tons/day]	NO_x [tons/day]	VOC [tons/day]	NH_3 [tons/day]	SO_2 [tons/day]	$PM_{2.5}$ [tons/day]	$PM_{2.5-10}$ [tons/day]
Coahuila	12.9	218.6	0.0	0.0	715.0	22.1	36.7
Chihuahua	6.4	32.9	0.4	0.0	102.1	3.9	1.3
Durango	2.7	15.3	0.2	0.0	60.2	2.3	0.8
Nuevo Leon	4.3	22.9	0.3	0.0	127.9	3.0	1.0
Sinaloa	1.1	8.5	0.1	0.0	49.5	1.8	0.7
Tamaulipas	2.7	20.1	0.3	0.0	129.1	4.2	1.6
Total	**29.9**	**318.2**	**1.3**	**0.0**	**1,183.8**	**37.2**	**41.9**

2.4 Initial and Boundary Conditions

Four-month BRAVO simulations run from July 2 to October 30, 1999 (hereafter referred to as the BRAVO period). On July 1, eight to ten measurement sites within the modeling domain measured concentrations for sulfur dioxide (SO_2) and three PM species (sulfate, sodium and chloride). These values were interpolated using an inverse squared radius approach, with a radius of influence for each measurement set to ten cells (about 360 km). Concentrations in grid cells located beyond the radius of influence of any measurements were assigned an average value of all measurements. On July 1, 1999, only one site (K-Bar) measured concentrations for nitric acid, ammonia, and other PM species (organic carbon and elemental carbon, also referred to as black carbon); these values were applied as the initial conditions for the species throughout the entire domain. Default CMAQ initial condition values (Byun and Ching, 1999) were applied for species not measured.

Boundary conditions for a preliminary CMAQ-MADRID base case simulation were generated from the output of the REMSAD base case simulation. Additional modifications, described in Section 2.5.3, were made to generate boundary conditions for SO_2 and particulate sulfate for the final base case simulation described in this report. The domain of REMSAD covered most of the continental U.S. and Mexico; REMSAD boundary conditions for SO_2 and primary sulfate were derived the Georgia Tech/Goddard Global Ozone Chemistry Aerosol Radiation Transport, GOCART (Chin *et al.,* 2000a; Chin *et al.,* 2000b). REMSAD hourly 3-D output files were obtained from the Cooperative Institute for Research in the Atmosphere (CIRA). The latitude and longitude of each CMAQ boundary grid cell was calculated, and the corresponding results from REMSAD were extracted. REMSAD outputs most gaseous and PM species in ppm, with the exception of secondary organic aerosol (SOA), fine and coarse PM species, which were output in μg/mole air. Therefore, a necessary step was to convert all PM concentrations to $\mu g/m^3$ for use in CMAQ, using temperature and pressure as functions of time and space at the CMAQ boundary. There were one-to-one correspondences between many REMSAD and CMAQ species (e.g., isoprene, NO, SO_2). Sulfate and ammonium species from REMSAD were aggregated into the corresponding CMAQ species. Chemical speciation was needed for terpenes, VOC (representing only anthropogenic VOC in REMSAD), and SOA. The speciation of terpene and VOC species was done based on emissions. Because less reactive compounds

tend to be enriched in aged air mass relative to fresh emissions, this assumption would likely overestimate the reactive compounds at the boundary at the expense of the less reactive compounds. Anthropogenic SOA species were allocated to the xylene and toluene aerosols in equal amounts, while biogenic SOA species were allocated to 34 terpene SOA species in equal amounts.

2.5 Modeling Methodology

BRAVO was one of the first large-scale modeling studies for PM and regional haze. As such, it provided a test bed for refining modeling strategies. A two-phase approach was envisioned. First, tracer simulations were to be conducted to evaluate transport processes. Once model performance for transport was assessed by comparing tracer simulation results with tracer data (which were sequestered for the two episodes), complete chemical transport model simulations with CMAQ-MADRID would then be performed.

2.5.1 Tracer Simulations

CMAQ was first applied to simulate tracer concentrations in an attempt to evaluate the dispersion characteristics of the model. Tracer emissions were developed based on information obtained from DRI (Pitchford et al., 2001). Visual inspection of initial tracer modeling results, performed on 12-km and 4-km resolution grids, indicated that tracer plumes were not sufficiently dispersed to reach BBNP when measurements indicated "hits" (Pun et al., 2003a). Several steps were taken to improve the model's dispersion characteristics based on the observed behavior of the tracer plumes. First, a coarser grid resolution (36 km) was used. By using a coarser grid size, emitted species become instantaneously diluted within a larger volume once they are emitted or transported into a grid cell. (There are also differences between the wind fields simulated at 36-km resolution and 12-km resolution.) Second, the Smagorinsky diffusion module (the same module as used in REMSAD) was implemented to provide diffusion characteristics commensurate with the tracer plumes observed during BRAVO. The Smagorinsky scheme is more diffusive than the module included in the original CMAQ distribution. For example, at a 36-km resolution, differences in eddy diffusivities approached two orders of magnitude. No other changes were made to the other transport modules – the Bott scheme for both horizontal and vertical advection and the eddy vertical diffusion scheme.

Version 2.1 of the Meteorology-Chemistry Interface Processor (MCIP) was used after its introduction in March 2003. Prior versions of MCIP contained an error in the calculation of wind fields when several MM5 layers are collapsed into a lesser number of layers for CMAQ application. Although the problem affects upper air transport characteristics, it can produce non-negligible effects in the prediction of surface concentrations. MCIP 2.1 was found to improve tracer simulation performance, especially for long-range transport; those results are presented in Section 3.

Figure 2-1
Modeling domain of CMAQ-MADRID

2.5.2 Chemical Transport Model Simulations

CMAQ-MADRID was used to simulate the gas-phase and particulate matter species for the four-month BRAVO period on a 36-km resolution grid. The configuration developed for transport processes in the CMAQ tracer simulation was adopted for use in the CMAQ-MADRID simulations. All 36-km resolution meteorological files were processed using MCIP 2.1 before applying the SMOKE emissions processor and modeling with CMAQ-MADRID. The modeling domain for the 36-km resolution simulations is shown in Figure 2-1. The size of the domain was constrained by the availability of spatial surrogate data for the generation of emission input. The southwest corner of the domain is located at –106.71 degrees longitude (easting) and 23.16 degrees latitude (northing). From this corner, the domain extends 1728 km east and 1584 km north, and extends vertically to the tropopause.

A preliminary CMAQ-MADRID base case chemistry simulation was performed using output from the Regional Modeling System for Aerosols and Deposition – REMSAD – as an outer nest that provided lateral boundary conditions to the CMAQ domain. (The REMSAD domain covered nearly the entirety of the continental U.S. and Mexico and in turn its boundary conditions for SO_2 and sulfate were provided by the GOCART global model.) The preliminary base case simulation was analyzed for any potential biases, including any bias carried over from the REMSAD simulations. The following text describes the analysis of the preliminary base case and the development of the final CMAQ-MADRID base case.

Performance of the preliminary CMAQ-MADRID base case was appraised by comparing 24-hour predictions of several species with 24-hour observations at corresponding sites. The species evaluated were $PM_{2.5}$ total mass, $PM_{2.5}$ sulfate, $PM_{2.5}$ ammonium, $PM_{2.5}$ nitrate, $PM_{2.5}$ organic mass (OM), $PM_{2.5}$ black carbon (BC), and gas-phase SO_2. In addition, weekly SO_2 predictions and measurements were also compared. Several statistical measures of performance – coefficient of determination (r-squared), gross bias, normalized bias, fractional bias, gross error, normalized error, fractional error, root mean square error – were calculated for each site of the BRAVO network and for the BRAVO network as a whole.

The preliminary CMAQ-MADRID base case simulation revealed poor performance for several species, particularly SO_2 and sulfate over the eastern half of the CMAQ domain. Due to the CMAQ-MADRID dependency on REMSAD for boundary conditions, a statistical analysis was prepared to establish whether REMSAD predictions were biased near the CMAQ-domain boundary. REMSAD-predicted concentrations of SO_2 and sulfate were compared to measurements at nearby Clean Air Status and Trends Network (CASTNet) and Interagency Monitoring of Protected Visual Environments (IMPROVE) sites during the BRAVO period. As shown in Table 2-6, REMSAD overpredicted sulfate by approximately 40% and overpredicted SO_2 by a factor of ~3.8 systematically for all measurements near the CMAQ-domain boundary. The bias exhibited by REMSAD in SO_2 and sulfate predictions could, therefore, carry over via transport through the boundary to the CMAQ-MADRID simulations.

A second potential bias was noted in the analysis of the CMAQ-MADRID preliminary base case simulation: during periods in July when there was a predominance of southerly winds, the model systematically underestimated sulfate concentrations at K-Bar in BBNP. At the time the BRAVO emission inventories were developed, no official emission inventory existed for Mexico (Vukovich and Kuhns, 2003). Although developed with the best available data at the time, the emissions of SO_2 and other primary species from Mexico in the BRAVO emissions inventory were highly uncertain. In September 2002, in a presentation titled "Mexico and USA Power Plant Emissions in Perspective," an Undersecretary of the Mexican Ministry of Energy presented total SO_2 emissions for three Mexican states bordering the United States, which constitute a large portion of the CMAQ modeling domain. The emission estimates from the Mexican Department of Energy were compared with the BRAVO inventory as shown in Table 2-7. Comparing SO_2 emissions from all sources other than the Carbon power plants, the BRAVO estimate (225,000 tons/year) disagreed with the estimate of the Mexican Ministry of Energy (398,000 tons/year). An underestimation factor of ~ 1.8 was associated with area-source and low-level point-source emissions of SO_2 within the Mexican portion of CMAQ modeling domain.

Table 2-6
Performance statistics of REMSAD compared to CASTNet and IMPROVE data.

Statistical Metric	Units	Weekly SO_2	24-hour SO_4^{2-}
Observed mean	$\mu g/m^3$	3.70	2.00
Predicted mean	$\mu g/m^3$	10.25	2.08
Coefficient of determination (r^2)		0.62	0.70
Mean bias	$\mu g/m^3$	6.55	0.07
Normalized bias		275%	41%
Mean error	$\mu g/m^3$	6.60	0.88
Normalized error		275%	63%
Root mean square, RMS, error	$\mu g/m^3$	8.72	1.57
Valid Points		309	843

Table 2-7
Comparison of SO_2 emissions (tons/year) for three U.S.-bordering Mexican states.

	Secretaría de Energía de México Estimate (2000)	BRAVO Estimate (1999)
Coahuila	160,000	270,000
Nuevo Leon	230,000	85,000
Tamaulipas	160,000	112,000
Total	**550,000**	**466,000**
Carbon (1)	152,000	241,000
Total – Carbon	**398,000**	**225,000**

(1) Carbon emissions included in Coahuila total

As a result of the above analyses (i.e., effects of overpredicted sulfur in the CMAQ-MADRID boundary conditions due to overpredictions in REMSAD and uncertainties in Mexican emissions), two sensitivity simulations were performed. First, emissions of SO_2 and sulfate within the Mexican portion of the CMAQ-MADRID domain, with the exception of emissions from the Carbon power plants, were increased by a factor of two. Doubling non-Carbon Mexican emissions resulted in an increase of total Mexican SO_2 emissions within the CMAQ domain (including the Carbon facilities) by a factor of 1.54, i.e., 54%. REMSAD simulations with similar increases to the Mexican emissions were not performed and, therefore, REMSAD-provided boundary conditions were not altered in a similar fashion. Thus, anthropogenic Mexican emissions of SO_2 in the greater BRAVO domain were increased by 22%. (If the Popocatépetl volcano emissions were included in the analysis, overall Mexican SO_2 emissions were increased by 10%.) As shown in Table 2-8, performance statistics for SO_2 and sulfate in

the sensitivity simulation yielded values similar to those of the preliminary simulation. The increase in Mexican emissions resulted in small changes to the fine particulate sulfate concentrations at K-Bar. For the month of July, when there was a predominance of southerly winds and the preliminary simulation systematically underestimated sulfate concentrations at K-Bar, the additional Mexican sulfur emissions increased the fine particulate sulfate in a fairly consistent range of 0.1 to 0.2 $\mu g/m^3$, equivalent to 8% to 17% of the observed mean monthly sulfate concentration of 1.21 $\mu g/m^3$. For the duration of the BRAVO period and over the entire BRAVO network, the sensitivity simulation yielded more subtle results: a 0.05 $\mu g/m^3$ increase in model-predicted mean sulfate, and a 0.07 $\mu g/m^3$ increase in the bias (4% on a normalized basis) when comparing model predictions to observations. The increases to these statistical measures are due to the superposition of additional sulfate to the predictions of the preliminary base case simulation that displayed an inherent bias of 1.57 $\mu g/m^3$ (+57% on a normalized basis).

Table 2-8
Comparison of SO_2 and fine SO_4^{2-} statistics for preliminary, sensitivity and base case simulations.

Statistical Metric	Units	Weekly SO_2			24-hour fine SO_4^{2-}		
		Prelim. Base Case	Mexican Emissions Sensitivity	Final Base Case	Prelim. Base Case	Mexican Emissions Sensitivity	Final Base Case
Observed mean	$\mu g/m^3$	1.48	1.48	1.48	3.1	3.1	3.1
Predicted mean	$\mu g/m^3$	1.74	1.79	1.61	4.67	4.74	3.97
Coefficient of Determination (r^2)		0.45	0.45	0.46	0.47	0.47	0.47
Mean bias	$\mu g/m^3$	0.26	0.31	0.12	1.57	1.64	0.87
Normalized bias		48%	56%	40%	57%	61%	37%
Mean error	$\mu g/m^3$	0.69	0.70	0.60	2.24	2.26	1.67
Normalized error		71%	74%	64%	82%	83%	65%
RMS error	$\mu g/m^3$	1.09	1.10	0.97	3.58	3.6	2.65
Valid Points		283	283	283	3607	3607	3607

For the second sensitivity simulation, Mexican SO_2 and sulfate emissions were increased as in the first sensitivity simulation. Additionally, lateral boundary conditions for SO_2 and sulfate were modified to reduce the bias imposed by the REMSAD predictions. The modification process involved four steps:

1. REMSAD results were compared to observations from the CASTNet and IMPROVE networks. 23 IMPROVE sites and 21 CASTNet sites were selected within 4 degrees (longitude or latitude) of the CMAQ-domain boundary. The 23 IMPROVE sites measured 24-hour fine particulate sulfate samples on every Wednesday and Saturday. CASTNet reported values weekly of SO_2 concentrations at 19 sites and 24-hour sulfate on every sixth day. (One CASTNet station provided values on every 12th day.)

2. Scaling factors were obtained by pairing observations to predictions.

3. Temporally, scaling factors were interpolated linearly for each station.

4. Spatially across grid cells, scaling factors were interpolated horizontally (up to a radius of influence of 600 km) using an inverse squared approach and propagated vertically to the top of the domain. The scaling factor at a grid cell, f_{cell}, is:

$$f_{cell} = \sum_{i=1}^{n|_{r_i \le 600\,km}} w_i f_i \text{ , where } w_i = \frac{1/r_i^2}{\sum_{j=1}^{n|_{r_i \le 600\,km}} 1/r_j^2} \text{ such that } \sum_{i=1}^{n|_{r_i \le 600\,km}} w_i = 1 .$$

In the above equations, f_{cell} denotes the scaling factor a particular grid cell, $n|_{ri<600km}$ is the number of stations located within 600 km of the grid cell, f_i is the scaling factor at a station i, w_i is the weight of the scaling factor from station i. The weight w_i is defined as the inverse square distance ($1/r_i^2$) normalized by the sum of the inverse square distance over all sites (j) located within 600 km of the grid cell. r_i and r_j are the distance from the center of the grid cell to the location of station i or j. Alternatively, in condensed form, the above expressions are equivalent to

$$f_{cell} = \frac{\sum_{i=1}^{n|_{r_i \le 600\,km}} f_i/r_i^2}{\sum_{i=1}^{n|_{r_i \le 600\,km}} 1/r_i^2} .$$

Model performance for the second sensitivity simulation improved over the performance of the preliminary base case simulation for SO_2 and sulfate, with bias and error reduced for both species throughout the BRAVO network, as shown in Table 2-8. Statistically, the second sensitivity case better represents the conditions present during the BRAVO study than the preliminary base case (parent) simulation, albeit with unsettled uncertainties remaining in the modeling system. In the end, the second sensitivity simulation was selected as the CMAQ-MADRID base case simulation and served as a basis for estimating source attribution.

Source attribution was conducted for fine particulate sulfate at K-Bar, BBNP during the BRAVO period. The CMAQ domain was divided into four geographical source areas consistent with the selection of source regions for attribution analysis with REMSAD (see Figure 2-2), i.e. Mexico, Texas, the eastern U.S. and the western U.S. excluding Texas. A fifth source region representing the boundary conditions provided to the REMSAD domain by the GOCART global model was also analyzed.

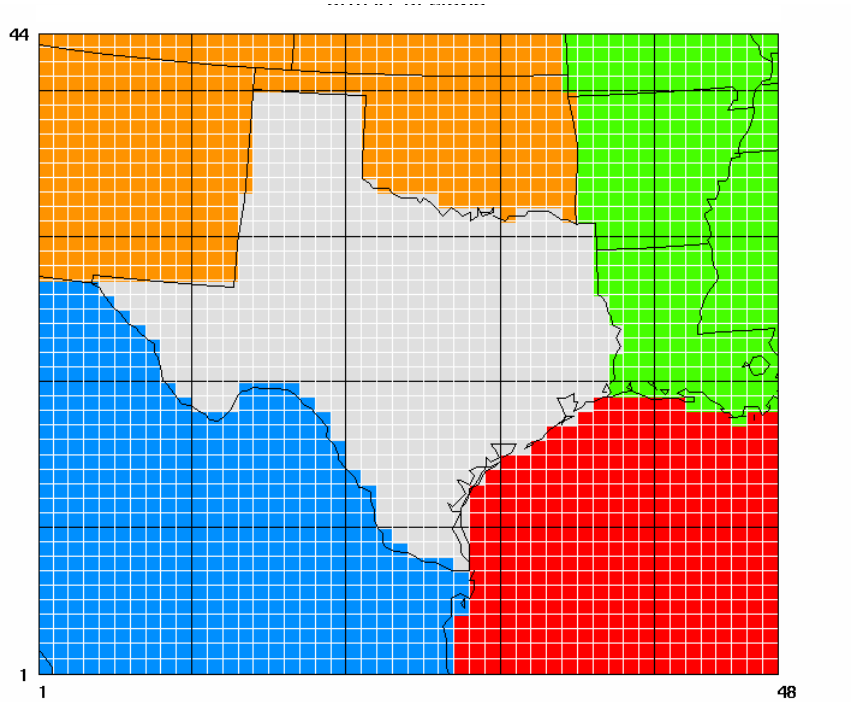

Figure 2-2
Source regions in CMAQ-MADRID. Color coded regions: orange for Western U.S.; green for Eastern U.S.; grey for Texas; blue for Mexico. Red for open-water of Gulf of Mexico, not included in any source attribution sensitivity simulation.

Source attribution was estimated by apportioning the in-domain and boundary contributions from the five source regions to the fine particulate sulfate concentrations predicted by CMAQ-MADRID at BBNP.

1. Complete 2-dimensional output for the surface layer was analyzed from the five REMSAD source attribution sensitivity simulations. For each source region, fractions were determined for SO_2 and sulfate at each grid cell of the CMAQ boundary using the corresponding file. Due to data limitations, the fractions computed at the surface were assumed to remain constant in the vertical direction.

2. The fractions for each region were multiplied by the scaling factors obtained via comparison with IMPROVE and CASTNet data as described earlier. The resultant factors when applied to the REMSAD output represent the contribution to the concentration of SO_2 and sulfate at each boundary cell corresponding to each source region.

3. When conducting the source attribution simulation, the emissions of SO_2 and sulfate from a source region were removed along with the corresponding contribution to the SO_2 and sulfate concentrations at each boundary cell.

The contribution from a source region to fine particulate sulfate at K-Bar, BBNP is defined as the difference between the base case fine sulfate concentration and the fine sulfate concentration predicted by the attribution sensitivity simulation, i.e.

$$\text{Contribution} = [SO_4^{2-}]_{\text{base case}} - [SO_4^{2-}]_{\text{sensitivity case}}.$$

Source attribution was estimated for the whole BRAVO period, for each month of the BRAVO period, and for seven episodes.

3
TRACER RESULTS

The transport and dispersion algorithms of the CMAQ three-dimensional Eulerian air-quality model were tested by simulating the transport of inert tracers emitted from specific point sources to receptor sites. (Hereafter, we refer to advective transport and dispersion (or diffusion) processes collectively as transport processes.) During BRAVO, four perfluorocarbon tracers – oPDCH, PDCB, PTCH, and i-PPCH – were released from locations near the cities of Eagle Pass (adjacent to the Texas/Mexico border), San Antonio, and Houston, and from a site in northeast Texas, respectively. The Eagle Pass tracer was released closest to BBNP, whereas the Northeast Texas tracer was released farthest away. From early July to mid September, "timing" tracers were released at intermittent periods from Eagle Pass in addition to the continuous tracer. Six BRAVO network stations – San Vincente, K-Bar (BBNP), Persimmon Gap, Marathon, Fort Stockton and Monahans Sandhills – measured tracer concentrations during the study.

As discussed in the previous section, CMAQ was configured with the Bott advection scheme for horizontal and vertical advection, the eddy diffusion scheme for vertical diffusion, and the Smagorinsky scheme for horizontal diffusion. For the inert tracer simulation, the chemistry, aerosol, and dry deposition modules were disabled. Meteorological fields were generated by processing the MM5 output with MCIP version 2.1 and a four-month simulation was conducted from July 2 to October 30, 1999 (i.e., the BRAVO period).

3.1 Spatial Distributions

Major transport pathways were inferred by inspecting the spatial distribution of tracers. The Eagle Pass tracer, chosen to simulate plumes from the Carbón I/II power-plant facilities in Mexico, was frequently transported to the north or northwest during summer and fall months, affecting BBNP on days with transport toward the west or with significant horizontal dispersion of the tracer plumes. During late August and September, the Eagle Pass tracer could also be transported into Mexico due to a shift in the wind direction. Tracer material from Eagle Pass was transported to eastern Texas infrequently.

The northeast Texas tracer did not reach BBNP frequently during July and the first part of August because the tracer plume was confined to the northern part of the domain. Several episodes during the later part of August, September and October featured plumes of the northeast Texas tracer dispersed quite widely in Texas and Mexico and that eventually moved along the Rio Grande to reach BBNP.

Release of the PTCH tracer from Houston and the PDCB tracer from San Antonio started in late September. The Houston tracer was typically transported to the north or south, except during the first 20 days in October, when the plume of tracer material moved southwest into Mexico and then dispersed in the northwest direction to reach BBNP. For the San Antonio plume, the spatial distributions alternate between a discernable plume to the north to widespread concentrations in southern Texas and Mexico.

Given the prevalence of southerly winds, air masses from Mexico frequently influence the air quality at BBNP. In the second half of the BRAVO period, air masses from source areas in northeast Texas affected BBNP more frequently than during the first half of the BRAVO period.

Table 3-1
Tracer statistics at K-Bar, BBNP.

C008-BIBE		Eagle Pass	NE Texas	Houston	San Antonio	Eagle Pass	Eagle Pass
STATISTIC	Unit	PDCH	PPCH	PTCH	PDCB	PTCH	PDCB
Observed Mean	ppq	0.14	-0.005	0.07	0.67	0.10	0.42
Predicted Mean	ppq	0.13	0.02	0.04	0.31	0.08	0.68
Ratio of Means		0.96	-4.30	0.49	0.46	0.86	1.64
Std Dev (Observed)	ppq	0.30	0.03	0.09	1.01	0.32	2.25
Std Dev (Predicted)	ppq	0.25	0.06	0.06	0.53	0.19	1.71
Coef of Variation (Obs)		2.19	-5.85	1.26	1.51	3.33	5.41
Coef of Variation (Pred)		1.89	3.19	1.62	1.71	2.25	2.51
RMS Error	ppq	0.33	0.07	0.10	0.88	0.33	2.53
RMSE / Observed Mean		2.37	-13.88	1.35	1.30	3.41	6.06
Coef of Correlation (r)		0.31	0.36	0.33	0.63	0.25	0.22

Table 3-2
Tracer statistics at Fort Stockton.

C113-FTST		Eagle Pass	NE Texas	Houston	San Antonio	Eagle Pass	Eagle Pass
STATISTIC	**Unit**	**PDCH**	**PPCH**	**PTCH**	**PDCB**	**PTCH**	**PDCB**
Observed Mean	ppq	0.44	0.02	0.09	0.40	0.19	1.01
Predicted Mean	ppq	0.23	0.02	0.02	0.29	0.17	1.38
Ratio of Means (Pred/Obs)		0.51	1.34	0.24	0.72	0.92	1.37
Std Dev (Observed)	ppq	0.62	0.05	0.10	0.63	0.54	2.70
Std Dev (Predicted)	ppq	0.29	0.05	0.05	0.60	0.27	2.33
Coef of Variation (Obs)		1.40	2.78	1.13	1.58	2.88	2.68
Coef of Variation (Pred)		1.31	1.95	2.32	2.08	1.56	1.69
RMS Error	ppq	0.63	0.06	0.12	0.65	0.54	3.15
RMSE / Observed Mean		1.43	3.29	1.38	1.64	2.85	3.13
Coef of Correlation (r)		0.32	0.26	0.20	0.45	0.27	0.23

Table 3-3
Tracer statistics at Marathon.

C112-MARA		Eagle Pass	NE Texas	Houston	San Antonio	Eagle Pass	Eagle Pass
STATISTIC	**Unit**	**PDCH**	**PPCH**	**PTCH**	**PDCB**	**PTCH**	**PDCB**
Observed Mean	ppq	0.46	0.01	0.07	0.55	0.31	1.50
Predicted Mean	ppq	0.21	0.03	0.03	0.33	0.14	1.07
Ratio of Means		0.45	3.99	0.35	0.61	0.44	0.72
Std Dev (Observed)	ppq	0.75	0.05	0.08	0.88	0.73	3.43
Std Dev (Predicted)	ppq	0.32	0.05	0.04	0.51	0.25	2.04
Coef of Variation (Obs)		1.62	7.21	1.10	1.61	2.36	2.28
Coef of Variation (Pred)		1.51	2.16	1.74	1.52	1.80	1.90
RMS Error	ppq	0.77	0.06	0.10	0.72	0.71	3.37
RMSE / Observed Mean		1.66	10.21	1.34	1.31	2.28	2.25
Coef of Correlation (r)		0.29	0.25	0.14	0.63	0.36	0.34

Table 3-4
Tracer statistics at Monahans Sandhills.

C114-MONA		Eagle Pass	NE Texas	Houston	San Antonio	Eagle Pass	Eagle Pass
STATISTIC	**Unit**	**PDCH**	**PPCH**	**PTCH**	**PDCB**	**PTCH**	**PDCB**
Observed Mean	ppq	0.49	0.02	0.06	0.50	0.18	1.60
Predicted Mean	ppq	0.25	0.03	0.03	0.39	0.19	1.52
Ratio of Means		0.51	1.29	0.50	0.78	1.08	0.95
Std Dev (Observed)	ppq	0.77	0.06	0.10	0.97	0.51	4.45
Std Dev (Predicted)	ppq	0.33	0.05	0.05	0.83	0.29	2.60
Coef of Variation (Obs)		1.55	3.10	1.79	1.94	2.85	2.79
Coef of Variation (Pred)		1.29	2.15	1.68	2.13	1.51	1.71
RMS Error	ppq	0.78	0.07	0.10	0.92	0.53	4.96
RMSE / Observed Mean		1.57	3.38	1.78	1.84	2.95	3.10
Coef of Correlation (r)		0.29	0.35	0.33	0.49	0.22	0.09

Table 3-5
Tracer statistics at Persimmon Gap.

C111-PRSG		Eagle Pass	NE Texas	Houston	San Antonio	Eagle Pass	Eagle Pass
STATISTIC	**Unit**	**PDCH**	**PPCH**	**PTCH**	**PDCB**	**PTCH**	**PDCB**
Observed Mean	ppq	0.40	0.01	0.05	0.39	0.30	1.15
Predicted Mean	ppq	0.18	0.02	0.03	0.33	0.12	0.89
Ratio of Means		0.45	1.87	0.51	0.84	0.39	0.77
Std Dev (Observed)	ppq	0.67	0.05	0.12	0.79	0.64	3.06
Std Dev (Predicted)	ppq	0.30	0.05	0.05	0.50	0.23	1.90
Coef of Variation (Obs)		1.68	4.38	2.45	2.00	2.14	2.67
Coef of Variation (Pred)		1.66	2.14	1.85	1.52	2.02	2.14
RMS Error	ppq	0.72	0.06	0.12	0.63	0.66	3.38
RMSE / Observed Mean		1.79	4.77	2.38	1.61	2.23	2.95
Coef of Correlation (r)		0.19	0.38	0.31	0.60	0.18	0.14

Table 3-6
Tracer statistics at San Vicente.

C110-SNVI		Eagle Pass	NE Texas	Houston	San Antonio	Eagle Pass	Eagle Pass
STATISTIC	**Unit**	**PDCH**	**PPCH**	**PTCH**	**PDCB**	**PTCH**	**PDCB**
Observed Mean	ppq	0.15	0.01	0.07	0.41	0.03	0.46
Predicted Mean	ppq	0.11	0.02	0.02	0.30	0.07	0.62
Ratio of Means		0.75	3.43	0.35	0.73	2.34	1.35
Std Dev (Observed)	ppq	0.40	0.04	0.08	0.72	0.34	2.37
Std Dev (Predicted)	ppq	0.26	0.05	0.05	0.55	0.20	1.86
Coef of Variation (Obs)		2.70	7.03	1.24	1.77	11.02	5.20
Coef of Variation (Pred)		2.34	2.62	2.12	1.85	2.71	3.01
RMS Error	ppq	0.40	0.04	0.10	0.73	0.37	2.64
RMSE / Observed Mean		2.73	8.16	1.44	1.79	12.07	5.78
Coef of Correlation (r)		0.32	0.55	0.24	0.38	0.13	0.25

3.2 Performance Statistics

The performance statistics of the various tracers at the 6-hour monitoring sites (see Figure 1-1) are summarized in Tables 3-1 to 3-6. Note that the units of volume mixing ratios are given as parts per quadrillion, ppq (1 ppq = 1 fL/L). The measurement data used in these comparisons were obtained from Dr. Mark Green, DRI (29 January 2003 version). Mixing ratios are reported as the mixing ratio above the background value and performance statistics are calculated on this basis. The performance statistics selected to test the simulations of the tracer campaign differ from those selected to test the chemical transport model. This is a consequence of the generally low signal-to-noise ratios observed during measurements. The percent of observations (over all six tracer measurement sites) that were greater than twice the analytical uncertainty (2σ) was less than 10% and 12% for the distant northeast Texas tracer and Houston tracers, respectively. For the San Antonio tracer, the percent of values greater than 2σ ranged from 15 to 34%, and for the Eagle Pass tracer, the percent of values greater than 2σ ranged from 16 to 59%. At the K-Bar site, the percent of values greater than 2σ for the San Antonio, Eagle Pass, Houston and northeast Texas tracer were 30%, 22%, 10% and 1%, respectively. Due to the low occurrence of sufficiently high signal-to-noise ratios, normalized performance metrics that gauge error between the magnitudes of simulated tracer mixing ratios and observations (e.g., normalized error and normalized bias) were not selected. Ultimately, the metrics chosen to test tracer performance relate more to the characteristics of the distribution and timing of the tracer (e.g., ratio of means and coefficient of variation).

The continuous tracer (PDCH) released at Eagle Pass is generally underpredicted at all 6-hour monitoring sites, especially at Fort Stockton, Marathon, Monahans Hills, and Persimmon Gap. The best prediction is obtained at the K-Bar site in BBNP, where the ratio of mean predicted mixing ratios with respect to mean observed mixing ratios approaches unity (0.96). However, coefficients of correlation (r) fall in a low range of values from 0.19 to 0.32.

The model performance with respect to the timing tracers PTCH and PDCB released from Eagle Pass exhibits a greater degree of variability. The ratios of mean simulated mixing ratios with respect to mean observed mixing ratios of the timing tracers are found to be as high as 2.3 for the PTCH tracer at San Vicente and as low as 0.39 for the same tracer at Persimmon Gap. Low correlation coefficients (r) are calculated as well, with values ranging from 0.08 to 0.36. These results indicate the inherent difficulty of simulating narrow plumes from nearby sources in 3-D models. Small errors in the wind fields or dispersion characteristics may cause the simulated plume to miss the receptor when the tracer from Eagle Pass reached the receptor in the ambient atmosphere, and vice versa.

Due to its remote location from BBNP, low mixing ratios for the northeast Texas tracer (PPCH) were measured typically at the 6-hour monitors located in the vicinity of BBNP. Indeed, the average mixing ratio was slightly negative at the K-Bar site in BBNP. Negative concentrations are "observed" when the background mixing ratio is subtracted from an even lower measured concentration. Standard deviations are high at all monitors compared to the average mixing ratio since high mixing ratios are sometimes observed when the plume directly "hits" the monitoring sites. Low average concentrations and high standard deviations are also predicted at all sites. The correlation coefficients (r) ranged from 0.25 to 0.55, despite repeated measurements below the background mixing ratio.

The correlation coefficients for the Houston tracer ranged from 0.14 to 0.33, and those for the San Antonio tracer ranged from 0.38 to 0.63. The correlation of the San Antonio tracer was typically better than that of the Houston tracer, although the trend was not consistent for other performance metrics, such as the ratio of means.

3.3 Time Series

The time series of both the observed and simulated tracer mixing ratios are shown in Figures 3-1 to 3-4 for the northeast Texas, Eagle Pass, Houston and San Antonio tracers at K-Bar, BBNP. For the northeast Texas tracer, "negative" or zero mixing ratios were observed during much of the 4-month period. Only a few measurements were observed where the tracer signal was clearly distinguishable from the noise, i.e. implying detectable hits. The highest observed mixing ratios (~0.2 ppq) occurred in the last part of October. Several lower peaks (0.05 to 0.1 ppq) were observed: July 31, August 22, August 31, October 7, and October 11. CMAQ was able to reproduce the timing of all but the July 31 tracer hits. However, of these simulated tracer signals, all except the late October peak were overpredicted. CMAQ also predicted mixing ratios in excess of 0.4 ppq on October 5, when significant signal-to-noise ratios were not observed.

The Eagle Pass tracer was observed at BBNP in several clusters. Several matching clusters were predicted by CMAQ, although the magnitudes of the predicted mixing ratios were not always

consistent with the observed values. For example, the highest simulated mixing ratios were approximately 1 ppq whereas a peak in the observations was observed at 3.5 ppq. In addition, the model also predicted mixing ratios near 1 ppq when appreciable tracer signals were not observed.

The measured Houston tracer showed two periods of elevated mixing ratios around October 7 and October 13. CMAQ also predicted elevated mixing ratios near those dates, although the simulated peak mixing ratios were shifted back in time for the former hit yet forward in time for the latter hit.

The timing of several predicted San Antonio tracer hits at K-Bar matched observations. However, a peak on October 16 was simulated when observed concentrations were negligible, possibly due to back shift in the timing of a later observed hit. Maximum simulated concentrations were lower than the observed peak concentrations,

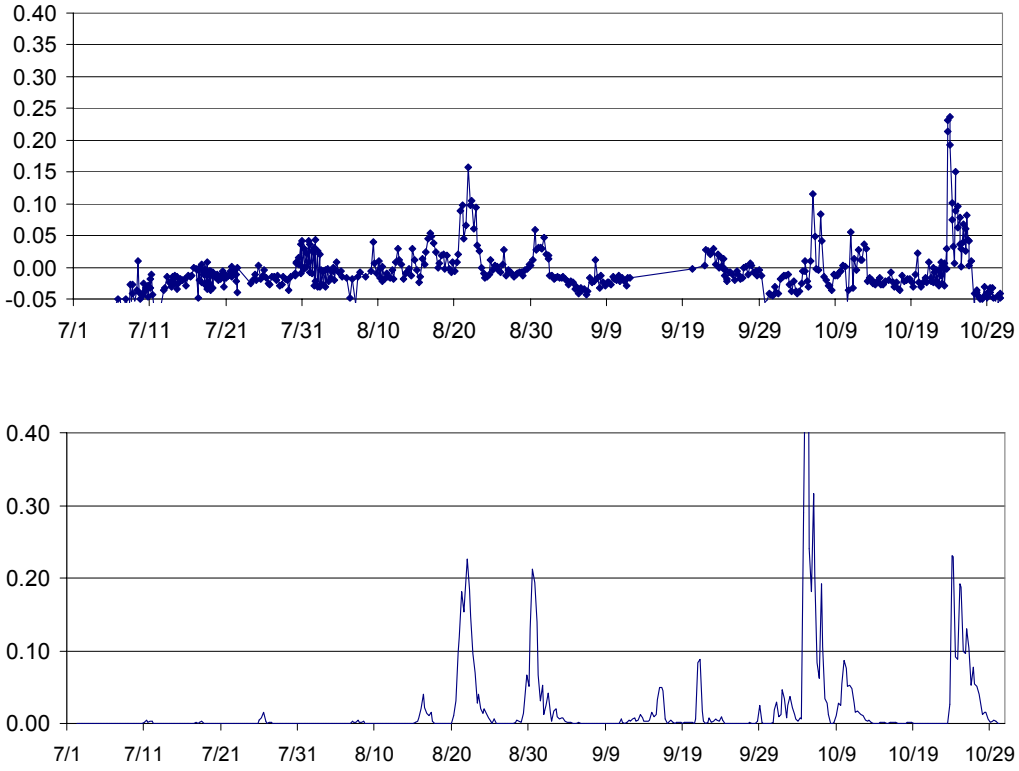

Figure 3-1
Observed (top) and simulated (bottom) time series of the NE Texas tracer at K-Bar, BBNP.

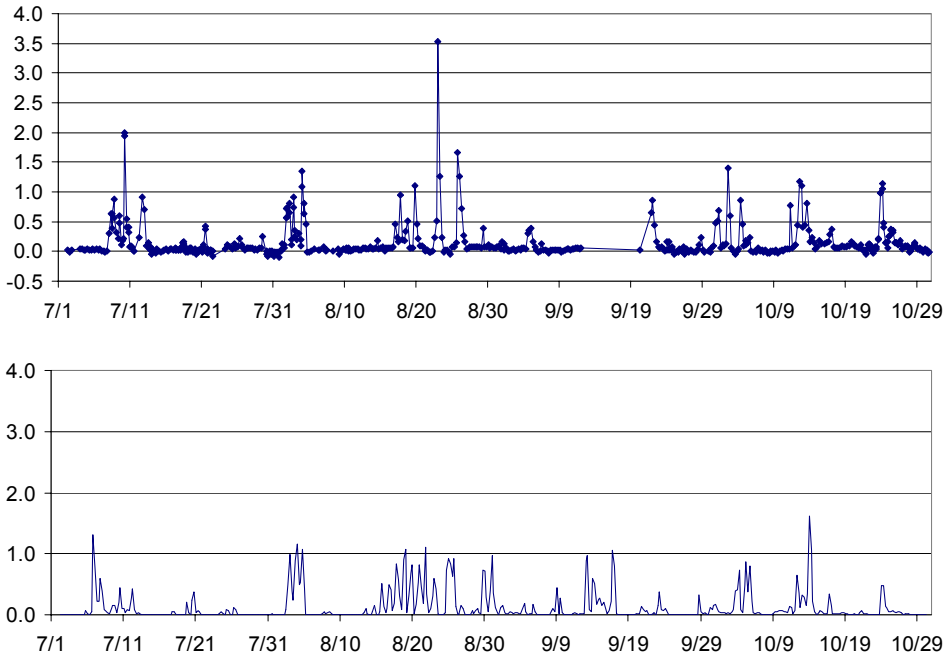

Figure 3-2
Observed (top) and simulated (bottom) time series of the Eagle Pass tracer at K-Bar, BBNP.

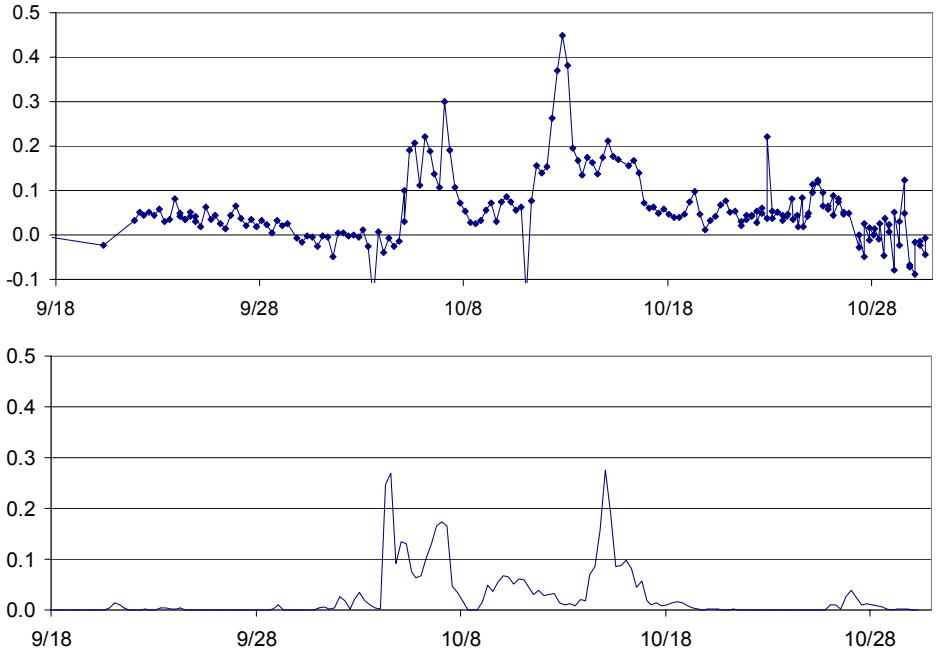

Figure 3-3
Observed (top) and simulated (bottom) time series of the Houston tracer at K-Bar, BBNP.

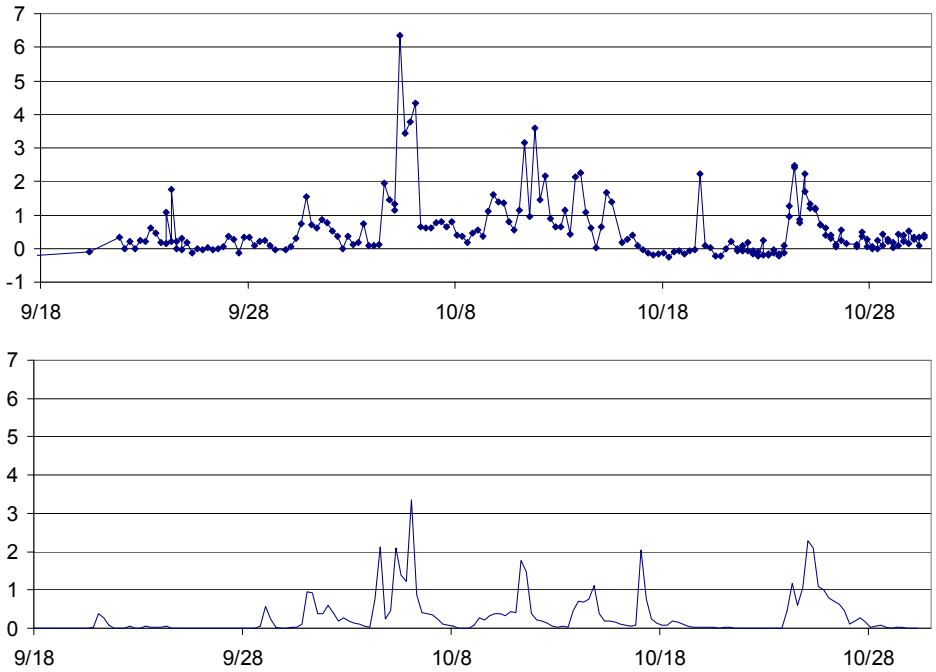

Figure 3-4
Observed (top) and simulated (bottom) time series of the San Antonio tracer at K-Bar, BBNP.

3.4 Discussion of the Tracer Results

Transport processes are seldom evaluated independently in routine applications of 3-D Eulerian models for ozone, particulate matter, haze, air toxics, and atmospheric deposition. The BRAVO tracer simulations reveal that transport processes can serve as a significant source of uncertainty. The relatively poor performance of the model is indicative of the inherent difficulty in the simulation of narrow plumes from single point sources in 3-D models. Small errors in the dispersion algorithms or in the MM5/MCIP2.1 wind fields can cause the simulated plume to miss the receptor when a tracer reached a receptor in the real atmosphere or vice-versa.

In application to BRAVO, coarse grid resolutions provide better performance for predicting the transport – with respect to distribution and timing – of inert tracers. Simulated plumes are generally more dispersed with a coarse grid resolution, resulting in a higher probability of reaching the monitoring site as the plume travels to the vicinity of the monitor. This is partly due to the artificial dilution inherent to emitting and transporting species within larger grid cell volumes. (Diffusion in 3-D air-quality models results from both the diffusion module and numerical diffusion.) In addition to the artificial dilution that occurs in a grid cell, differences in the wind speed and wind direction in the meteorological input used to drive the transport modules can contribute to differences in the location of the tracer plumes. It is reasonable to infer that simulation of inert tracers may require a higher accuracy in meteorological inputs than regionally distributed pollutants. While higher spatial resolutions reduce uncertainties in the numerical representation of various physicochemical processes in Eulerian models (e.g., plume chemistry, cloud effects), finer resolutions may not always yield better results in situations where transport plays a dominant role in the distribution of the simulated species of interest.

BRAVO provided an opportunity to evaluate the transport components of Eulerian models independently of chemical processes. Overall, CMAQ was capable of explaining only 5 to 13% of the variance (as estimated by the coefficient of determination, r^2) for all but one of the six tracers at K-Bar, BBNP (40% of the variance could be explained by the model for the San Antonio tracer at K-Bar). Performance results with respect to the timing of tracers indicate that CMAQ may be more apt in depicting regional scale transport of more-distributed pollutants from multiple sources and restricted in its ability of capturing transport from a single source to specific receptors.

Fine aerosol particles are regionally distributed due to their long atmospheric lifetimes in the absence of wet deposition. CMAQ-MADRID is subsequently used to estimate the relative impacts of sources on particulate matter concentrations at BBNP. However, due to the recognition that significant uncertainties are associated with the use of CMAQ-MADRID to conduct PM attribution for individual sources, source attribution was limited to larger geographical source regions.

4
AIR QUALITY RESULTS

The CMAQ-MADRID chemical transport model base case simulation was developed following the analysis of a preliminary base case simulation. The preliminary simulation used emissions estimated by the BRAVO emissions inventory and boundary conditions prescribed by the continental-scale REMSAD model simulation of the BRAVO study using a one-way nesting approach. As described in Chapter 2, two important issues were raised during the analysis of the preliminary simulation: underestimation of Mexican sulfur emissions and transfer of the bias in SO_2 and sulfate predictions of the REMSAD model through the boundary conditions into the CMAQ domain. The development of the final CMAQ-MADRID base case, based on the results of sensitivity simulations addressing these issues, was discussed in Chapter 2. The results from the final base case simulation are presented in this section.

4.1 Statistical Model Performance

Table 4-1 shows the performance statistics of the CMAQ-MADRID base case simulation in simulating fine particulate matter ($PM_{2.5}$) and its components as determined by comparing 24-hour average model predictions to observations of several species at K-Bar, BBNP. Sulfate and $PM_{2.5}$ mass were also measured at two other sites within BBNP: San Vicente and Persimmon Gap. The overall performance of CMAQ-MADRID at the three sites within BBNP is summarized in Table 4-2. In general, total $PM_{2.5}$ mass loadings at K-Bar, BBNP were underpredicted in the base case simulation, with an absolute mean bias of -1.7 $\mu g/m^3$; however, when normalized to observations, the model showed a positive (relative) bias of 7%. Considering all BBNP sites, the mean bias for $PM_{2.5}$ was -2.7 $\mu g/m^3$, with a positive normalized bias of 13%. This seemingly paradoxical result is due to a general tendency in the model to overpredict $PM_{2.5}$ mass at low concentrations and underpredict $PM_{2.5}$ mass at high concentrations. In turn, this tendency can be explained by the combination of the positive bias exhibited by the model in the predictions of sulfate superimposed on the negative bias in the prediction of other important constituents of aerosol mass. These other components, principally organic material (OM) and dust/crustal species, as well as elemental (black) carbon and nitrate, often constituted significant portions of the particulate mass at BBNP during events of high aerosol particle mass. Accordingly, the fractional bias is approximately zero; the fractional bias weighs the bias in individual measurements based on the average of the simulated and observed values, thus removing the tendency of the metric to approach infinity when the model overpredicts a relatively small concentration. As indicated by the coefficient of determination (r^2), the model accounts for 52% of the variance in fine sulfate mass and 23% of the variance in total fine particulate mass at K-Bar, BBNP. For three BBNP sites, the model accounted for much less of the $PM_{2.5}$ variation despite a similar r^2 value for sulfate, the main PM component. The normalized error in the predictions for all species is greater than 50% at K-Bar; however, the normalized error is species-dependent and ranges from 51% and 55% for ammonium and sulfate

to 96% for nitrate at K-Bar. The normalized error for sulfate at the three sites in BBNP is 48%; for $PM_{2.5}$, it is 96%.

Table 4-3 shows the performance statistics of CMAQ-MADRID for the entire BRAVO network for 24-hour concentrations of PM and components. Thirty-seven stations in the BRAVO network measured fine sulfate and total $PM_{2.5}$. With respect to the overall BRAVO network, the model also exhibited positive (absolute and relative) bias in its predictions of fine particulate sulfate in conjunction with a negative absolute bias and a positive normalized (relative to observation) bias in its predictions of total $PM_{2.5}$. Both organic mass and elemental (black) carbon were measured at six stations of the BRAVO network, traversing the state of Texas from west to east (K-Bar/BBNP, Langtry, Lyndon B. Johnson National Historic Park, Stephenville, Somerville Lake and Big Thicket). The model showed a small bias in BC prediction, but the lack of correlation in the predictions compared to observations suggests that the small bias may be due to compensating errors. Organic material predictions yielded a coefficient of determination of 0.61; however, when interpreted in conjunction with the negative mean bias of –1.14 $\mu g/m^3$ and the negative normalized bias of –50%, a consistent underprediction by the model of particulate organic matter concentrations across the sites is identified. (Ammonium and nitrate concentrations were measured only at BBNP.) The normalized error in the predictions of individual $PM_{2.5}$ species ranges from 51% (ammonium) to 96% (nitrate). For the BRAVO network, fractional errors are generally higher than normalized errors due to underpredictions.

Table 4-1
Statistical model performance at K-Bar, BBNP, during BRAVO [1, 2]

Statistical Metric (BIBE)	units	SO_4^{2-}	NO_3^-	NH_4^+	BC	OM	$PM_{2.5}$
Observed mean	$\mu g/m^3$	2.49	0.23	0.82	0.23	1.25	6.33
Predicted mean	$\mu g/m^3$	2.61	0.03	0.7	0.05	0.45	4.61
Coef. of determination (r^2)		0.52	0.01	0.47	0.13	0.1	0.23
Mean bias	$\mu g/m^3$	0.12	-0.19	-0.12	-0.18	-0.8	-1.72
Normalized bias		20%	-79%	7%	-76%	-59%	7%
Fractional bias		0%	-166%	-12%	-135%	-98%	-31%
Mean error	$\mu g/m^3$	1.08	0.21	0.35	0.18	0.81	3.09
Normalized error		55%	96%	51%	76%	62%	70%
Fractional error		46%	173%	48%	135%	100%	62%
Root mean square, RMS, error	$\mu g/m^3$	1.51	0.24	0.45	0.14	1.08	4.05
Valid Points		109	89	105	41	110	106

(1) A threshold of 0.1 $\mu g/m^3$ was applied for all species.

(2) CMAQ-MADRID modeling period corresponds to July 2 – October 28, 1999.

Table 4-2
Combined statistical model performance at the K-Bar, San Vincente and Persimmon Gap stations in BBNP, during BRAVO [1, 2]

Statistical Metric	units	SO_4^{2-}	$PM_{2.5}$
Observed mean	$\mu g/m^3$	2.53	6.30
Predicted mean	$\mu g/m^3$	2.66	3.66
Coef. of determination (r^2)		0.51	0.05
Mean bias	$\mu g/m^3$	0.09	-2.66
Normalized bias		13%	13%
Fractional bias		-4%	-51%
Mean error	$\mu g/m^3$	1.06	3.71
Normalized error		48%	96%
Fractional error		43%	76%
Root mean square, RMS, error	$\mu g/m^3$	1.5	4.76
Valid Points		323	147

(1) A threshold of 0.1 $\mu g/m^3$ was applied for all species.

(2) CMAQ-MADRID modeling period corresponds to July 2 – October 28, 1999.

Table 4-3
Statistical model performance over all BRAVO sites during BRAVO [1, 2]

Statistical Metric (BRAVO Network)	units	SO_4^{2-}	NO_3^{-} [3]	NH_4^{+} [3]	BC	OM	$PM_{2.5}$
Observed mean	$\mu g/m^3$	3.10	0.23	0.82	0.17	2.36	9.92
Predicted mean	$\mu g/m^3$	3.97	0.03	0.70	0.15	1.22	9.54
Coef. of determination (r^2)		0.47	0.01	0.47	0.03	0.61	0.21
Mean bias	$\mu g/m^3$	0.87	-0.19	-0.12	-0.03	-1.14	-0.39
Normalized bias		37%	-79%	7%	4%	-50%	16%
Fractional bias		8%	-166%	-12%	-34%	-78%	-15%
Mean error	$\mu g/m^3$	1.67	0.21	0.35	0.12	1.23	5.04
Normalized error		65%	96%	51%	73%	55%	65%
Fractional error		47%	173%	48%	81%	82%	56%
Root mean square, RMS, error	$\mu g/m^3$	2.65	0.24	0.45	0.2	1.55	7.06
Valid Points		3607	89	105	131	508	3169
Valid Stations		37	1	1	6	6	37

(1) A threshold of 0.1 $\mu g/m^3$ was applied for all species.

(2) CMAQ-MADRID modeling period corresponds to July 2 – October 28, 1999.

(3) The statistics (shown in grey) for ammonium and nitrate observations reflect measurement at one station (K-Bar, BBNP) and may not reflect model performance over larger regions.

4.2 Sulfur Dioxide, Fine Particulate Sulfate and Total Sulfur – BRAVO Network

Table 4-4 provides several statistical measures of model performance across the BRAVO Network as determined by comparison of 24-hour and weekly sulfur dioxide (SO_2), in addition to 24-hour sulfate and total ambient sulfur. Concentrations of SO_2 were measured at 24 of the 37 monitoring stations of the BRAVO network and these measurements, therefore, provide data for comparing to SO_2 and total sulfur concentrations.

Although 24-hour SO_2 predictions exhibited a mean bias of 0.12 $\mu g/m^3$, less than 10% of the observed mean concentration, the normalized bias was 83%. Furthermore, the mean error was nearly 1 $\mu g/m^3$ or 120% when normalized to observations. These statistics are illustrated in a scatterplot of predicted versus observed daily SO_2 in the upper plot of Figure 4-1. The blue line denoting the linear regression through the data points crosses the 1:1 line at 2 $\mu g/m^3$ (equivalent to a formation potential of 3 $\mu g/m^3$ of sulfate). Over ¾ of the data points lie in this region (i.e., over ¾ of the observations were less than 2 $\mu g/m^3$) where the model showed a tendency to overpredict SO_2 more often. Beyond this region the model was more likely to underpredict SO_2, although the model overpredicted SO_2 for one third of the data points. The bottom panel in Figure 4-1 illustrates more clearly the region with concentrations less than 8 $\mu g/m^3$ that represents the preponderance (> 98%) of data points. The scatterplot demonstrates the low correlation ($r^2 = 0.25$) between model predictions and observations. Overall, the model tended to overpredict SO_2 at typical concentrations, hence the high normalized bias. The low absolute mean bias is due to the dampening effect of the underprediction of a few episodes of high SO_2.

With the exception of a minor yield from dimethylsulfide oxidation over oceans, SO_2 is a primary (i.e., directly emitted) gas-phase compound subject to sharp local gradients in concentrations due to the effects of dilution, transport, chemical transformation, particle/droplet uptake and deposition. These conditions make it inherently difficult to compare model results and measurement data. The representation in coarse-grid simulations does not always yield values representative of the area near the monitoring site. Spatial variability and temporal variability are not equivalent, but they can be related in an idealized environment. Hence, concentrations representative of weekly averages were compared to evaluate whether the bias and error are also evident over longer time periods. Figure 4-2 shows weekly SO_2 predictions versus observations at the monitoring sites. As expected, the statistical results exhibit some improvement. However, some trends remain consistent with the 24-hour statistics; the normalized bias is 40% and the normalized error is 64% on a weekly basis. The region with weekly average concentrations of SO_2 less than 2 $\mu g/m^3$, containing ¾ of the data points, shows mainly overpredictions by the model. Beyond this region, the model is more likely to underpredict, it does so less often than for the 24-hour observations, with roughly 40% of the data points corresponding to overpredictions. Finally, weekly SO_2 concentrations are better correlated to their corresponding observations than the 24-hour predictions; the model statistically can account for approximately half of the variance in the weekly SO_2 observations.

Table 4-4
Statistical model performance for sulfur species across the BRAVO Network during BRAVO [1,2]

Statistical Metric (BRAVO Network)	Units	24-hr SO_2	Weekly SO_2	24-hr SO_4^{2-}	24-hr Total S
Observed mean	$\mu g/m^3$	1.52	1.48	3.10	1.72
Predicted mean	$\mu g/m^3$	1.64	1.61	3.97	2.05
Coef. of determination (r^2)		0.25	0.46	0.47	0.39
Mean bias	$\mu g/m^3$	0.12	0.12	0.87	0.33
Normalized bias		83%	40%	37%	38%
Fractional bias		9%	10%	8%	12%
Mean error	$\mu g/m^3$	0.99	0.60	1.67	0.83
Normalized error		120%	64%	65%	62%
Fractional error		63%	40%	47%	44%
Root mean square, RMS, error		1.73	0.97	2.65	1.29
Valid Points		2009	283	3607	2051

(1) A threshold of 0.1 $\mu g/m^3$ was applied for all species.

(2) CMAQ-MADRID modeling period corresponds to July 2 – October 28, 1999.

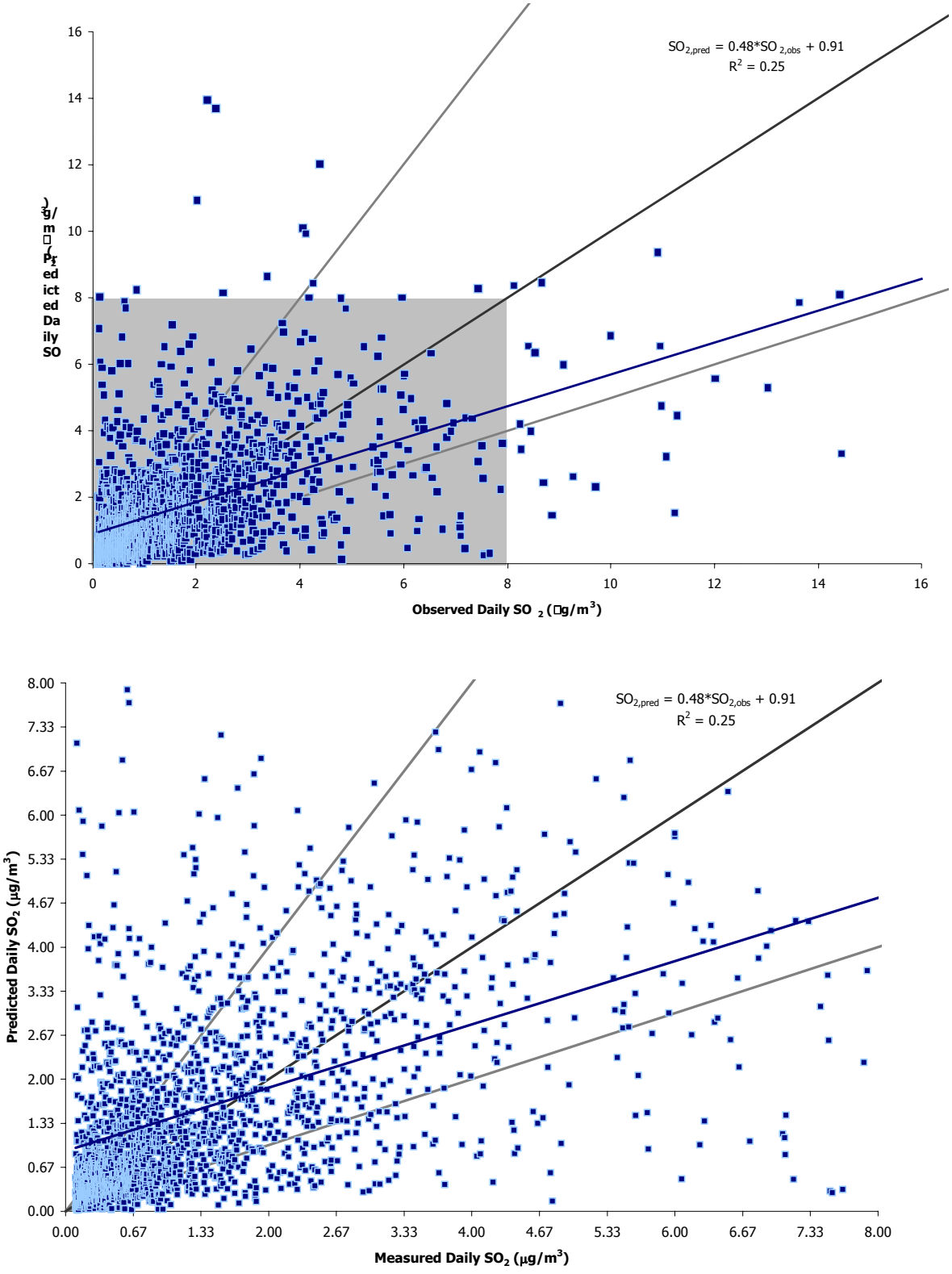

Figure 4-1
Predicted and observed 24-hr SO_2 concentrations across the BRAVO network

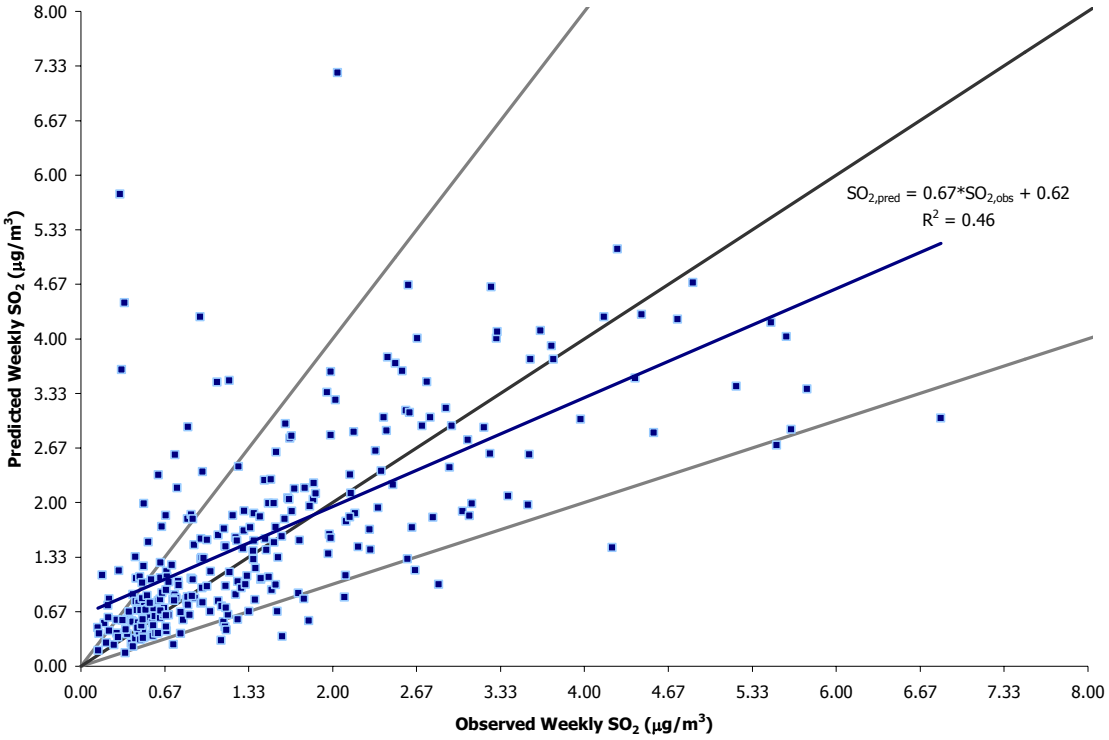

Figure 4-2
Predicted and observed weekly SO_2 concentrations across the BRAVO network.

The coefficient of determination, normalized bias and normalized error statistics of the 24-hr fine sulfate predictions are better than those of the 24-hr SO_2 predictions, with values of 0.47, 37% and 65%, respectively (see Table 4-4). Statistics of daily sulfate are expected to be better than those of daily SO_2 because sulfate has a longer lifetime and a more regional distribution than SO_2. Longer lifetime and regional distribution are characteristics that make both measurements and coarse-grid predictions more likely to represent regional ambient conditions. It is interesting to note that the coefficient of determination, normalized bias and normalized error statistics of the spatially homogeneous 24-hr fine sulfate are similar to those of the temporally (weekly) averaged SO_2. However, in the 24-hr fine particulate sulfate performance statistics, the absolute mean bias (0.87 $\mu g/m^3$, respectively) is much higher than expected merely from the 1.5 ratio of molecular weights among the species. This comparison is complicated by the fact that SO_2 and sulfate measurements were not always taken at the same sites at the same time. Even if all measurement sites can be considered representative, an exact relation between the two species is not expected due to the different loss rates (e.g., deposition velocities) between the species and regional/transient differences (e.g., oxidant fields and clouds) affecting the conversion rate of SO_2 to sulfate. Predictions of sulfate are influenced by factors other than the emissions of SO_2 within the domain and the sulfate mean bias may indicate that the net effect of these extra-domain influences is inclined towards augmenting the positive bias in the overall predictions.

In order to further explore the bias exhibited by the model in sulfate predictions, the distribution of data points comparing predictions versus observations of 24-hr fine sulfate is graphed in Figure 4-3. Although the model is generally biased towards overpredictions of fine particulate sulfate (the regression line is always above the 1:1 line), approximately 40% of the all data points in Figure 4-3 correspond to underpredictions, suggesting that wide variations in the bias could exist across the domain. The spatial distribution of the normalized bias and normalized error are analyzed by graphing their values in Figure 4-4. The normalized error is a positive number that is greater than or equal to (by definition) the normalized bias; the normalized bias decreases in value with respect to the value of the normalized error due to the presence of underpredictions in the comparison data. Thus, regions with a high normalized bias and a similarly high normalized error represent areas of consistent overpredictions. In the CMAQ-MADRID base simulations, at the eight stations that exhibited the highest bias in predicted sulfate normalized to observations (53-130%), the normalized bias represented a significant portion (on average ~80%) of the normalized error (66-159%). Of these stations, seven are located in eastern Texas (Wright Patman, Center, Big Thicket, Somerville, Everton Ranch, Lake Corpus Christi and Padre Island), showing a marked propensity of the model to overpredict sulfate in the eastern region of the domain. (The predicted signal at the other station, Eagle Pass in southern Texas near the Mexican border, is affected detrimentally by collocation of the Carbon power plant plume in the model grid cell.) In particular, significant normalized error and bias near the Gulf coast call into question the representation of cloud, where sulfate-processing takes place, in the region. On the other hand, eleven stations where the normalized bias represented a lesser portion (on average ~30%) of the normalized error (33-78%) are located in the vicinity of BBNP and/or near the U.S.-Mexico border (Guadalupe Mountains, Monahans Sandhills, McDonald, Esperanza, Marathon, Persimmon Gap, Langtry, Big Bend/K-Bar, San Vicente/Rio Grande, Brackettville and Laguna Atascosa), showing a tendency of the model to underpredict more often in these regions compared to other regions of the domain. (A twelfth station at Wichita Mountains that shares the same characteristics with respect to normalized error and bias yielded only 36 data points, which corresponded to less than 30% data capture, and was excluded from the analysis.) These stations also displayed the lowest bias in predicted sulfate normalized to observation (5-24%) due to the counteracting effect of underpredictions and overpredictions in the time series.

Table 4-4 also provides performance statistics for total sulfur predictions compared to observations. The data points used in the analysis are graphed in Figure 4-5. Total sulfur in the context of this study is defined as the sum of one-half of the mass of gas-phase SO_2 and one-third of the mass of fine particulate sulfate. The statistics for total sulfur are various hybrids of the statistics for the two individual components. The blue line denoting the linear regression through the data points in Figure 4-5 crosses the 1:1 line at 3 $\mu g/m^3$ of sulfur (equivalent to a potential concentration of 9 $\mu g/m^3$ of sulfate). In the region with 24-hr average total concentrations less than 3 $\mu g/m^3$, representing ~85% of data points, the model tends to overpredict approximately two-thirds of all observations. Beyond this region, where the model is more likely to underpredict sulfur concentrations, roughly 40% of the data points correspond to overpredictions.

For the duration of the BRAVO period and across the entire BRAVO network, particulate sulfate accounted for 62% of the observed total sulfur concentrations, comparable to a sulfate fraction of 61% for the predicted total. However, as shown in Figure 4-6 when comparing predicted sulfate fractions versus observed sulfate fractions on a 24-hr basis, the model rarely predicts the accurate sulfate fraction although the results show relatively low bias (a linear regression fit with the intercept forced through the origin yields an r^2 value of 0.09 but a slope of 0.93). The standard deviations of predictions and observations are similar at ~20% and ¾ of the predicted sulfate fraction data points in Figure 4-6 lie within ±20% of the observed value. The bottom plot of Figure 4-6 shows the predicted and observed sulfate fractions as a function of the corresponding sulfate concentrations. Both data sets display a similar trend showing an increasing likelihood of high sulfate fractions as the sulfate concentration increases. The above analysis suggests that the deterioration in model performance is likely attributable to factors such as emissions of SO_2 and primary sulfate, meteorology (clouds, winds), deposition/settling, and emissions and photochemistry leading to the formation of the requisite oxidant fields (i.e., OH, H_2O_2, O_3 concentrations), than to the model formulation for SO_2 oxidation: the chemical mechanisms for SO_2 oxidation – primarily gas-phase oxidation by the hydroxyl radical, aqueous-phase oxidation by hydrogen peroxide and ozone, and aqueous-phase oxidation by O_2 catalyzed by metals – and their rate constants are well known and properly represented in the model.

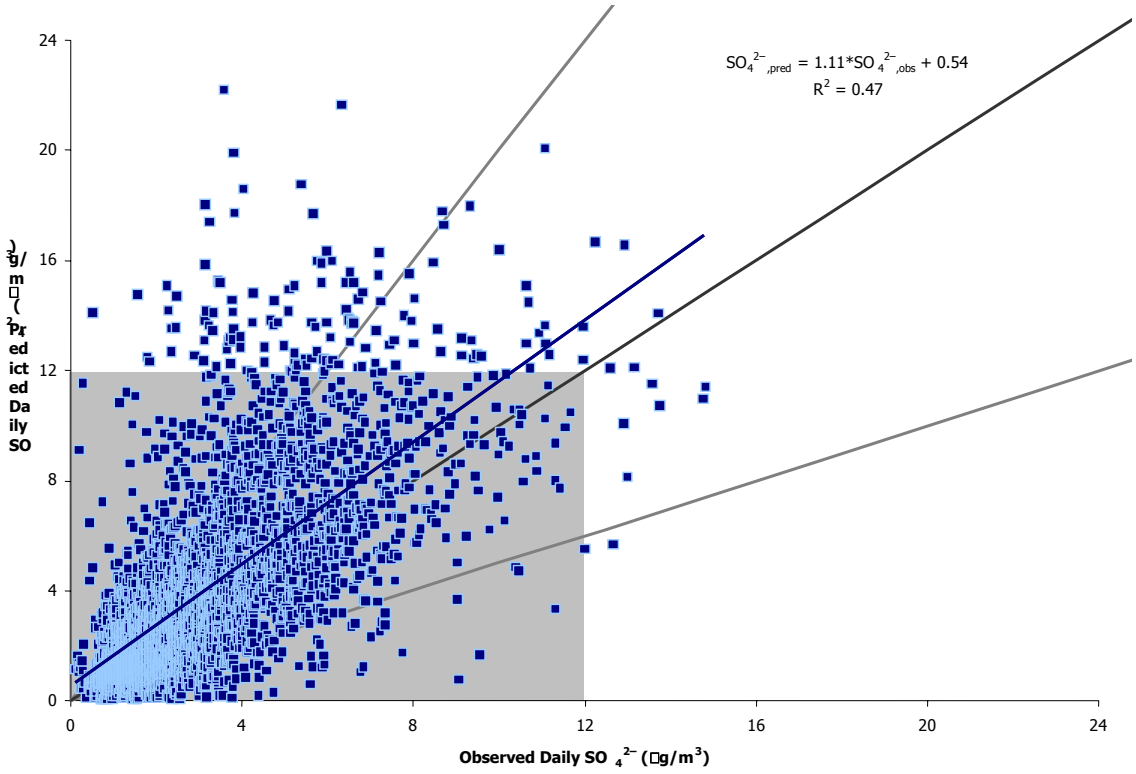
$SO_4^{2-}_{,pred}$ = 1.11*$SO_4^{2-}_{,obs}$ + 0.54
R^2 = 0.47
Predicted Daily SO_4^{2-} (µg/m³)
Observed Daily SO_4^{2-} (µg/m³)
0
4
8
12
16
20
24

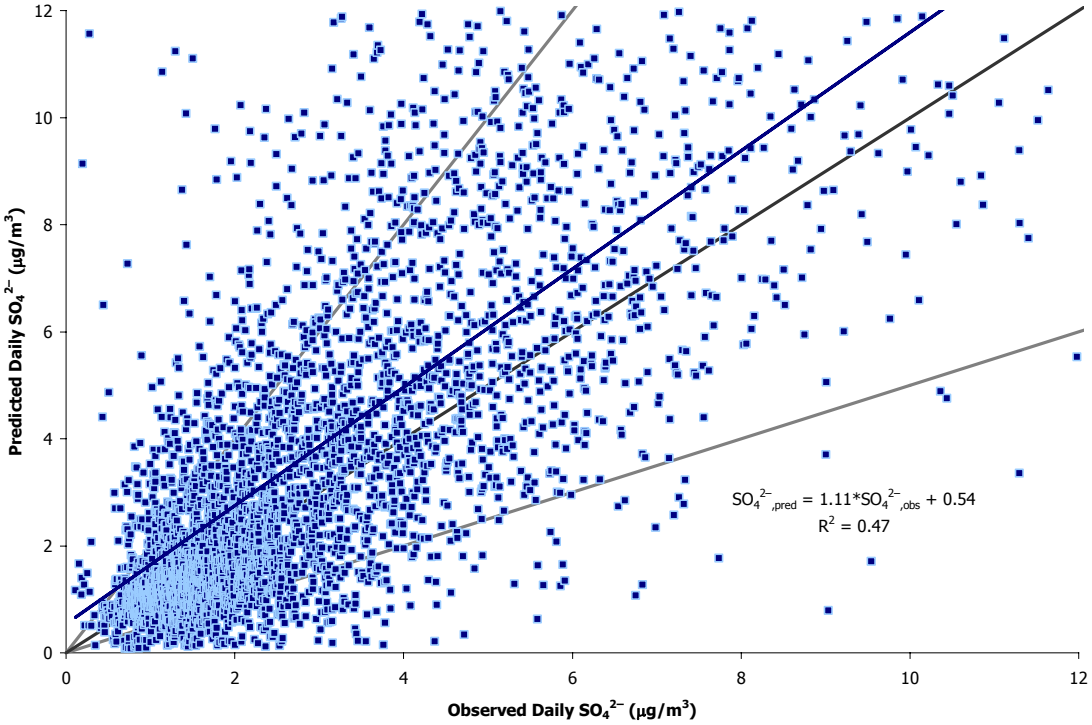
$SO_4^{2-}_{,pred}$ = 1.11*$SO_4^{2-}_{,obs}$ + 0.54
R^2 = 0.47
Predicted Daily SO_4^{2-} (µg/m³)
Observed Daily SO_4^{2-} (µg/m³)
0
2
4
6
8
10
12

Figure 4-3
Predicted and observed 24-hr fine sulfate concentrations across the BRAVO network.

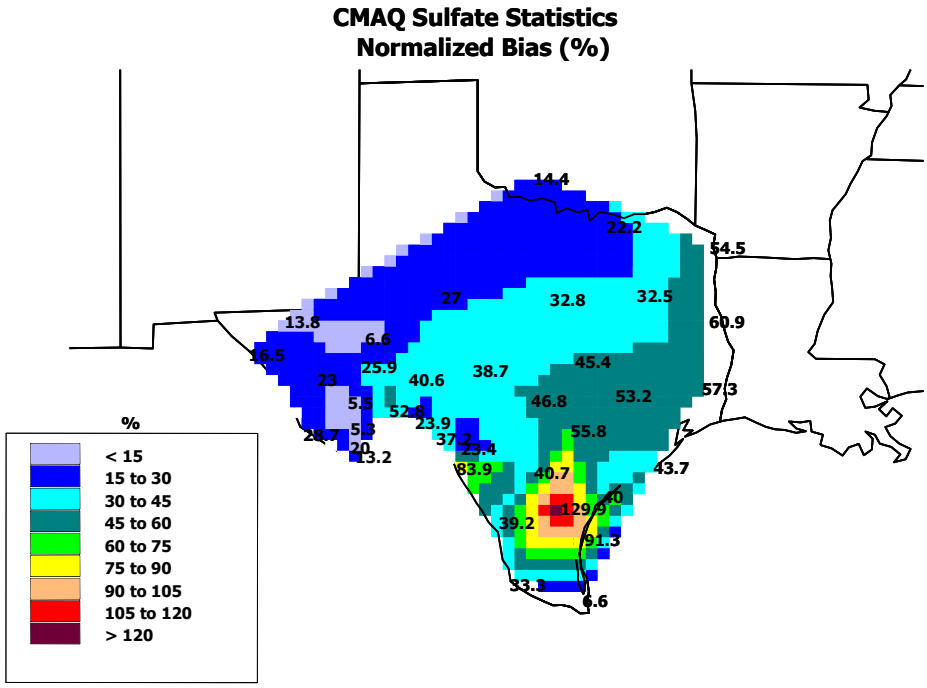

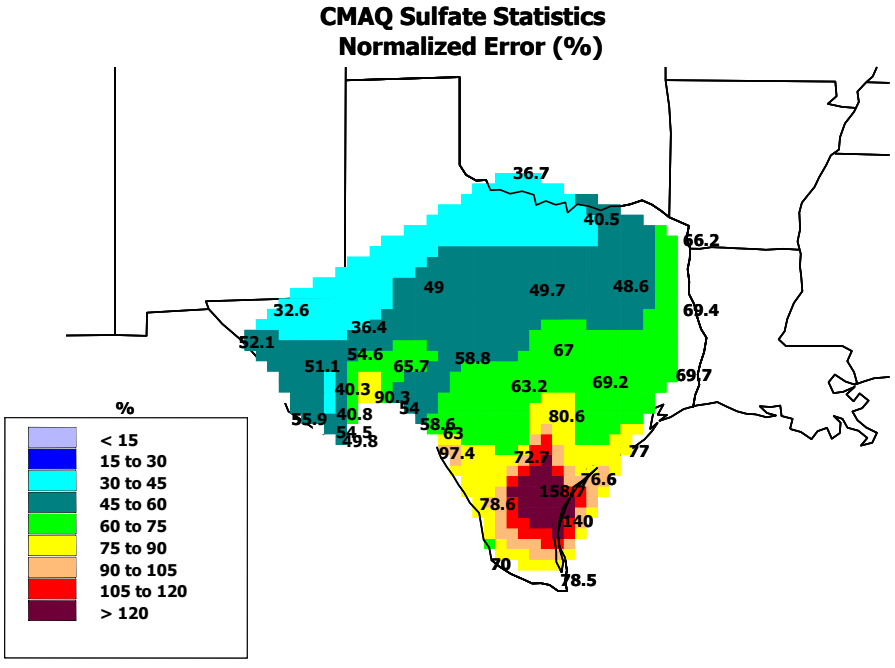

Figure 4-4
Spatial distribution of normalized bias and normalized error in CMAQ-MADRID predictions of fine sulfate across the BRAVO Network.

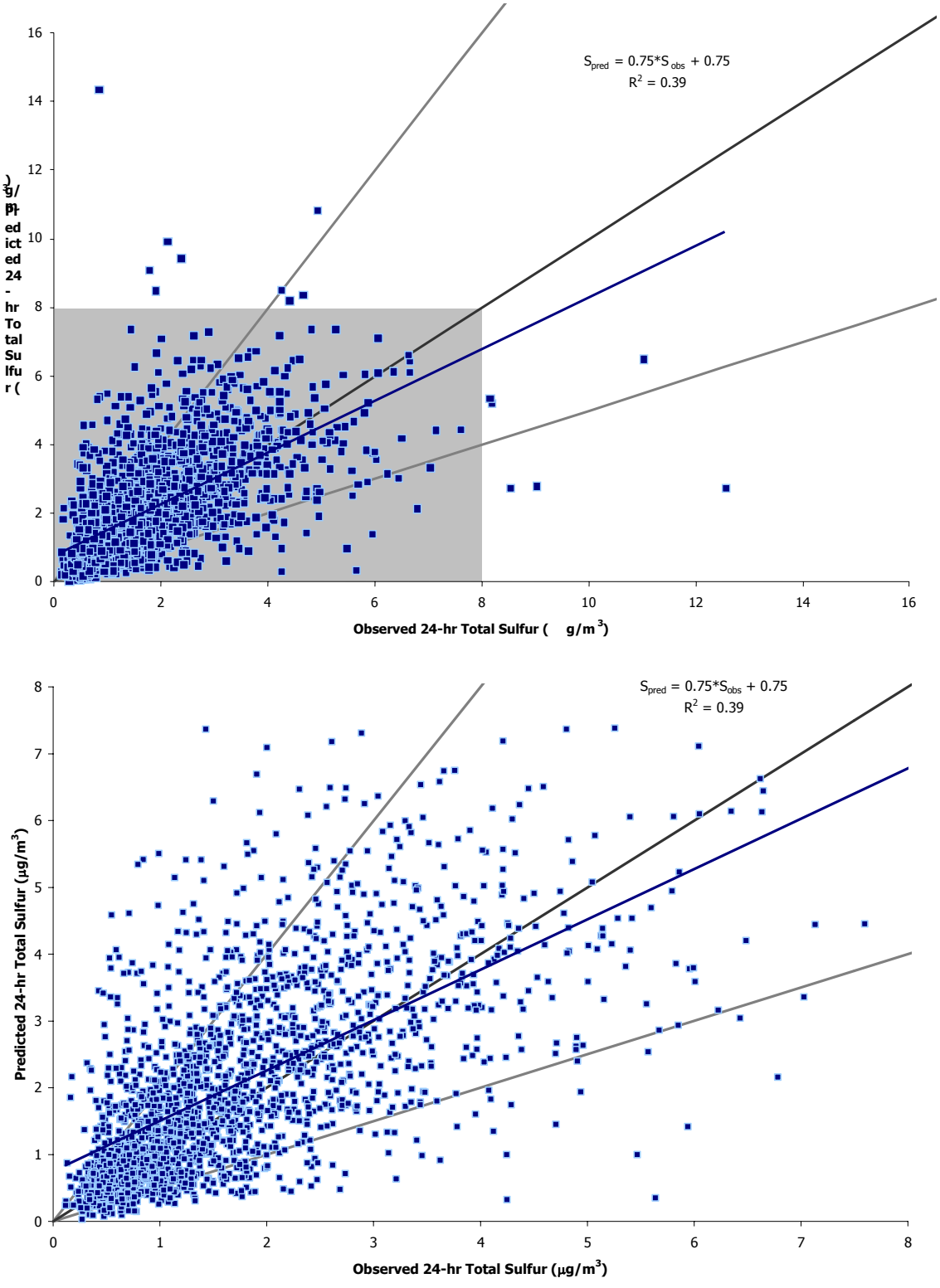

Figure 4-5
Predicted and observed 24-hr total sulfur concentrations across the BRAVO network.

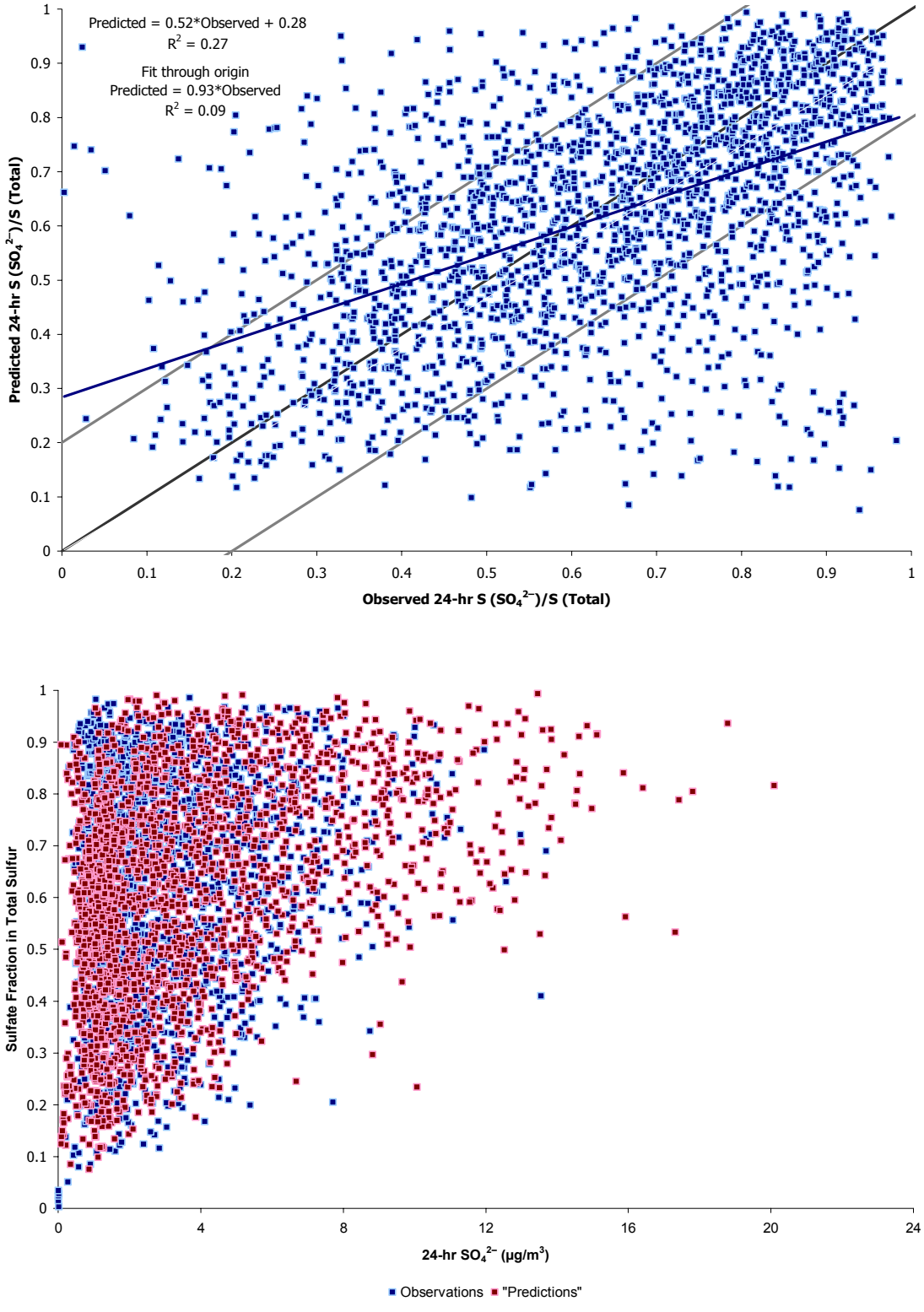

Figure 4-6
Predicted and observed sulfate fraction of total sulfur concentrations (top) and sulfate fraction as a function of 24-hr sulfate concentrations (bottom) across the BRAVO network.

4.3 Sulfur Dioxide, Fine Particulate Sulfate and Total Sulfur at K-Bar, BBNP and Big Thicket

Performance statistics for the BRAVO network with respect to sulfur species provide an overview of the model's capacity to describe the temporal and spatial distribution of the species. This section presents a more focused analysis of the model's ability to capture the daily variations of these species at specific stations, in particular the K-Bar, BBNP and Big Thicket stations. As described above, the K-Bar station in BBNP, apart from being the focal station of the study, is representative of the region where the model was more likely to occasionally underpredict concentrations of sulfur species. The Big Thicket station is representative of the eastern portion of the domain, where the model showed high positive bias in simulated concentrations of sulfur species due to consistent overpredictions in the region.

K-Bar. Table 4-5 shows performance statistics comparing model predictions to observations for 24-hr and weekly SO_2, 24-hour fine particulate sulfate, and 24-hr and weekly total sulfur at the K-Bar site. As illustrated in Figure 4-7, the model does not capture well the evolution of SO_2 concentrations at K-Bar, BBNP, as reflected by the low coefficient of determination ($r^2 = 0.03$, i.e. the model cannot account for essentially any of the variance in SO_2 concentrations at K-Bar, BBNP). The model fails to capture the two principal peak SO_2 events (underpredicting for August 20-24 and September 3-4), and predicts only one of the three lesser peak SO_2 events (matching for August 16-17 but underpredicting for September 13-14 and October 23). The model also predicts five sharp SO_2 peaks that were not observed – one abrupt spike on September 16 and other overpredictions on August 28-30, September 8, October 2 and October 13-14. With the exception of peak events, concentrations of SO_2 at K-Bar, BBNP were relatively low. Therefore, underpredictions occurred during events of unusually high concentrations, whereas overpredictions occurred over periods of typically low concentrations. Thus, the absolute mean bias in SO_2 predictions was low (–0.04 $\mu g/m^3$), and the normalized bias yielded a value of +85%, driven by overpredictions when the observed concentrations were low. Performance statistics for weekly SO_2 showed improvement due to the averaging of overpredictions and underpredictions. The failure to capture SO_2 peaks accurately is unlikely to be due to temporal shifts, as most of the peaks and valleys are separated by multiple days and the concentrations of a previously or subsequently predicted event are not commensurate with the failed predictions.

Fine particulate sulfate concentrations at K-Bar, BBNP are predicted by the model with a lower bias and normalized error than obtained for SO_2. The model can explain more than half of the variance in fine sulfate observations (i.e., $r^2=0.52$ – nearly double the value of the coefficient of determination for weekly SO_2). However, the model fails to accurately capture events of peak sulfate concentration. In order to address the trends observed, the time series can be divided into four stages.

The first stage begins after the first week of observations, during which there are indications that the measurements may have been faulty. During this segment from July 12 to August 27, the model regularly underpredicted (33 of the 43 days with reliable data) fine sulfate concentrations. The normalized bias during the 33 days when the model underpredicted fine sulfate is –46% compared to a normalized bias of 19% for the ten days in the stage for which the model

overpredicted fine sulfate. The model captures two individual daily peaks observed during August 3-4 and August 16-17, but fails to capture the peak sulfate concentrations observed during July 26-28, August 1-2, August 5-9 and August 20-23.

The second stage is observed from August 28 to September 19, when the model overpredicted fine particulate sulfate on 19 of the 23 days. The normalized bias in this period during the 19 days when the model overpredicted sulfate is 76% compared to a normalized bias of –16% for the four days when the model underpredicted sulfate. During this segment, the model prematurely predicted the peak period observed during August 28 to September 4, resulting in an overestimation by a factor of 2 or more during the four days in August and an underestimation by a factor of 2 on September 4. The model also predicted a smaller peak on September 8 that was not observed at the K-Bar, BBNP site. Finally, the model overpredicted sulfate during the peak segment from September 13 to September 19 with a normalized bias of 23%.

Table 4-5
Statistical model performance for sulfur species at K-Bar, BBNP, during the BRAVO study[1, 2]

Statistical Metric (BIBE)	Units	24-hr SO_2	Weekly SO_2	24-hr SO_4^{2-}	24-hr Total S	Weekly Total S
Observed mean	$\mu g/m^3$	0.88	0.87	2.49	1.25	1.30
Predicted mean	$\mu g/m^3$	0.85	0.87	2.61	1.33	1.41
Coef of determination (r^2)		0.03	0.29	0.52	0.30	0.38
Mean bias	$\mu g/m^3$	-0.04	-0.01	0.12	0.08	0.11
Normalized bias		85%	16%	20%	34%	9%
Fractional bias		0%	5%	0%	8%	4%
Mean error	$\mu g/m^3$	0.72	0.33	1.08	0.64	0.39
Normalized error		134%	42%	55%	64%	28%
Fractional error		72%	38%	46%	48%	27%
Root mean square, RMS, error	$\mu g/m^3$	1.24	0.46	1.51	0.95	0.50
Valid Points		86	12	109	91	12

(1) A threshold of 0.1 $\mu g/m^3$ was applied for all species.

(2) CMAQ-MADRID modeling period corresponds to July 2 – October 28, 1999.

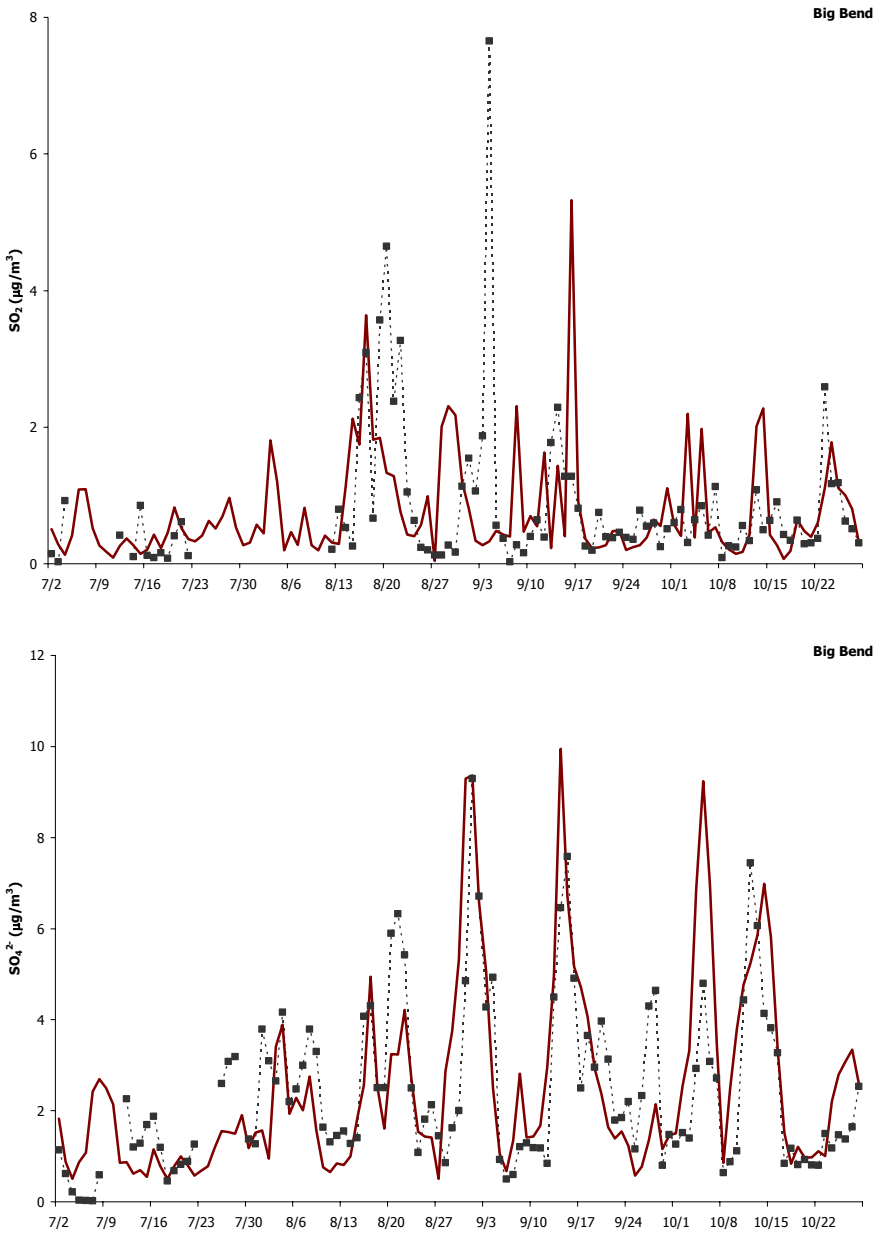

Figure 4-7
Time series of SO_2 (top) and fine sulfate concentrations (bottom) at K-Bar, BBNP.

The third stage is observed during September 20-30. During this segment, the model underestimated fine sulfate at K-Bar, BBNP for ten of the eleven days, resulting in an overall normalized bias of –33% for the time period. For the first two days at the onset of this stage, the model failed to capture what was either a tertiary peak of the final segment of the second stage or a separate and distinct sulfate peak event with a normalized bias of –44% compared to observations. The peak particulate sulfate concentrations observed during September 26-28 were underestimated by the model with a normalized bias of –63%, i.e., approximately a factor of 2.5. The final 10 days of September are analyzed further in the source region attribution section of Chapter 5.

The final stage encompasses the remaining days simulated by CMAQ-MADRID (October 1-28). During this period, the model overpredicted on 24 of the 28 days, with a corresponding normalized bias of 75% compared to observations. On the 4 remaining days, the model exhibited a normalized bias of –24%. Two distinct peak sulfate segments were observed during the segment, with a final peak event forming near the end of the simulation. The first peak sulfate event, during October 4-7, was greatly overpredicted by the model. During October 2-7, the model overpredicted sulfate at K-Bar, BBNP on average by a factor of 2, including an overestimation of the peak sulfate observed on October 5 by nearly a factor of two (an observation of 4.80 $\mu g/m^3$ vs. a prediction of 9.24 $\mu g/m^3$). For the second peak sulfate event, the observations and predictions during October 11-16 are skewed in time with respect to one another: overprediction on October 9-10, followed by underprediction on October 12 and overprediction on October 14-15. The overall sulfate load during the period of October 9-16 was overpredicted by 23% (with a normalized bias of 65%). Finally, in the time interval during October 24-27, the model predicted a peak sulfate event not present in the observations, resulting in overpredictions equal to double the value of sulfate concentrations observed during these days.

A final analysis of the CMAQ-MADRID model performance comprises a comparison of the observations and simulation results for total sulfur – gas-phase SO_2 and fine particulate sulfate – at K-Bar, BBNP. The top portion of Figure 4-8 shows valid observations of total sulfur concentrations at K-Bar and predicted values corresponding to those same dates. While the observations and simulations share several common features of sulfur peaks, the figure also depicts several periods of underestimation and overestimation. Several small and large peaks were either underpredicted or missed by the model, e.g., middle of July, August 19-22, September 4 (this is the most significant "miss", where 5.47 $\mu g/m^3$ S was observed vs. 1.00 $\mu g/m^3$ S predicted), and September 20-28. For several other peaks, early accumulation of sulfur caused significant overpredictions prior to peaks, e.g., August 15, August 28-31, and October 9-10. Sulfur peaks were predicted but not observed in the measurements on September 8 (2.09 $\mu g/m^3$ S predicted vs. 0.54 $\mu g/m^3$ S observed) and October 24-27. The model overpredicted by over a factor of 2 the total sulfur peak event from October 3-6. For other sulfate events, the model predicted the magnitude of total sulfur reasonably well but not the time evolution of peaks (e.g., September 11 to September 16, October 8 to October 15).

Inspection of the top portion of Figure 4-8 prompted further analysis of weekly total sulfur model trends in order to ascertain the influence of minor temporal shifts in the predictions compared to observations and to account for the same influences discussed earlier during the analysis of weekly SO_2 trends. Table 4-5 shows statistics for weekly total sulfur concentrations at K-Bar, BBNP. The bottom portion of Figure 4-8 illustrates the twelve weeks for which observational data could be computed. Of the twelve weeks, four weeks displayed weekly predicted total sulfur values within ±10% of the observations. For the remaining time period, the model underpredicted total sulfur concentrations for three weeks (by factors of 1.7, 1.4 and 1.6) and overpredicted total sulfur concentrations for five weeks (by factors of 1.5, 1.3, 1.8, 1.3 and 1.3). Overall, the low bias shown for weekly total sulfur concentrations is due to the offsetting effect that underpredictions have on the overpredictions and the lower error is due to the averaging over longer periods of time thus dampening the effect of "outlying" data points present on a finer temporal scale.

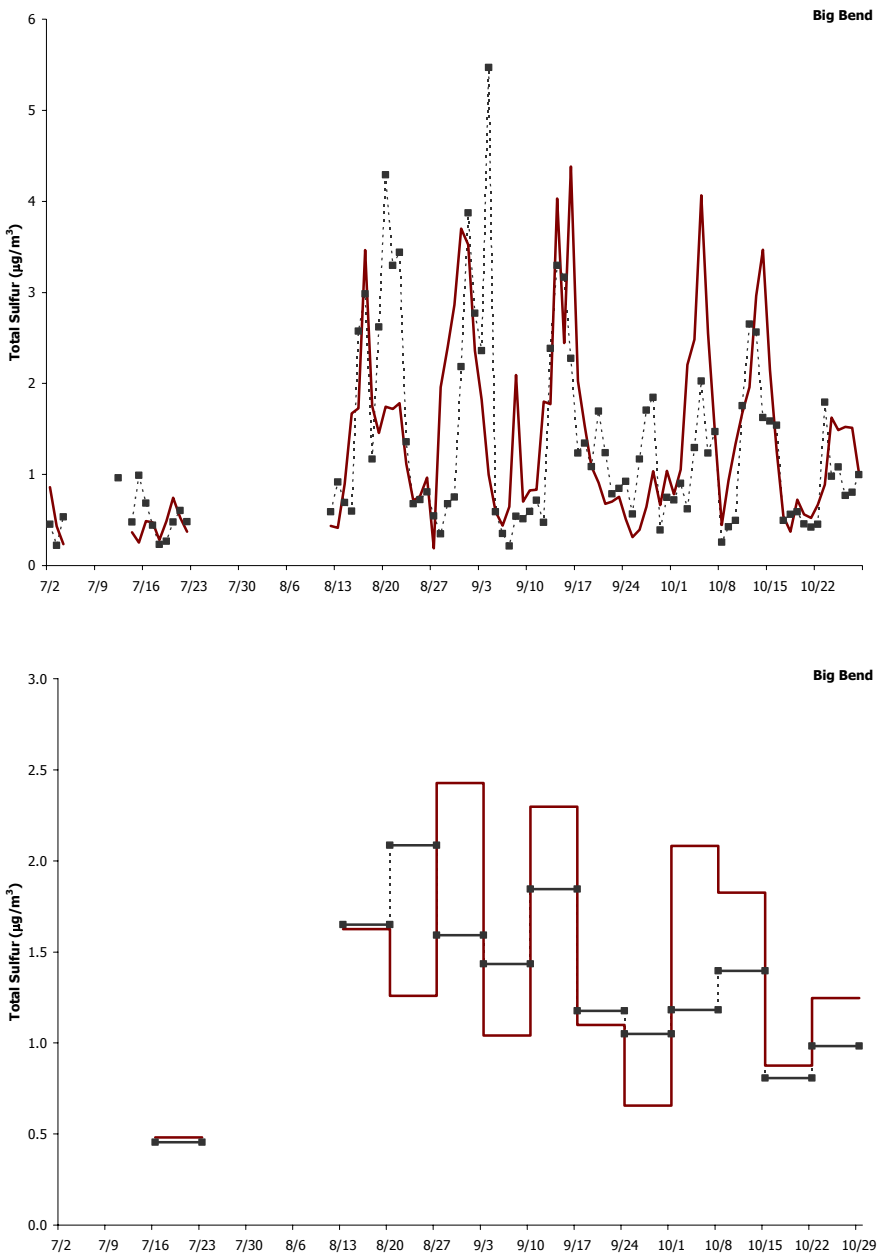

Figure 4-8
Time series of 24-hr (top) and weekly (bottom) total sulfur concentrations at K-Bar, BBNP.

Big Thicket. As discussed above, the model exhibited a propensity for overpredicting fine particulate sulfate concentrations over the eastern region of the domain. Performance statistics for the Big Thicket station, a station representative of the region and where valid measurements of both ambient SO_2 and fine sulfate concentrations are available, are listed in Table 4-6 for 24-hr and weekly SO_2, 24-hour fine particulate sulfate, and 24-hr and weekly total sulfur. For all species and timescales of comparison, the normalized bias corresponds to a large (80-100%) portion of the normalized error, indicating that there were few, if any, events of underpredictions. Following is a brief discussion of the individual statistics.

In Figure 4-9 (top panel), 24-hour SO_2 predictions are plotted alongside concentrations measured at Big Thicket. The model overpredicted on 64 of the 75 days with valid observations for comparison. In particular, the model predicted "large" SO_2 overprediction spikes (a "large" SO_2 overprediction is defined as a prediction > 2.66 $\mu g/m^3$, equivalent to the potential for forming 4 $\mu g/m^3$ of sulfate, that is also greater than twice the observed value) on August 16 and 22; September 10-11, 14, 16, 23, 27; and October 1-2, 5, 14-15, 19, 21-22, and 25-28. Elevated SO_2 concentrations were predicted in early and mid July; however, observational data were not available until August 6. Overall, the model predictions exhibit a normalized bias of +239% compared to observations, equivalent to an average overprediction factor (normalized to observations) of 3.4.

As expected based on the discussion on the difficulties of reproducing daily SO_2 trends, the model did not adequately reproduce daily fluctuations in SO_2 concentrations at Big Thicket, as determined by the low coefficient of determination (r^2=0.28). However, model performance improved substantially when evaluating SO_2 concentrations on a weekly basis, with the r-squared value increasing to 0.65. Weekly SO_2 concentrations were overpredicted for all but one of the 10 weeks with valid data. In summary, the normalized bias of weekly SO_2 predictions is 149%, equivalent to an average overprediction factor (normalized to observations) of 2.5. This value is commensurate with the ratio of 24-hr and weekly SO_2 predicted mean concentrations versus observed mean concentrations. The higher value of the coefficient of determination implies that the model captures weekly fluctuations in SO_2 concentrations (accounting for approximately two-thirds of the variance), and thereby overpredicts SO_2 concentrations in a consistent fashion.

The lower portion of Figure 4-9 shows 24-hour fine particulate sulfate predictions at Big Thicket. The model overestimated the daily sulfate load at Big Thicket on 64 of the 88 days with valid measurement data for comparison. In particular, the model predicted "large" fine sulfate overprediction spikes (a "large" fine particulate sulfate overprediction is defined as a prediction > 4.00 $\mu g/m^3$ that is also 50% greater than the observed value) on July 24-30; August 5, 9, 15-16, 18, 21-22, 27, and 30-31; September 11-13, and 19; October 1-6, 10-12, 14-18, and 26-28. Overall, fine particulate sulfate concentrations were predicted with a normalized bias of 57%; similarly, the ratio of mean predicted sulfate concentrations to the mean observed sulfate concentrations is equal to ~1.5. The bias in the prediction in combination with the high coefficient of determination (r^2=0.63) indicates that the model is able to capture the daily fluctuation in fine particulate sulfate concentrations but regularly overpredicts their values by approximately 50%.

Table 4-6
Statistical model performance for sulfur species at Big Thicket during BRAVO [1, 2]

Statistical Metric (BGTH)	units	24-hr SO_2	Weekly SO_2	24-hr SO_4^{2-}	24-hr Total S	Weekly Total S
Observed mean	$\mu g/m^3$	1.03	1.04	4.18	1.91	1.94
Predicted mean	$\mu g/m^3$	2.56	2.62	6.44	3.40	3.48
Coef of determination (r^2)		0.28	0.65	0.63	0.43	0.16
Mean bias	$\mu g/m^3$	1.53	1.58	2.26	1.48	1.54
Normalized bias		239%	149%	57%	95%	81%
Fractional bias		63%	73%	32%	50%	53%
Mean error	$\mu g/m^3$	1.73	1.63	2.67	1.60	1.54
Normalized error		255%	154%	70%	101%	81%
Fractional error		88%	79%	47%	58%	53%
Root mean square, RMS, error	$\mu g/m^3$	2.66	2.12	3.66	2.23	1.86
Valid Points		75	10	88	77	10

(1) A statistical threshold of 0.1 $\mu g/m^3$ was applied for all species.

(2) CMAQ-MADRID modeling period corresponds to July 2 – October 28, 1999.

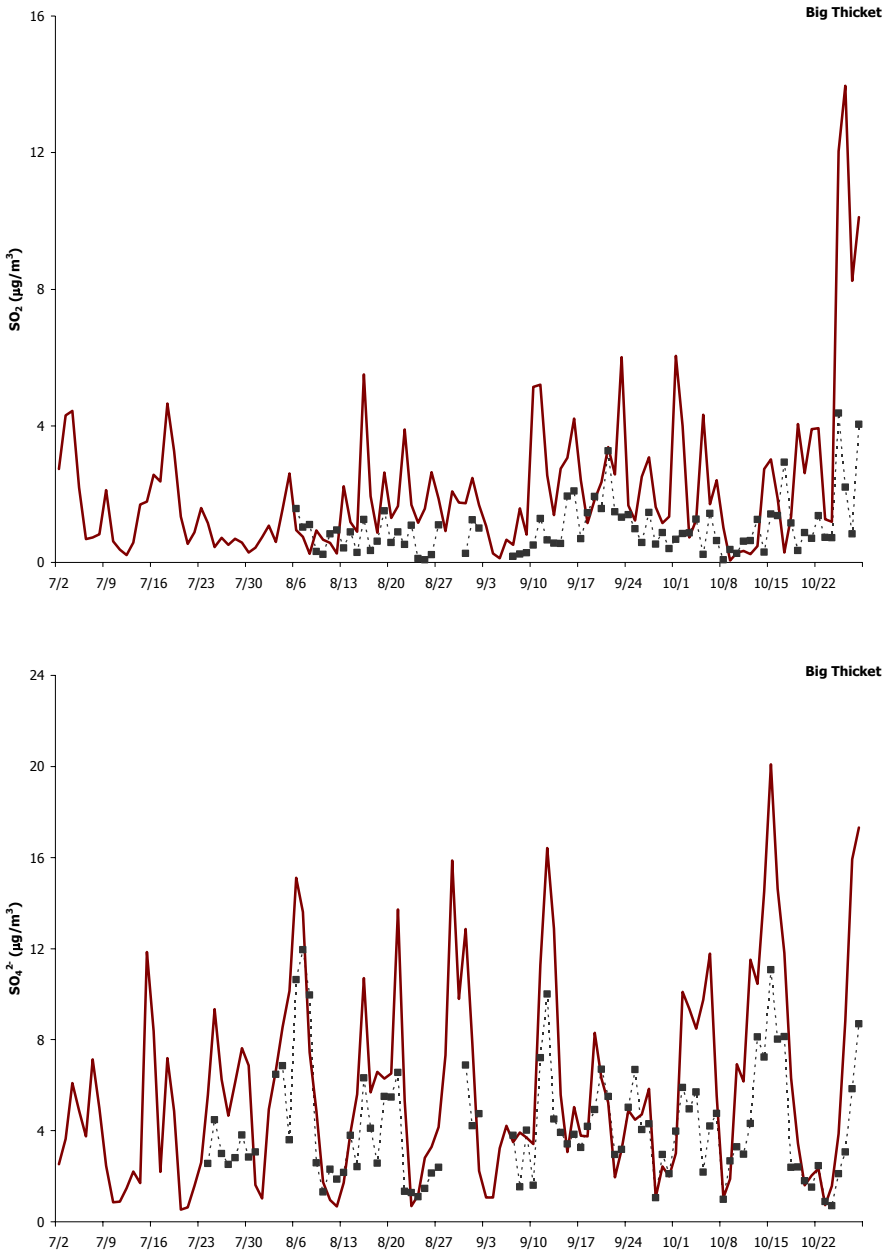

Figure 4-9
Time series of SO_2 (top) and fine sulfate concentrations (bottom) at Big Thicket.

Figure 4-10 shows 24-hr and weekly total sulfur predictions. As expected, the coefficient of determination for 24-hr total concentrations lies between that of 24-hr SO_2 and 24-hr fine sulfate concentrations. Nonetheless, the model regularly overpredicted daily total sulfur concentrations by approximately a factor of two. Fine sulfate contributed on average to 73% of the daily total sulfur observed at Big Thicket, whereas, in accordance with the higher degree of SO_2 overpredictions, fine sulfate constitutes on average ~61% of the daily total sulfur observed at Big Thicket. When compared on a weekly timescale, the correlation between total sulfur predictions and observations deteriorates. Whereas total sulfur fluctuations were fairly well captured by the model, albeit with regular overestimations of twice the observed value, the model failed to represent the lower and more consistent longer-term average concentrations. On a weekly basis, the total sulfur concentrations observed at Big Thicket ranged from 1.2 to 2.4 $\mu g/m^3$ S, with a mean concentration of approximately 2 $\mu g/m^3$ S and coefficient of variation (standard deviation/mean) of 0.20; in contrast, predicted total sulfur concentrations for Big Thicket ranged from 2.1 to 6.0 $\mu g/m^3$ S, with a mean concentration of approximately 3.5 $\mu g/m^3$ S and a coefficient of variation (standard deviation/mean) of 0.35. Overall, total sulfur concentrations were predicted with a normalized bias of 81%; similarly, the ratio of mean predicted total sulfur concentrations to the mean observed total sulfur concentrations is equal to ~1.8.

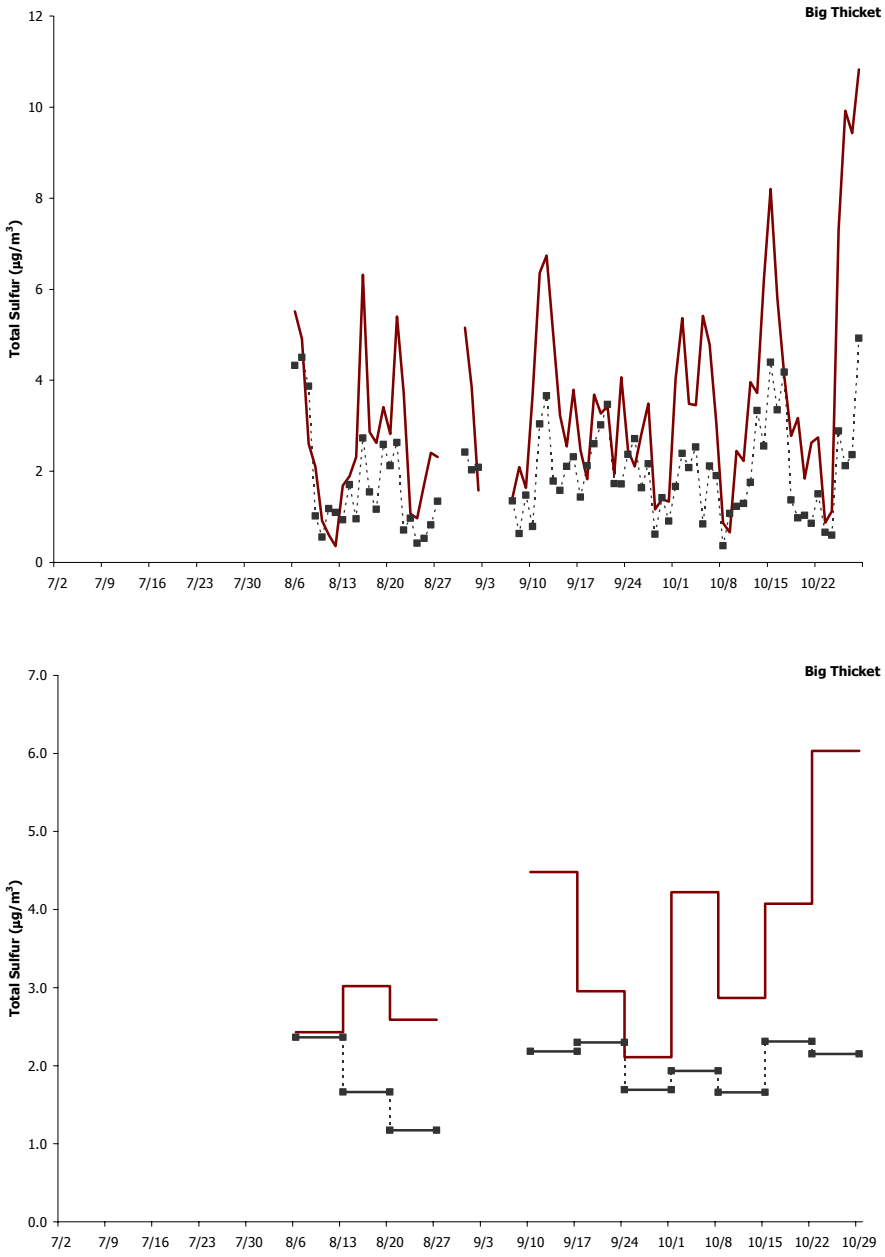

Figure 4-10
Time series of 24-hr (top) and weekly (bottom) total sulfur concentrations at Big Thicket.

4.4 Organic Material

As the second most prominent component of $PM_{2.5}$ in BBNP and across the BRAVO network from July to October, 1999, organic material warrants specific analysis. As shown in Table 4-3, CMAQ-MADRID has a general tendency to underestimate organic particulate matter. At all six sites where organic carbon measurements were taken, organic material, calculated as 1.4 × measured organic carbon, was underpredicted by the model (Figure 4-11) on a four-month basis. Turpin and Lim (2001) suggest that 1.4 may be a lower limit for the conversion factor from OC to OM in remote areas, where the fraction of highly oxidized secondary organic compounds is higher than in urban/suburban locations. Selection of a higher value for the OC-to-OM conversion factor, as suggested by the study, would result in an inherent negative bias in model predictions for BRAVO.

Figure 4-11 also shows that despite the difference in predicted concentrations of OM, the relative fractions of primary and secondary OM were fairly consistent at different sites. Primary OM accounted for 23 to 41% of OM at all sites. At BBNP, primary OM accounted for 25% of the predicted OM, consistent with its remote location. Of the secondary OM, biogenic secondary organic aerosol (SOA) dominated over anthropogenic SOA at all sites. The fraction of biogenic SOA ranged from 47 to 67% of the total predicted OM. Whereas anthropogenic SOA accounted for only 10 to 12% of the total predicted OM at all sites.

Figure 4-12 contrasts the OM time series at Big Thicket and K-Bar, BBNP. The average fractions of primary organic compounds, anthropogenic SOA, and biogenic SOA represent quite well the daily fractions of these components. An interesting observation is that while the underprediction of OM is consistent throughout August, September, and October in Big Thicket (only a few measurements were available in July at Big Thicket), the time series at K-Bar, BBNP indicates large underpredictions in July, August, and September, and smaller underpredictions in October. The difference in temporal patterns in the model performance may be indicative of different sources of uncertainties at these two locations. Big Thicket may be downwind of a source area or a source type of primary PM organic matter that is consistently under-represented. Alternatively, Big Thicket may be affected by a source or source area of VOC, whose conversion to SOA is underpredicted. BBNP, on the other hand, may be affected by an source area or source type that contributed to the observed OM in July through September, which may be severely under-represented in the emission inventories. One such possibility is biomass burning in Mexico. BBNP seemed to receive a higher OM load from a different source area or source type during the fall season that may be better represented in the inventories used as inputs to the models.

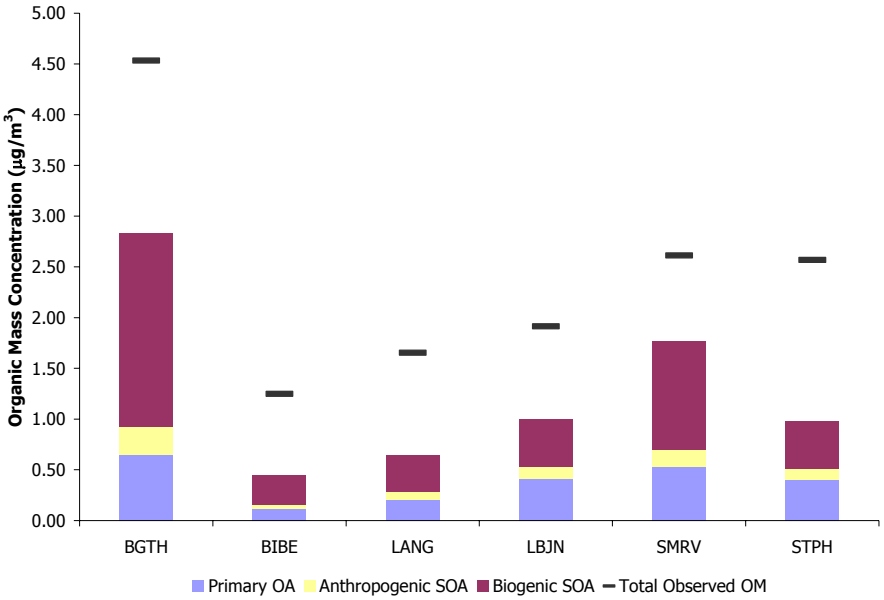

Figure 4-11
Composition of predicted $PM_{2.5}$ organic material at 6 sites averaged over the duration of BRAVO .

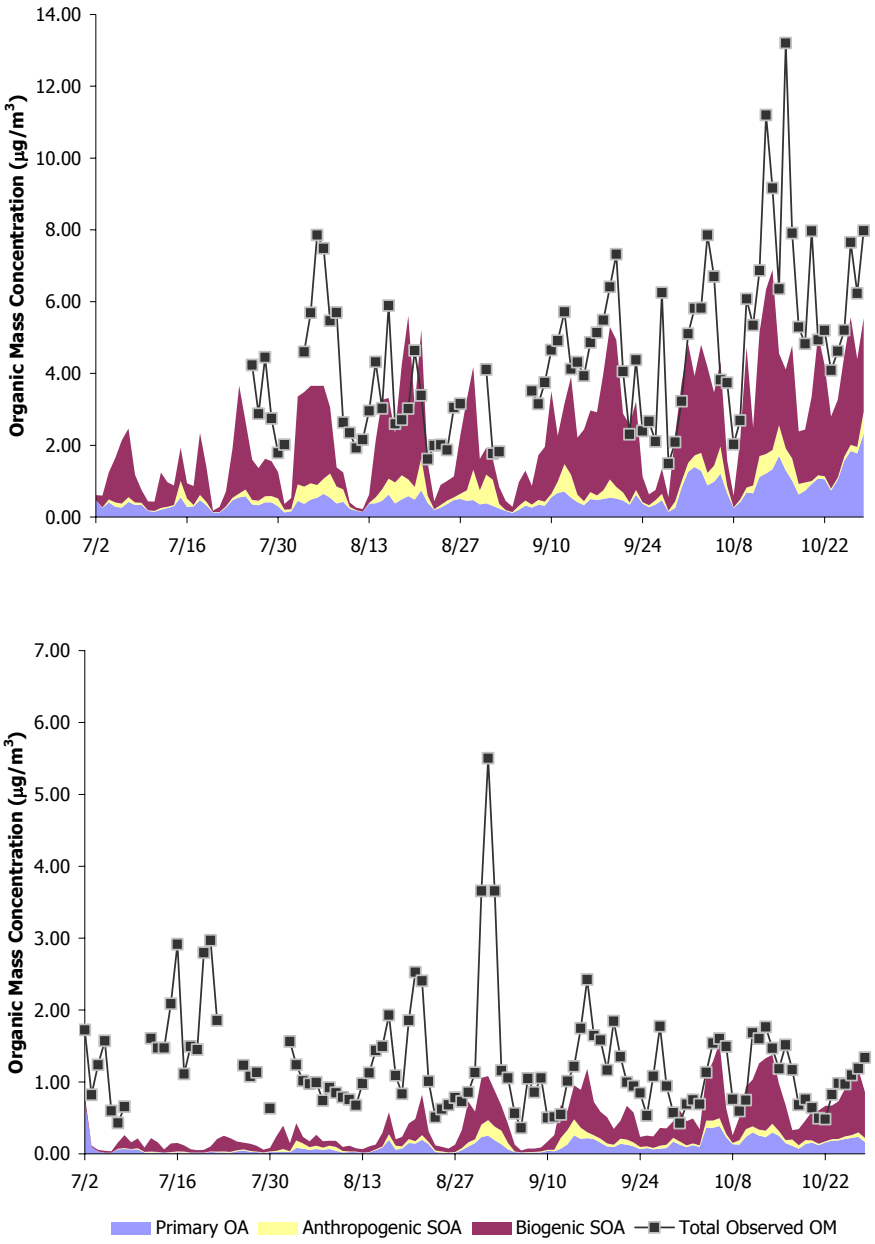

Figure 4-12
Time series of organic material at Big Thicket (top) and K-Bar, BBNP (bottom).

4.5 Particulate Matter Components and Total Mass

This section completes the evaluation of model performance for predicting fine particulate matter by analyzing the ability of the model to reproduce daily variations of the components of $PM_{2.5}$ other than sulfate, as well as the total $PM_{2.5}$ mass, measured by the BRAVO network. The five major *identified* components of fine particulate matter – ammonium, black carbon, nitrate, organic material and sulfate – and total $PM_{2.5}$ were only measured at the K-Bar station. In addition to the five major components and total mass, an "other" category composed of all other unidentified species will form the basis of the ensuing discussion of model performance with respect to $PM_{2.5}$ composition at Big Bend National Park.

Measurements of fine chloride and fine sodium concentrations were attempted at 37 and 20 stations respectively, including the K-Bar station at BBNP. Combined sodium and chloride concentrations greater than 1 $\mu g/m^3$ were measured at coastal sites (e.g., Padre Island, Laguna Atascosa, Aransas, and San Bernard) and even fairly inland sites (e.g. Laredo, Pleasanton). Combined concentrations as high as 0.5 $\mu g/m^3$ were detected on several days as far inland as Eagle Pass and the Lyndon B. Johnson National Historic Park. However, concentrations of these species at K-Bar were typically (for 70% of observations) less than 0.1 $\mu g/m^3$. Similarly, the mean concentration of sodium and chloride at K-Bar during the BRAVO study was ~0.1 $\mu g/m^3$. In order to focus the following discussion, sodium and chloride will be grouped in the "other" category, both for the model results and for the measurements.

Two features of organic and total $PM_{2.5}$ mass noted earlier and shown in Table 4-3 are recalled. CMAQ-MADRID reproduced total $PM_{2.5}$ mass throughout the network with a negative mean bias (–0.39 $\mu g/m^3$) and a positive normalized bias (16%). This result is due to two factors:

1. the propensity of the model to overpredict lower observed concentrations more often than higher concentrations, and,

2. the combination of the positive bias exhibited by the model in the predictions of sulfate superimposed with the negative bias in the prediction of other important constituents of aerosol mass, principally organic material (OM).

The predictions of organic material when compared to observations (measured at six stations of the BRAVO Network) exhibited a normalized bias (–50%) nearly equal in magnitude but opposite in sign to the normalized error, indicating that the model underpredicted virtually all organic material concentrations. The coefficient of determination (r^2=0.61) shows that the model could reproduce fairly accurately the fluctuations in organic mass. These statistical results indicate that the model regularly predicted approximately half of the organic mass observed at the monitoring stations. A factor of 1.4 was used to convert organic carbon measurements to organic mass in order to account for other atoms such as hydrogen, oxygen and nitrogen. Recent studies suggest that this factor may need to be increased depending on location (Turpin and Lim, 2001), which would increase the degree of underestimation of organic mass exhibited by the model.

Attention is now focused to particle composition as predicted by CMAQ-MADRID and observed at K-Bar, BBNP. Table 4-7, a modified version of Table 4-1, lists model performance statistics

as determined from comparing predictions to observations on the 103 days (of 119 simulation days) when concentrations were measured at the K-Bar site for all 5 major fine particulate components and total $PM_{2.5}$ mass. A component denoted as "other" represents the difference between the total mass and the sum of the major components; this "other" component is likely to be dominated by dust, crustal material, metal oxides, and sea-salt. In addition, since individual components of $PM_{2.5}$ may volatilize during sample handling and measurement, negative concentrations can be recorded for the "other" component in the measurements. Statistics are computed without the cutoff value of 0.1 $\mu g/m^3$, and thus test model performance at levels lower than those shown in Table 4-1. The lack of a cutoff affects (apart from "other" that is expected to have some negative values) 18 values of nitrate, 2 values of ammonium, and 63 values of elemental (black) carbon. However, the concentrations still remain within acceptable values for analysis, with only 1 nitrate observation and 6 black carbon observations below 0.02 $\mu g/m^3$.

Table 4-7
Statistical model performance at K-Bar, BBNP, for 103 common days(1) with no cutoff concentration.

Statistical Metric (BIBE)	units	SO_4^{2-}	NO_3^-	NH_4^+	BC	OM	Other	$PM_{2.5}$
Observed mean	$\mu g/m^3$	2.52	0.20	0.82	0.12	1.27	1.56	6.49
Predicted mean	$\mu g/m^3$	2.63	0.04	0.68	0.06	0.44	0.80	4.66
Coef of determination (r^2)		0.53	0.03	0.50	0.00	0.10	0.02	0.23
Mean bias	$\mu g/m^3$	0.11	-0.16	-0.13	-0.06	-0.82	-0.76	-1.83
Normalized bias		19%	26%	6%	8%	-60%	-45%	-13%
Fractional bias		-1%	-154%	-13%	-13%	-116%	163%	-31%
Mean error	$\mu g/m^3$	1.08	0.20	0.34	0.09	0.84	1.47	3.13
Normalized error		54%	194%	51%	89%	63%	160%	51%
Fractional error		46%	169%	48%	19%	121%	282%	87%
Root mean square, RMS, error	$\mu g/m^3$	1.51	0.24	0.45	0.14	1.10	2.37	4.11

(1) CMAQ-MADRID modeling period corresponds to July 2 – October 28, 1999.

Figure 4-13 presents two pie charts illustrating the average composition of $PM_{2.5}$ at K-Bar, BBNP observed during 103 days with full compositional data during the BRAVO study and the corresponding prediction for the same period by CMAQ- MADRID. The pie charts are scaled by surface area according to the appropriate (observed or predicted) total mass value. Figure 4-14 shows the same information on an absolute mass basis as a pair of stacked bar charts. The characteristics of sulfate predictions were discussed in the preceding section. As a result of the balancing effects of overpredictions and underpredictions, the overall sulfate mass was overpredicted by a little less than five percent during the analysis period. However, due to the underprediction of all non-sulfate components, the model predicts a higher contribution of fine sulfate to $PM_{2.5}$ mass, increasing the sulfate fraction from an observed 39% to 56%.

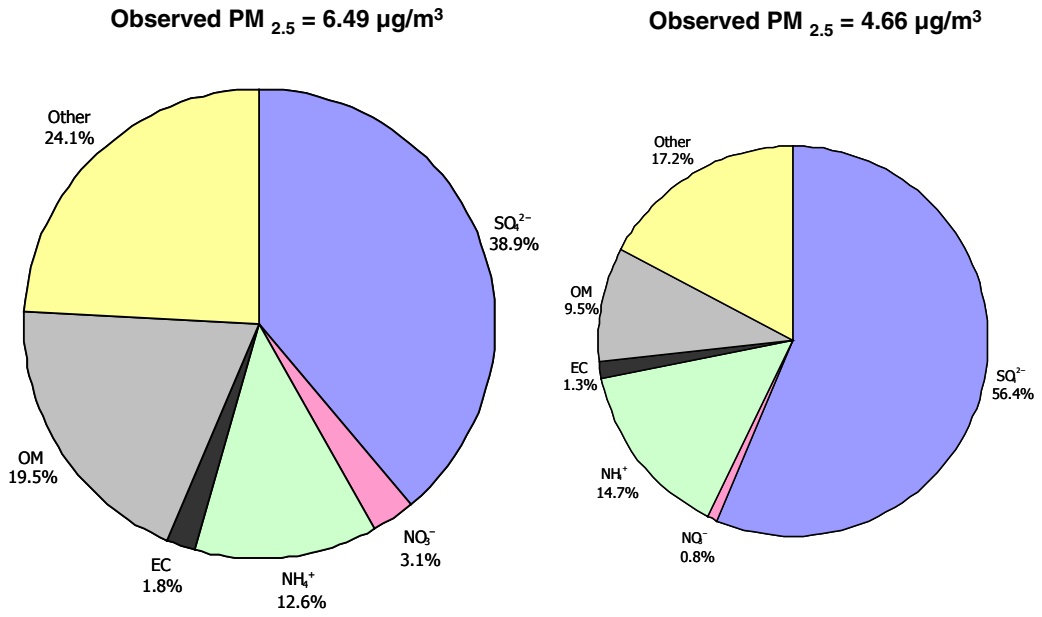

Figure 4-13
Relative composition of observed and predicted $PM_{2.5}$ at K-Bar, BBNP, averaged over the duration of BRAVO. Pie charts scaled relative to total mass.

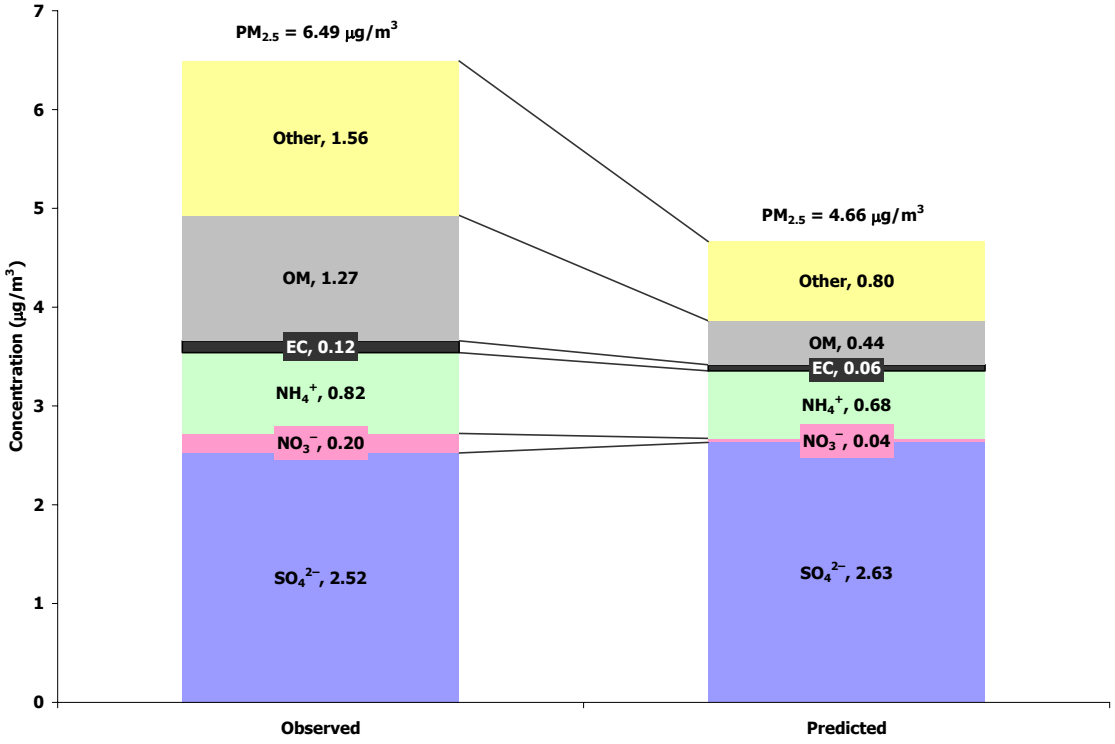

Figure 4-14
Mass composition of observed and predicted $PM_{2.5}$ at K-Bar, BBNP, averaged over duration of BRAVO.

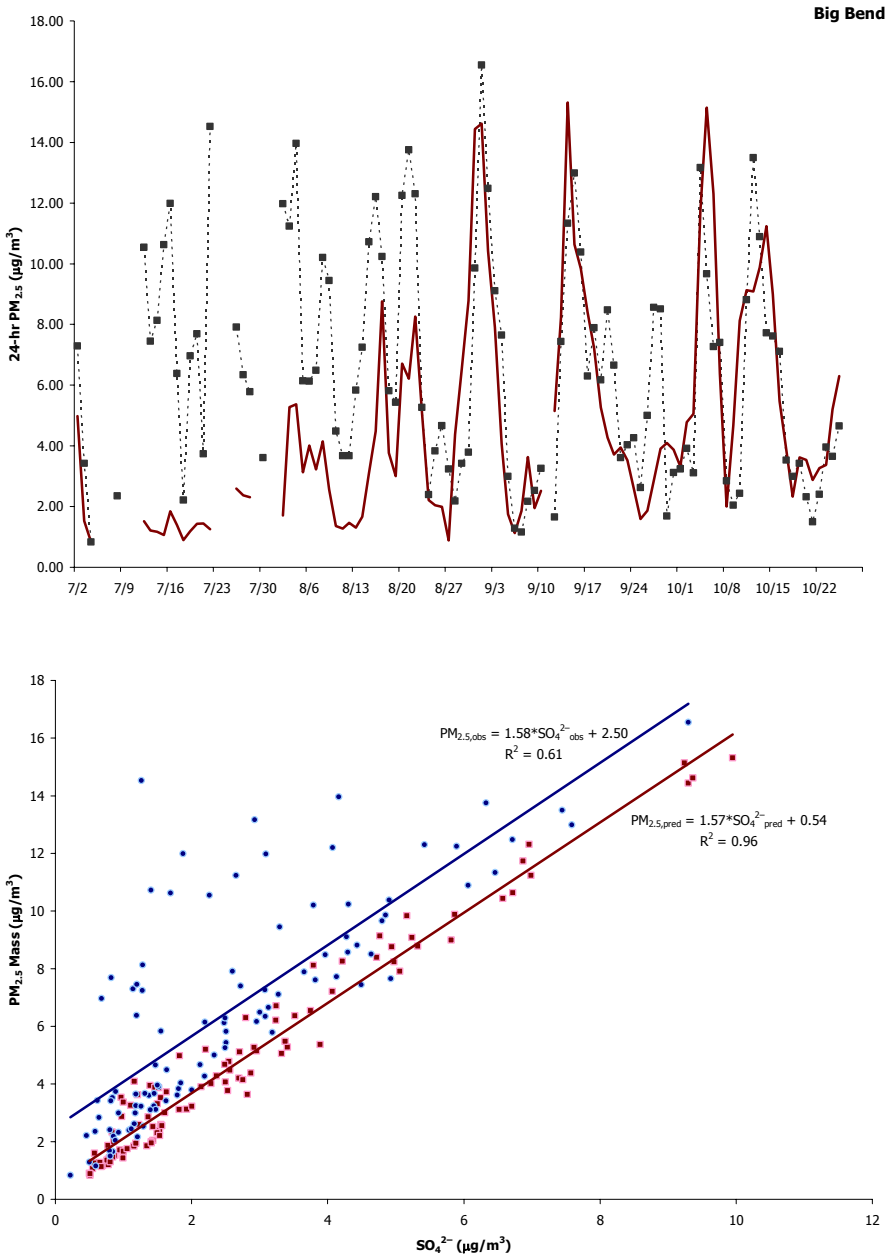

Figure 4-15
Time series of total $PM_{2.5}$ mass (top) and predicted (pink) and observed (blue) total $PM_{2.5}$ mass as a function of fine particulate sulfate (bottom) at K-Bar, BBNP.

Over the analysis period, the mean $PM_{2.5}$ mass is underestimated by a factor of 1.4, equivalent to an underprediction of 1.83 $\mu g/m^3$. The top portion of Figure 4-15 shows time series of observed and predicted $PM_{2.5}$ mass. From July to late August and during the final eleven-day period of September, the model consistently underpredicted $PM_{2.5}$ mass. These periods include the entire duration of the two stages of sulfate underprediction discussed previously; fine particulate sulfate underprediction accounts on average for roughly 20% (1 $\mu g/m^3$) and 50% (1.5 $\mu g/m^3$) of the missing $PM_{2.5}$ mass on corresponding days during the July-August and late September stages, respectively. Conversely, part of the reason for better agreement between the model and observations during four $PM_{2.5}$ peaks is the sulfate overpredictions. During these two stages, the overpredicted portions of sulfate mass contributed on average to 33% (1.4 $\mu g/m^3$) of total $PM_{2.5}$ mass observed on corresponding days.

The bottom panel of Figure 4-15 depicts $PM_{2.5}$ mass concentrations as a function of fine particulate sulfate for both observations and model predictions. The figure illustrates that the lack of agreement in model predictions to observations of total $PM_{2.5}$ mass cannot be explained solely by discrepancies in model predictions for sulfate. CMAQ-MADRID predicted a much tighter relationship between fine sulfate and $PM_{2.5}$ mass than is evidenced in the observations. The coefficient of determination is much higher for the simulation (r^2=0.91) than for the ambient data (r^2=0.61). The model failed to simulate peak $PM_{2.5}$ mass events when sulfate contributed to lesser fractions of the fine particle mass. Finally, inspection of the plotted diagram reveals the two linear regressions through the observed and predicted data points yield similar slopes, but the separation between the two lines (and thus the intercept) is underpredicted by the model by 1.96 $\mu g/m^3$. This separation is consistent with the mean bias of –1.83 $\mu g/m^3$ shown in Table 4-7.

Organic material is the principal PM component contributing to the underprediction of total $PM_{2.5}$ mass. The average mean predicted organic mass is approximately one-third of the observed organic material. Even in the smaller predicted pie (due to underestimated total particulate mass) on Figure 4-13, organic material only accounts for 9.5% of the total predicted $PM_{2.5}$ mass, whereas organic material corresponds to 19.5% of the mass in the ambient data for the analysis period, i.e. the undeprediction in organic mass is proportionally greater than the underprediction in total mass. The negative normalized bias of -60% and its approximately equal magnitude to the normalized error indicates that the model consistently underpredicted organic mass concentration on average by a factor of 2.5. This is clearly illustrated in the time series graph on Figure 4-16. The time series plot also displays how the model failed to capture many peak organic mass events (defined as days when measured organic carbon was > 1 $\mu g/m^3$ C, which, after multiplication by the 1.4 factor, yields an estimated observed organic mass of 1.4 $\mu g/m^3$) – July 12-16, July 18-July 22, August 14-17, August 20-22, August 31-September 3, September 15-20, September 27 – by an average factor of 2.5. Better agreements were observed in October; even then, two periods at the end of October were underpredicted by a factor of 1.4.

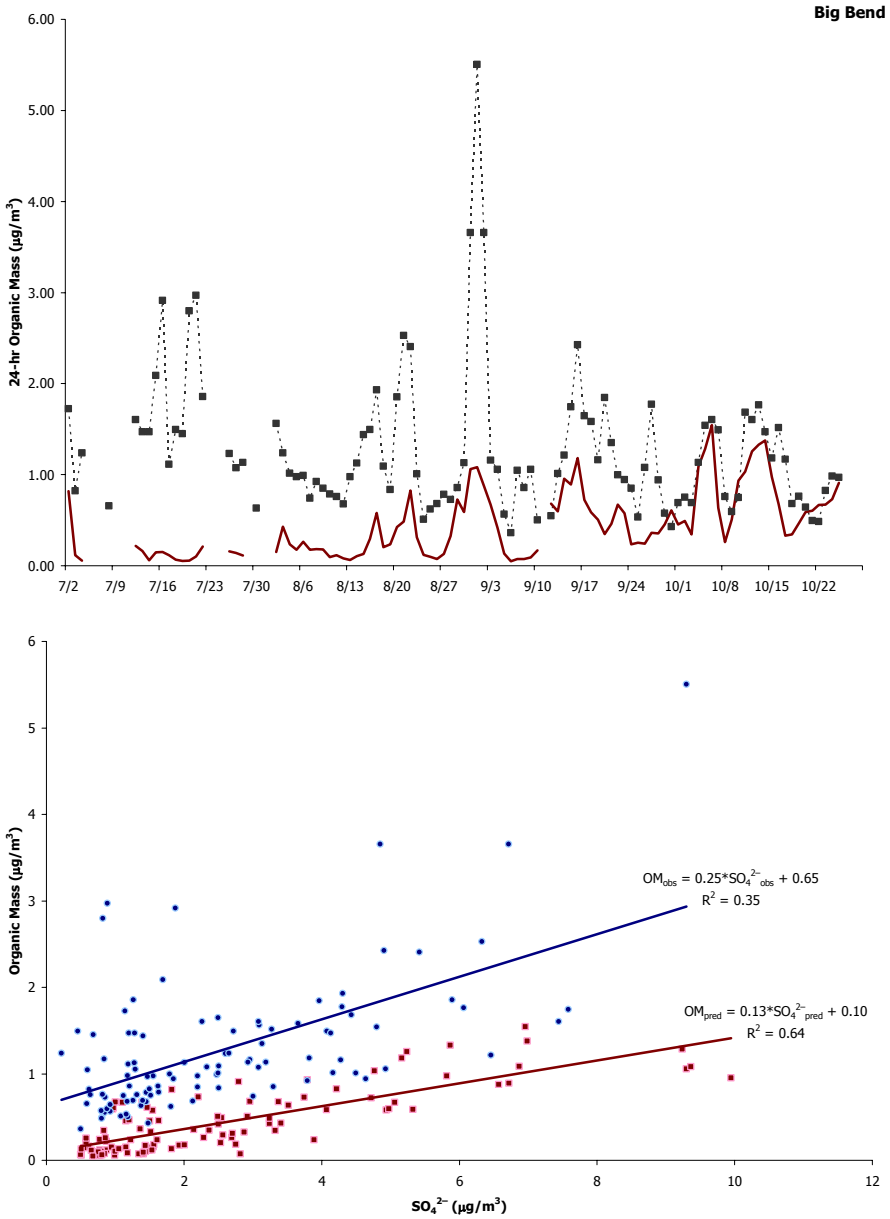

Figure 4-16
Time series of fine organic material concentrations (top) and predicted (red) and observed (blue) organic material as a function of fine particulate sulfate (bottom) at K-Bar, BBNP.

The lower graph on Figure 4-16, showing fine organic material (OM) concentrations as a function of fine particulate sulfate for both observations and predictions, illustrates the propensity of the model to underestimate OM. Fifty-one observed OM values, nearly half of the observed data, yielded values equal to or greater than half of the observed fine sulfate mass; on seventeen days, observed OM concentrations were greater than the sulfate mass. In contrast, the model only predicted fine OM greater than half of the predicted fine sulfate mass on four occasions. The graph also depicts the tendency of the model to predict a closer relation among sulfate and OM (r^2=0.61) than actually observed in the ambient data (r^2=0.35). The slopes of the

regression lines show that the contribution of OM relative to sulfate mass increases more rapidly in the observed data set than in the model predictions, indicating a tendency of the model to increasingly underpredict the contribution of OM at higher $PM_{2.5}$ sulfate concentrations.

The third most prevalent identified component in the observations was particulate ammonium. In contrast to particulate sulfate, particulate ammonium was underpredicted by the model with a mean bias of –0.13 $\mu g/m^3$. However, the normalized bias was 6%, due to a propensity of the model to overpredict often during days of low observed values, as shown in Figure 4-17. Ammonia is the most prevalent alkaline gas in the atmosphere and plays a key role in the neutralization of inorganic acids (e.g., sulfuric, nitric and hydrochloric acids) and organic acids (e.g., formic and acetic acids). The degree of neutralization was estimated by plotting the charge concentration of ammonia versus the charge concentration of sulfate and nitrate (in units of thousandths of charge equivalents per m^3, mEq/m^3) in the upper graph of Figure 4-18. This figure evaluates the capacity of the model to predict the overall neutralization trend observed at K-Bar, BBNP, regardless of the model predictions on any particular day. (Contributions to negative charge by chloride and organic anions cannot be calculated with the available data, but are likely to be minor and should not affect the conclusions of the analysis.) The average degree of neutralization observed at K-Bar, BBNP was 0.77, which in the absence of nitrate would correspond to a composition consistent with letovicite, i.e. $(NH_4)_3H(SO_4)_2$. However, as shown in Figure 4-18, the slope of the linear regression through the observed points suggests that the degree of neutralization was higher, with compositions of salts similar to mixture of letovocite, ammonium sulfate and ammonium nitrate. The average degree of neutralization predicted by the model was 0.73, similar to that observed at K-Bar, BBNP. However, the trends for the degree of neutralization as displayed by the model predictions are much more complex. Figure 4-18 shows that the model predicted wholly neutralized aerosol particles more often at lower concentrations than observed, but as anion concentrations increase, the model increasingly underpredicted the degree of neutralization. Model predictions also exhibited slightly higher variation from the linear regression (r^2_0.89) than observed (r^2=0.95) with several predictions across the concentration range representing degrees of neutralization more consistent (in the absence of nitrate) with ammonium bisulfate (NH_4HSO_4). The discrepancy between observed and predicted trends of neutralization could be symptomatic of problems in ammonia emissions.

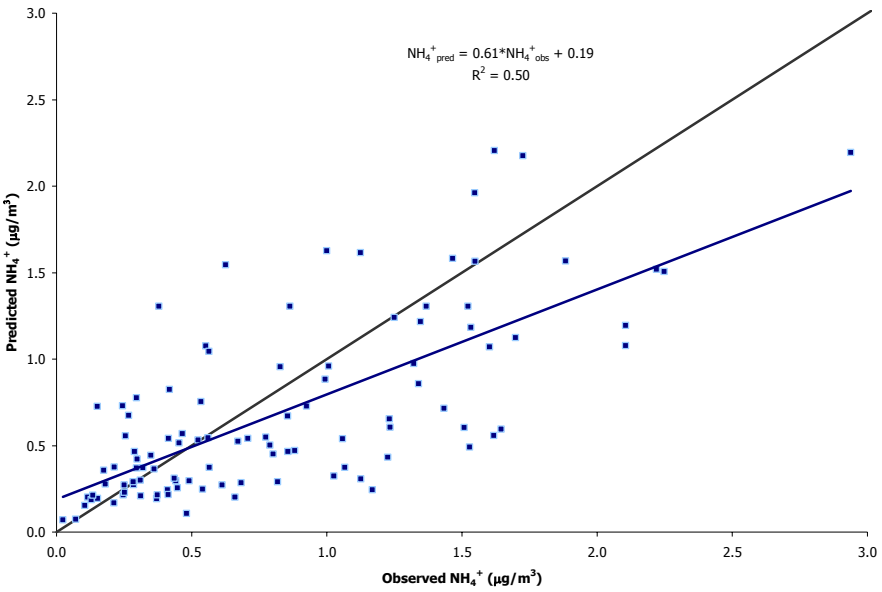

Figure 4-17
Predicted and observed fine ammonium concentrations at K-Bar, BBNP.

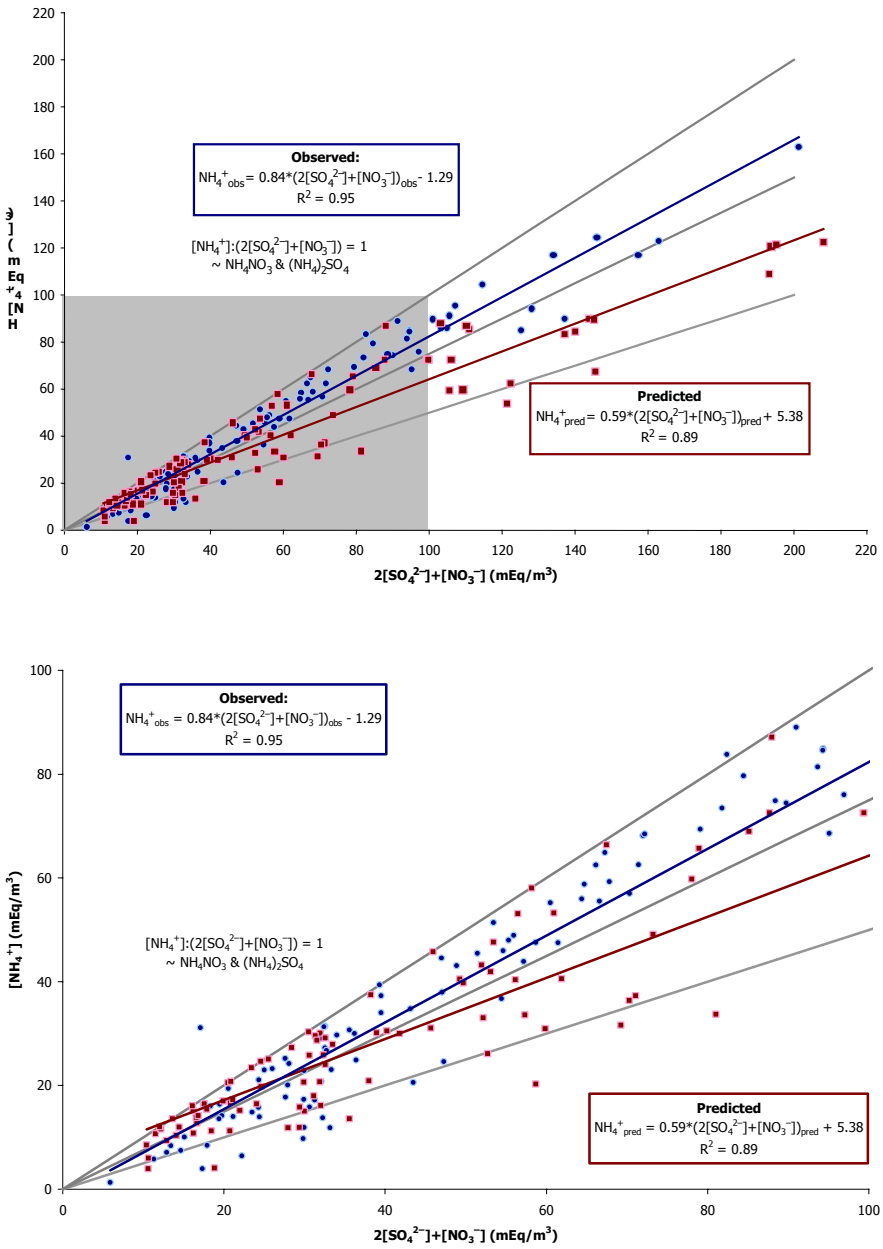

Figure 4-18
Predicted and observed degree of neutralization at K-Bar, BBNP. (Grey lines correspond to 1:1, 1:1.5, and 1:2 lines, from top to bottom.)

Another component worth discussing is the "other" component, which represents slightly different things in the model and in the observations. In the observations, the "other" component is the difference between total $PM_{2.5}$ mass and the sum of identified components in the measurement (in this case, sulfate, nitrate, ammonium, BC, OM; sodium and chloride are lumped into the "other" component). It can be primary or secondary, or a result of errors in the measurements of the explicit components. In the model, the "other" component is the sum of sodium, chloride, and any particulate matter from primary emissions not treated explicitly in the

model. Both the ratio of the mean predicted to mean observed concentration of "other" components and the normalized bias (-45%) suggest that "other" components were underestimated by a factor of two. As shown in Figure 4-13, this underestimation decreases the contribution of other components to total fine particulate mass from 24% in the observations to 17% in the "shrunken" pie of predictions. However, the low correlation between the observed and simulated values indicates that this underprediction is not consistent. Figure 4-19 shows that during July and August, the concentration of "other" components exceeded concentrations of 2 $\mu g/m^3$ on half of the days, yielding an average concentration of 2.5 $\mu g/m^3$ of "other" components during the two months of the analysis period. In contrast, the model predicted a repeatedly low concentration of 0.5 $\mu g/m^3$ of the "other" category. Model performance improved for the final two months, with the exception of two important events – a negative observed "other" event on September 1 (when predicted "other" concentrations exhibited a small spike) and underprediction of a substantial observed spike of other components on October 4. Removing these two events, the normalized bias in model predictions of "other" components during the final two months of analysis is –20%. The systematic and time dependent errors suggest the possibility of a missing PM source that was more important in the first two months than the last two.

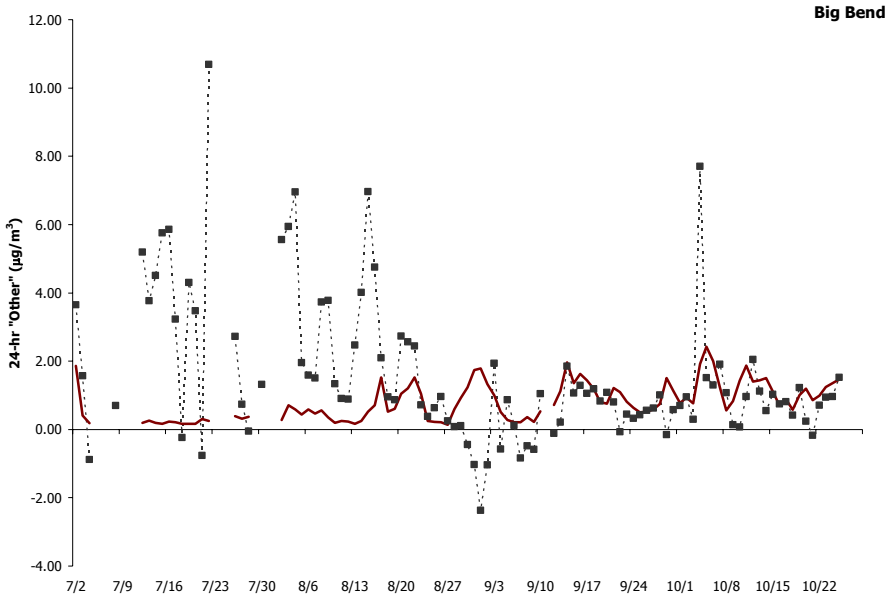

Figure 4-19
Time series of 24-hr concentrations of "other" $PM_{2.5}$ components at K-Bar, BBNP.

In order to place into perspective CMAQ-MADRID model performance for the remaining species, i.e., nitrate, black carbon and "other", Table 4-8 compares Pearson correlation matrices (i.e., matrices of coefficients of correlation, "r") among the individual species data arrays within a corresponding data set, i.e. observations and predictions. At first glance, correlations between $PM_{2.5}$ components are stronger in the Pearson matrix of the predictions compared to that of the observations. In other words, with the exception of nitrate, the predicted $PM_{2.5}$ mass co-varied with every component to a large extent. The observed $PM_{2.5}$ mass was also driven to a large extent by ammonium and sulfate components. However, only moderate correlations were found between $PM_{2.5}$ and nitrate, organic materials and the "other" component. $PM_{2.5}$ mass aside, the

model predicted a tendency for sulfate, ammonium, BC, OM, and the "other" component to fluctuate together, suggesting a common source or source area of these species or a common response to meteorology. This behavior is not as apparent in the measurements.

Table 4-8
Observed and predict Pearson correlation coefficient matrix(1)

OBSERVED PEARSON MATRIX

	SO_4^{2-}	NO_3^-	NH_4^+	BC	OM	Other	$PM_{2.5}$
SO_4^{2-}	**1.00**						
NO_3^-	0.19	**1.00**					
NH_4^+	0.98	0.14	**1.00**				
BC	0.29	0.53	0.24	**1.00**			
OM	0.59	0.48	0.56	0.65	**1.00**		
Other	-0.01	0.50	-0.05	0.10	0.08	**1.00**	
$PM_{2.5}$	**0.78**	0.55	**0.74**	0.42	0.67	0.58	**1.00**

PREDICTED PEARSON MATRIX

	SO_4^{2-}	NO_3^-	NH_4^+	BC	OM	Other	$PM_{2.5}$
SO_4^{2-}	**1.00**						
NO_3^-	-0.02	**1.00**					
NH_4^+	**0.94**	0.11	**1.00**				
BC	**0.88**	0.18	**0.92**	**1.00**			
OM	**0.80**	0.11	**0.80**	**0.90**	**1.00**		
Other	**0.78**	0.22	**0.84**	**0.96**	**0.91**	**1.00**	
$PM_{2.5}$	**0.98**	0.08	**0.97**	**0.95**	**0.88**	**0.88**	**1.00**

(1) The following ranges are considered for interpretation of correlations between variables: insignificant, $|r| <= 0.5$ ($r^2 <= 0.25$, i.e., one variable explains 0%-25% of the variance of the other); low, $0.5 < |r| <= 0.7$ ($0.25 < r^2 < \sim 0.5$); moderate – yellow shading, $0.7 < |r| < 0.9$ ($\sim 0.5 < r^2 < \sim .8$); and high – violet shading, $|r| <= 0.9$ ($r^2 <= \sim 0.8$).

In the observed Pearson matrix, the "other" constituent is moderately correlated with particulate nitrate with an r=0.50, indicating that the approximately one-quarter of the variance in the "other" category can be explained by the variability in nitrate concentrations. The observed "other" component shows no other correlation with $PM_{2.5}$ and components. One source that contributes to both particulate nitrate and the "other" component is motor vehicles. Nitrate may be formed from NO_x emissions from vehicles, which also contributes to mechanically-generated fugitive dust, which is a constituent of the "other" category. Following this line of reasoning, a quarter of the "other" $PM_{2.5}$ component may originate from road dust associated with mobile sources, and this $PM_{2.5}$ emission source may be under-represented in the simulation. Sodium and chloride, principal components of sea-salt, contribute to approximately one-tenth of the "other" category. Windblown fugitive dust, crustal material and metal oxides (e.g., from metallurgical processing, fly ash emissions, glass manufacturing, cement manufacturing, rust, and diesel engines) are likely to form the remainder of the "other" category.

In the observation data set, black carbon is somewhat correlated to organic material and nitrate. The correlations with other components are weak or nonexistent. This finding is consistent with concurrent emissions from multiple sources such as biomass burning (BC and OM emissions) and motor vehicle emissions (BC emissions and nitrate formation). However, the model showed moderate-to-high correlations of black carbon with sulfate, ammonium, and "other" components. In addition, the model predicted a much higher correlation with OM than observed in the atmosphere while failing to predict a correlation to nitrate. These results suggest that BC emissions associated with a source that also emit NO_x (resulting in the formation of nitrate) such as diesel soot motor vehicles, are underrepresented in the modeling system.

For the analysis period, BC concentrations were underpredicted by a factor of 2. As illustrated in Figure 4-20, observed BC concentrations were highest for the period starting in July and ending September 4, when observed BC concentrations exceeded 0.2 $\mu g/m^3$ on 19 days, more than one-third of the 53 days with available data, and exceeded 0.1 $\mu g/m^3$ on 36 days. In contrast, predicted BC concentrations for the same period exceeded 0.1 $\mu g/m^3$ on 6 days. Although, the model peaked in accordance with the most extreme BC event from August 27-September 4, it failed to capture the peak concentration by almost a factor of 4.

Finally, nitrate observations appear to correlate moderately with BC, OM and "other" components. These correlations may represent a signature of a common source or source areas. OM contains both primary (i.e. directly emitted) organic mass and secondary organic aerosol, formed from the oxidation of volatile organic compounds. It follows that this signature source may be associated with diesel and gasoline engines, which contains primary organic aerosol, secondary aerosol precursors, BC and is associated also with road dust. In the simulation data set, however, nitrate predictions show no significant correlation with any component of $PM_{2.5}$. It follows that the emissions of primary organic aerosol, secondary aerosol precursors, BC and road dust associated with diesel and gasoline engines are likely underestimated by the modeling system. Mean predicted fine nitrate concentrations are underpredicted at K-Bar, BBNP by a factor of five compared to mean observed nitrate concentrations. As shown in Figure 4-13, this underestimation of nitrate decreases its contribution to total fine particulate mass from 3% in the observations to less than 1% in the "shrunken" pie of predictions. As illustrated in Figure 4-21, the model failed to capture any of the fluctuations observed in the measurements.

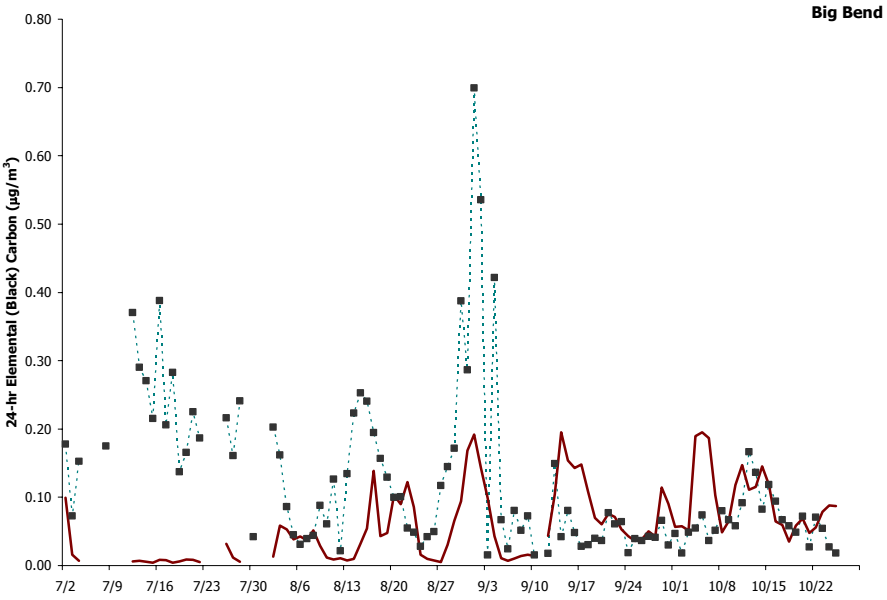

Figure 4-20
Time series of 24-hr fine BC concentrations at K-Bar, BBNP.

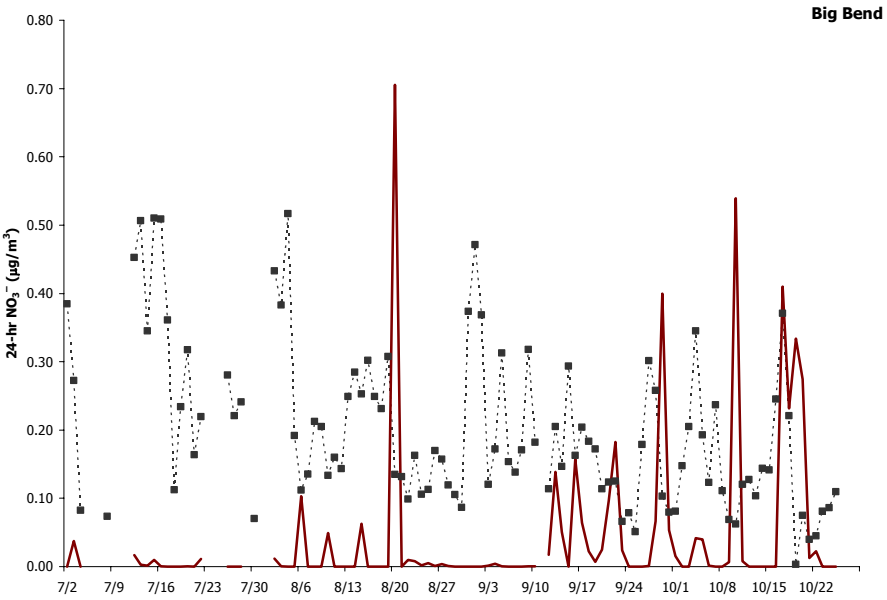

Figure 4-21
Time series of 24-hr fine nitrate concentrations at K-Bar, BBNP.

4.6 Discussion

Model performance with respect to fine sulfate predictions was explored in detail, including model performance for its gas-phase precursor, sulfur dioxide. The analysis showed that although for the overall study period sulfate predictions exhibited low bias, this bias was the result of the counterbalancing effects of periods of overprediction combined with periods of underprediction. Four distinct stages of the BRAVO study as defined by observations at K-Bar, BBNP were observed: two periods for which the model consistently underestimated fine sulfate extending from July 12 to August 27 and from September 20 to 30, and two periods, extending from August 28 to September 19 and from October 1 to 28, for which the model regularly overpredicted fine sulfate concentrations. The model could account for approximately half of the fluctuations in sulfate concentrations with a normalized error commensurate with the expected performance of current models. However, the model showed limitations in predicting short-term or long-term temporal variations of sulfate concentrations.

Overpredictions at BBNP were influenced by a marked positive bias of the model with respect to both gas-phase and particulate sulfur concentrations in the eastern portion of the domain. In this region, the model almost invariably overestimated the sulfur burden measured at the BRAVO Network sites. The exact causes for overpredictions of sulfur species in this region are unknown but may be influenced by the positive bias in boundary conditions from the eastern United States as prescribed by the REMSAD model, overvalued emissions of sulfur species in the eastern portion of the CMAQ domain or other physicochemical process affecting the conversion and loss of sulfur species within the model. Given that total sulfur concentrations were overestimated by the CMAQ-MADRID modeling system, a systematic investigation of the causes of sulfur overpredictions by the models is warranted.

In contrast to the overprediction of sulfur species at stations in eastern Texas, underpredictions of those species occur predominantly at the southern and southwestern stations (in the vicinity of BBNP) of the BRAVO network. During the two underprediction stages observed at K-Bar, BBNP during the four-month period, wind trajectories originated more often from Mexico than they did during the periods of overprediction. These observations, in conjunction with additional conclusions derived during analysis of the source-region attribution sensitivity simulation, indicate that emissions of sulfur compounds and accurate simulation of the factors controlling conversion of SO_2 to fine particulate sulfate need to be further explored for the Mexican domain.

In summary, several potential causes exist for the disagreement between fine sulfate model predictions and corresponding observations, including, but not limited to:

- Emissions – errors in emission inventories of SO_2, primary sulfate or errors in the emission inventories of other species necessary for the correct representation of oxidant fields (NO_x, VOC and CO) and aerosol nucleation/condensation rates (NH_3).
- Meteorology – errors in cloud predictions (location, size, liquid water content), precipitation, or wind fields.
- Transport – incorrect representation of the atmospheric dispersion of pollutants or deposition/settling velocities in the model.

- Chemistry – inaccurate estimates of SO_2 oxidation rates.

All of the above phenomena are closely related; for example, the accurate representation of aqueous-phase SO_2 oxidation rates does not only depend on properly simulated chemistry, but also requires suitable estimates of the emissions of atmospheric oxidant precursor species (and proper simulation of their photochemistry), correct representation of cloud liquid water content, and accurate transport of all reactants to the appropriate locations.

Concentrations of organic particulate compounds were also underestimated at K-Bar, BBNP. Organic fine particulate matter constitutes the second largest identified component of $PM_{2.5}$ mass. BRAVO network measurements indicate that organic compounds can constitute a large fraction of the $PM_{2.5}$ mass during events of high $PM_{2.5}$ loadings, even in the absence of significant fractions of sulfate. Developing a correct emissions inventory of primary organic particulate matter and the correct simulation of the formation of secondary organic aerosol are areas requiring further research in order to accurately represent their fate and transport in the air quality models. The inability to accurately represent these compounds (Pun et al., 2003b) could hinder the development of effective strategies to obtain continued improvement of visibility in Class I areas.

The concentration of "other" compounds – including mechanically-induced and windblown dust, crustal material, metal oxides (e.g., from metallurgical processing, fly ash emissions, glass manufacturing, cement manufacturing, rust, and diesel engines), and sea-salt – accounted for approximately 24% of the observed mass during the BRAVO study at K-Bar, BBNP. These "other" compounds were also underestimated by the model, in particular in the months of July and August when these "other" compounds accounted for large portions of the total fine particulate matter mass.

Nitrate concentrations at K-Bar, BBNP were also underestimated by the model; in addition the model could not represent the fluctuations of nitrate concentrations. The model also failed to reproduce the relationship between measured fine nitrate with three other components of fine particulate mass: organic compounds, black carbon and the "other" compounds, which is expected to include a portion relating to mechanically-generated road dust. These factors indicate that the components of gasoline and diesel vehicle emissions may be underestimated in the modeling domain.

Concentrations of organic compounds and black carbon were found to be correlated in the model predictions, in contrast to a lack of correlation between the two PM components in the observational data set at K-Bar, BBNP. The inability of the modeling system to reproduce the lack of correlation between BC and organic mass observed in the ambient data could be caused by omissions or errors in the BRAVO emissions inventory for estimates of biogenic SOA precursors or emissions from specific events, such as wild fires, remote biomass burning or refuse burning in Mexico.

5
SOURCE ATTRIBUTION

5.1 Source Attribution of Fine Particulate Sulfate Using CMAQ-MADRID

Following the methodology described in Section 2, the CMAQ domain was divided into four geographical source areas consistent with the selection of source regions for attribution analysis with REMSAD: Mexico, Texas, eastern U.S., and western U.S. (excluding Texas). Five sensitivity simulations were conducted. Since REMSAD serves as an outer nest to the CMAQ-MADRID simulations, the first sensitivity simulation evaluated the contribution from the boundary conditions of the REMSAD domain (as estimated from the GOCART model) to the fine particulate sulfate load in the CMAQ domain. Each of the ensuing sensitivity simulations evaluated the contribution of a particular source region to the fine particulate sulfate load by removing all primary sulfur emissions (SO_2 and primary sulfate) within the CMAQ domain and the corresponding contribution to the inner nest boundary conditions. The contribution from a source region to fine particulate sulfate at K-Bar, BBNP was defined as the difference between the base case fine sulfate concentration and the fine sulfate concentration predicted by the attribution sensitivity simulation. Source attribution values at K-Bar were estimated for the duration of BRAVO , for each month of the BRAVO period, and for seven selected episodes (the dates of those episodes are presented in Table 5-1). In spite of the potential for large perturbation in emissions to produce non-linear responses to SO_2 oxidation and aerosol sulfate dynamics, the contributions from the source regions and the outer nest boundary typically aggregated to within 3% of the total final particulate sulfate predicted by the base case simulation.

The analysis of source attribution during the BRAVO period is inextricably connected to model performance. A precise understanding of the underlying causes for models to overpredict or underpredict fine particulate sulfate, in combination with knowledge of the trends illustrated during the model performance analysis, is necessary to interpret attribution estimates. This understanding is important for all time periods, but above all for individual days and study episodes.

5.2 Daily and Episodic Attribution Estimates

In the case of CMAQ-MADRID, the predicted values of fine sulfate at K-Bar during the BRAVO episodes exhibited a degree of bias (as shown in Table 5-1) that obscures the analysis of the relative impact of different source regions. Three episodes displayed a positive bias higher than 30%, with sulfate loads during Episode VI overestimated by a factor of two. Three episodes exhibited a negative bias ranging from –21% to as much as –60%, equivalent to an underprediction by a factor of 2.5. The lowest episodic bias, 16%, was displayed during Episode VII; however, this value reflects a compensation of errors during the episode – an early segment of overprediction followed by a period of underprediction (as is shown later in time-series plots).

The scope of BRAVO does not explore or diagnose the causes for disagreement among the predictions of the Eulerian chemical transport modeling systems and the observations of the BRAVO network; consequently, the implications of the daily and episodic source region attribution estimates remain uncertain.

For consistency with previous chapters, estimates of the relative source region attribution for fine particulate sulfate at K-Bar, BBNP, are presented in Figures 5-1 and 5-2 for each day of the BRAVO period (shown separately for each month). Tables 5-2 and 5-3 provide source region attribution results for fine sulfate at K-Bar during the seven BRAVO episodes.

The relative contribution from the source regions is calculated using two metrics. The first metric is the apportionment of the overall sulfate load – the ratio of the average contribution (in $\mu g/m^3$) of fine sulfate from a source region during a time interval with respect to the overall average predicted concentration (in $\mu g/m^3$) during the same interval; this index provides a measure of impact strength from a particular region. The second metric is the average of daily apportionment – the average of individual daily percent contributions from a source region to the 24-hour fine sulfate concentrations during a time interval; this index provides a measure of the impact frequency from a particular region.

Table 5-1
Bias in the fine sulfate predictions by CMAQ-MADRID at K-Bar during the BRAVO episodes

Statistical Measure	Episode I 7/22 – 7/31	Episode II 8/16 – 8/23	Episode III 8/31 – 9/4	Episode IV 9/12 – 9/17	Episode V 9/25 – 9/28	Episode VI 10/3 – 10/7	Episode VII 10/11 – 10/16
Observed Mean SO_4^{2-} ($\mu g/m^3$)	2.13	4.19	5.35	4.46	3.11	2.99	4.86
Predicted Mean SO_4^{2-} ($\mu g/m^3$)	1.31	3.13	6.35	5.75	1.21	5.98	5.34
Ratio of Predicted Mean / Observed Mean	0.61	0.75	1.19	1.29	0.39	2.00	1.10
Normalized Bias	-32%	-21%	38%	66%	-60%	104%	16%

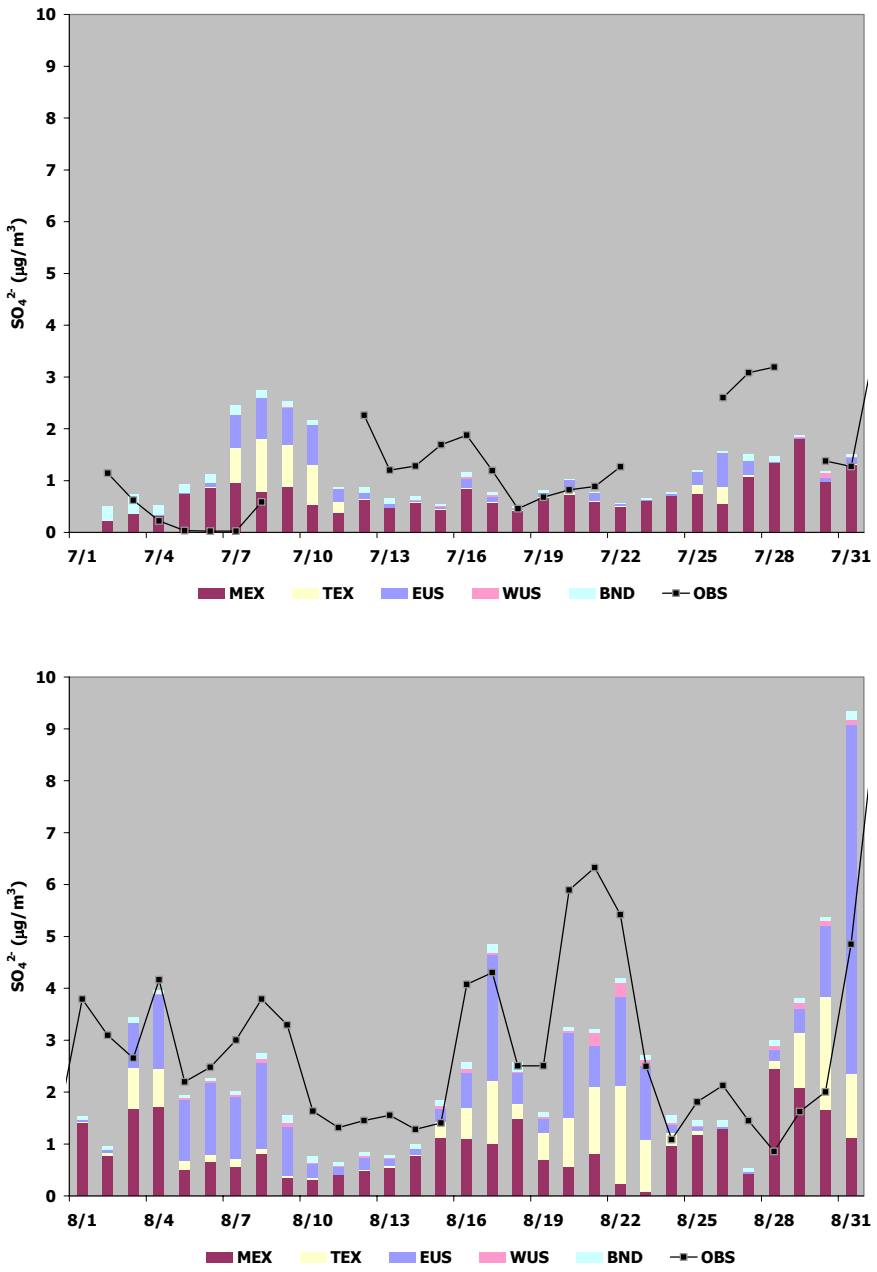

Figure 5-1
Daily source region attribution and observations (OBS) of fine particulate sulfate as predicted by CMAQ-MADRID at K-Bar, BBNP, during July (top) and August (bottom), 1999. Source regions are Mexico (MEX); Texas (TEX); eastern U.S. (EUS); western U.S. (WUS), excluding Texas; and boundary conditions (BND) provided by the GOCART model to REMSAD.

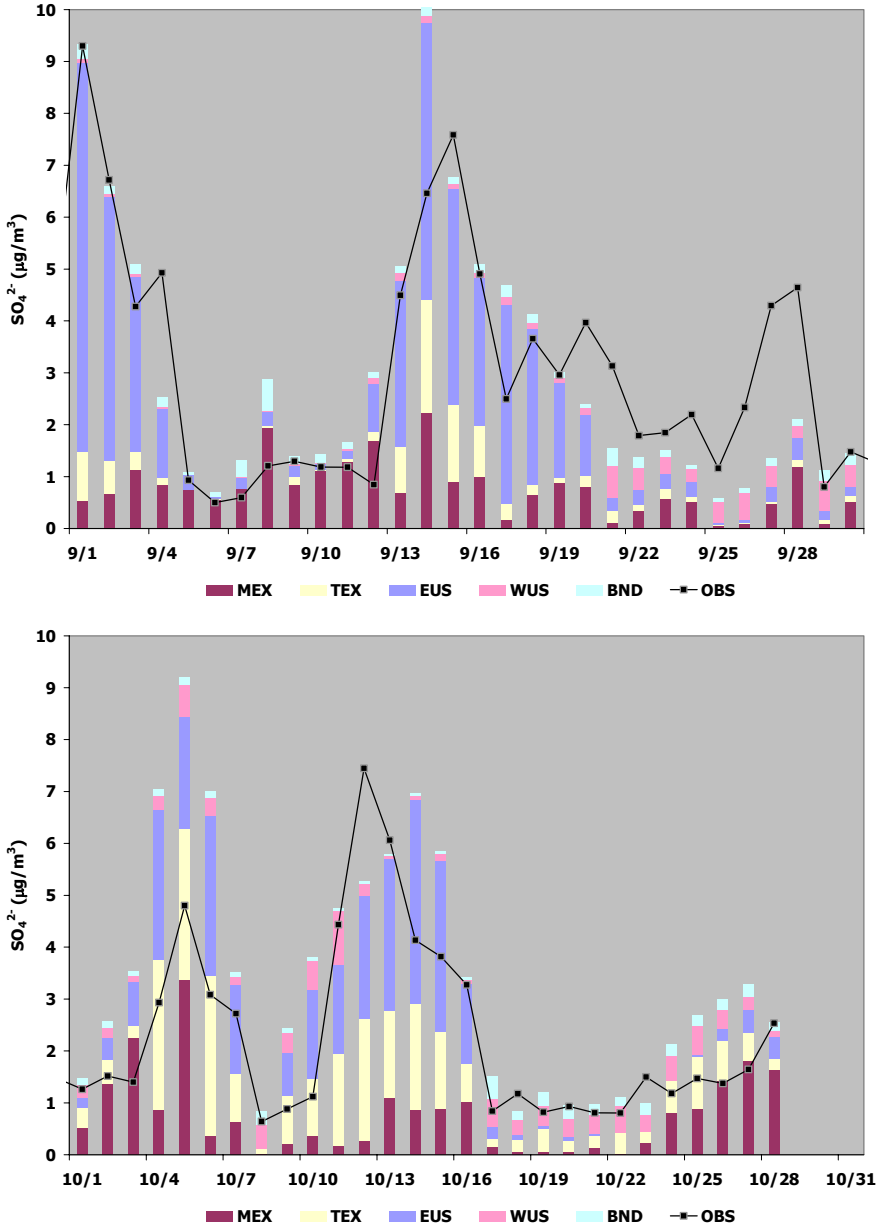

Figure 5-2
Daily source region attribution and observations (OBS) of fine particulate sulfate as predicted by CMAQ-MADRID at K-Bar, BBNP, during September (top) and October (bottom), 1999. Source regions are Mexico (MEX); Texas (TEX); eastern U.S. (EUS); western U.S. (WUS), excluding Texas; and boundary conditions (BND) provided by the GOCART model to REMSAD.

Table 5-2
Source region attribution of $PM_{2.5}$ sulfate as predicted by CMAQ-MADRID at K-Bar, BBNP, during seven selected episodes during BRAVO (July – October, 1999). The top row of values for an episode denotes the apportionment of the fine sulfate aerosol load at K-Bar, BBNP during the episode. The bottom row of values for an episode denotes the average of the individual daily sulfate apportionment fractions at K-Bar, BBNP during the episode. Contributions may not add up to 100% due to round-off and non-linearities.

	Mexico	Texas	Eastern U.S.	Western U.S.	GOCART Boundary
Episode I	78%	5%	12%	1%	4%
7/22-7/31	79%	4%	11%	1%	4%
Episode II	24%	31%	38%	3%	3%
8/16/-8/23	27%	31%	35%	3%	4%
Episode III	16%	14%	67%	1%	3%
8/31-9/4	19%	14%	63%	1%	3%
Episode IV	19%	18%	59%	2%	3%
9/12-9-17	22%	16%	58%	2%	3%
Episode V	37%	4%	16%	32%	9%
9/25-9/28	28%	4%	13%	44%	10%
Episode VI	25%	34%	36%	5%	2%
10/3-10/7	28%	30%	37%	5%	2%
Episode VII	13%	31%	49%	5%	1%
10/11-10/16	14%	31%	48%	6%	1%

Table 5-3
Average contributions from source regions to the $PM_{2.5}$ sulfate load (concentrations in $\mu g/m^3$) as predicted by CMAQ-MADRID and $PM_{2.5}$ sulfate observations at K-Bar, BBNP, during seven selected episodes during BRAVO (July-October, 1999).

	Mexico	Texas	Eastern U.S.	Western U.S.	GOCART Boundary	Other	Total Predicted	Observed
Episode I	0.96	0.06	0.15	0.01	0.05	0.01	1.24	2.13
Episode II	0.74	0.97	1.19	0.11	0.11	0.01	3.13	4.19
Episode III	1.00	0.91	4.23	0.07	0.17	-0.02	6.35	5.35
Episode IV	1.11	1.01	3.38	0.13	0.15	-0.03	5.75	4.46
Episode V	0.45	0.05	0.20	0.39	0.11	0.01	1.21	3.11
Episode VI	1.50	2.01	2.14	0.30	0.11	-0.07	5.98	2.99
Episode VII	0.72	1.67	2.63	0.28	0.04	0.00	5.34	4.86

An example of model performance issues with respect to source region attribution is illustrated during the final ten-day period of September 1999. During this time period, which includes Episode V, CMAQ-MADRID systematically underpredicted the concentrations of fine particulate sulfate at the K-Bar site. In addition, low predictions of fine sulfate from Mexico appear to modulate synchronously with the fine sulfate measurements, suggesting that the contribution from that region may have been underestimated. The predicted concentrations from the western U.S., which exhibited a large relative contribution during the period, did not modulate similarly. Considering the degree of underprediction (half of observed values during Episode V), any commensurate changes to the Mexican contribution would affect the source attribution results.

5.3 Assessment of the Effect of Model Performance on Attribution Estimates

In order to assess the nature of the negative and positive bias days as predicted by the model, the twenty days exhibiting the most intense relative underpredictions and the twenty days displaying the most intense relative overpredictions were aggregated into two groups. Table 5-4 shows a summary of the data for the two groups. Both groups show similar biases in opposite directions which compensate for each other when evaluated jointly – the dual-aggregate ratio of means is 0.90 and the dual-aggregate bias is 48%. Results from CMAQ-MADRID show that the modeling system yielded nearly a week of acute underpredictions of fine sulfate at K-Bar, BBNP during each of the first three months. CMAQ-MADRID exhibited large overpredictions of fine sulfate at K-Bar, BBNP during each month, with the least occurrences in July and the most frequent occurrences during October.

As evident in Figure 5-3, two distinct, highly correlated mechanisms are detected as separate contributors to the underprediction and overprediction at K-Bar, BBNP by plotting predicted fine sulfate versus observed fine sulfate concentrations during days of acute disagreement between the two values. These mechanisms were corroborated by plotting the 20 largest absolute underpredictions and overpredictions (not shown). In order to obtain additional insight on these mechanisms, source region attribution is also performed for the two groups, as shown in Table 5-5.

Table 5-4
Summary data of 20 largest relative underpredictions and 20 largest relative overpredictions of fine sulfate by CMAQ-MADRID at K-Bar, BBNP during the BRAVO period.

	Statistics				Number of Days in Specific Month & (Number of Days in Episodes)			
	Obs. Mean	Pred. Mean	Ratio of Means	Norm. Bias	Jul	Aug	Sep	Oct
20 Largest Relative Underpredictions	2.78	1.23	0.44	–56%	6 (3)	8 (2)	6 (5)	0
20 Largest Relative Overpredictions	1.76	4.02	2.29	151%	2 (0)	4 (2)	4 (2)	10 (4)

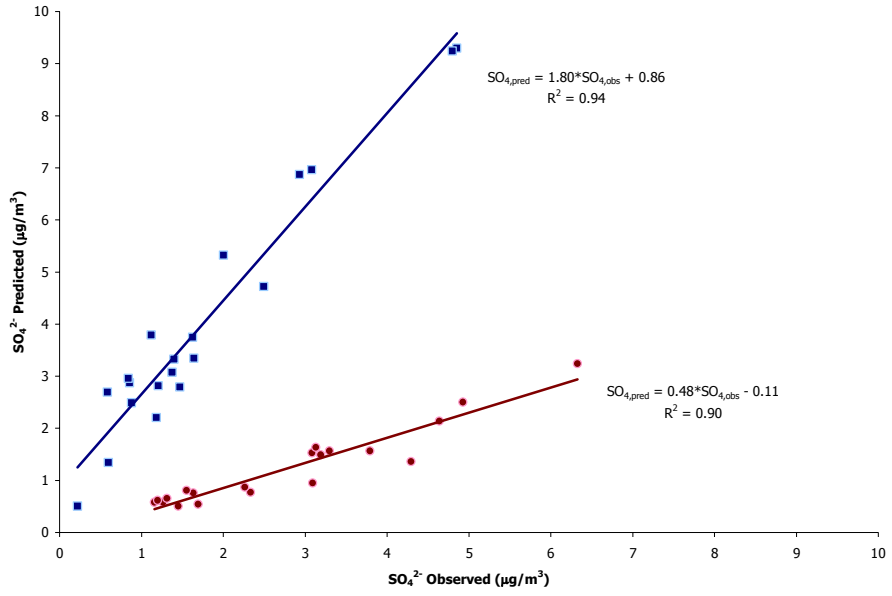

Figure 5-3
Two distinct non-random mechanisms for underprection (red) and overprediction (blue) displayed by the CMAQ-MADRID modeling system for fine sulfate at K-Bar, BBNP during the BRAVO period.

As shown in the model performance discussions of Chapter 4, the eastern portion of the CMAQ modeling domain exhibits the highest positive bias with respect to SO_2 and fine sulfate predictions. It follows that this bias carries over during transport of fine sulfate particles

(together with additional chemical conversion of SO_2 to sulfate) to the BBNP area, leading to overpredictions at the K-Bar site. As currently configured with respect to emissions, meteorology and chemical transport, CMAQ-MADRID estimates that events of large underpredictions of 24-hour fine sulfate at K-bar are predominantly characterized by relatively higher contributions to the fine sulfate load from sources in Mexico (50%) and lesser contributions from contribution from Texas and eastern U.S. sources (9% and 22%, respectively.) The lowermost trendline in Figure 5-3 illustrates that these underpredictions are strongly correlated with a specific but yet unidentified mechanism. As the contributions from the other main source regions (Texas and the eastern U.S.) are likely overestimated due to the carry-over of bias in fine sulfate concentrations originating in the eastern portions of the domain, the highly correlated mechanism of underprediction and high relative contribution from Mexico suggest that one or more aspects of the modeling system (emissions, meteorology or chemical transport) leads to a systematic underestimation of contribution from Mexican sources.

Continuing the analysis, it can be inferred that the circumstances leading to overpredictions in the eastern half of the domain are key contributing factors to the overprediction mechanism illustrated by the uppermost trendline in Figure 5-3. As shown in Table 5-5, CMAQ-MADRID currently estimates that daily events of acute overpredictions are characterized by approximately one-third contributions to the fine sulfate load from sources in Mexico and the eastern U.S. and current estimates of one-fourth contribution from sources in Texas. As the source region attribution values for both the eastern U.S. and Texas are likely overestimated during these days, correction of this bias would decrease the eastern U.S. and Texas contributions and increase the Mexican contribution, which as discussed earlier, is likely underestimated by CMAQ-MADRID.

Table 5-5
Source region attribution of fine sulfate at K-Bar, BBNP, as estimated by CMAQ-MADRID for the 20 most intense relative underpredictions and 20 most intense relative overpredictions. The top row of values denotes the apportionment of the fine sulfate aerosol load at K-Bar, BBNP for the twenty-day grouping. The bottom row of values denotes the average of the individual daily sulfate apportionment fractions at K-Bar, BBNP for the twenty-day grouping. Contributions may not add up to 100% due to round-off and non-linearities.

	Mexico	Texas	Eastern U.S.	Western U.S.	GOCART Boundary
20 Most Intense Relative Underpredictions	50%	9%	22%	11%	8%
	55%	5%	18%	12%	9%
20 Most Intense Relative Overpredictions	32%	25%	34%	6%	5%
	39%	22%	26%	6%	7%

Investigation of the mechanisms leading to the divergences between model predictions and observations of fine sulfate at K-Bar does not constitute part of the scope of BRAVO. As discussed in Chapter 4, these mechanisms may include errors in the emissions, meteorological and physicochemical data and/or algorithms used to develop emissions inventories, meteorological fields or used to drive the chemical transport model. Although efforts were made to reduce errors in SO_2 and sulfate concentrations carried over as boundary conditions from the outer (REMSAD) nest to the inner (CMAQ-MADRID) nest, errors may still exist for these species. Furthermore, a similar process was not followed in order to reduce errors in the CMAQ-domain boundary conditions of other critical species such as VOCs, NO_x and CO. In brief, source attribution estimates require careful inspection of the model performance in order to gauge the uncertainty of the attributions.

5.4 Monthly and Overall Attribution Estimates

Tables 5-6 and 5-7 provide a summary of the source contribution to sulfate at K-Bar, BBNP for each month and for the 4-month study period. The results for the 4-month period are also portrayed as pie charts in Figure 5-4. Table 5-8 summarizes the bias exhibited in fine sulfate predictions at K-Bar during each month. As shown in the previous analysis, the relatively lower bias in the overall four-month predictions at K-Bar during BRAVO is a consequence of a compensation of errors by two separate mechanisms of underprediction and overprediction that exhibit similar strengths and occur with similar frequency. It should also be noted that model performance for nitrate, black carbon and organic carbon, lesser contributors to visibility reduction and haze than sulfate, over the four-month period was inferior to model performance for sulfate.

Without accurate knowledge of the reasons for the discrepancy between the predictions and observations, even at extended timescales, using the percentage contributions from source regions can lead to erroneous interpretations of the data. Further research and development of air quality modeling systems, in conjunction with diagnostic evaluations of their component parts (emissions, meteorology and chemical transport), is required in order to elucidate the causes of the discrepancies, improve model performance and allow better interpretation of results.

Table 5-6
Source region attribution of $PM_{2.5}$ sulfate as predicted by CMAQ-MADRID at K-Bar, BBNP, for each month and for the duration of BRAVO (July – October, 1999). The top row of values for an episode denotes the apportionment of the fine sulfate aerosol load at K-Bar, BBNP during the episode. The bottom row of values for an episode denotes the average of the individual daily sulfate apportionment fractions at K-Bar, BBNP during the episode. Contributions may not add up to 100% due to round-off and non-linearities.

	Mexico	Texas	Eastern U.S.	Western U.S.	GOCART Boundary
July	63%	13%	17%	1%	6%
	70%	8%	14%	1%	8%
August	38%	20%	37%	2%	4%
	48%	15%	30%	2%	5%
September	26%	11%	52%	6%	6%
	35%	8%	35%	13%	9%
October	23%	30%	33%	10%	4%
	23%	27%	24%	17%	9%
July - October	32%	19%	38%	6%	5%
	44%	14%	26%	8%	8%

Table 5-7
Average contributions from source regions to the $PM_{2.5}$ sulfate load (concentrations in $\mu g/m^3$) as predicted by CMAQ-MADRID and $PM_{2.5}$ sulfate observations at K-Bar, BBNP, for each month and for the duration of BRAVO (July-October, 1999).

	Mexico	Texas	Eastern U.S.	Western U.S.	GOCART Boundary	Other	Total Predicted	Obs[1]
July	0.75	0.15	0.2	0.01	0.08	-0.01	1.19	1.24
August	0.94	0.50	0.92	0.06	0.09	-0.01	2.50	2.79
September	0.78	0.33	1.57	0.19	0.17	-0.01	3.03	3.10
October	0.77	1.00	1.12	0.34	0.15	0.00	3.38	2.31
July - October	0.81	0.49	0.96	0.15	0.12	-0.01	2.53	2.46

[1] Observed mean data reflects the Jul 4-Oct 28 timeframe without a concentration threshold. Due to lack of measurements, seven days in July that are included in the attribution analysis are not included in the observed mean for July and July-October.

Table 5-8
Bias displayed in the fine sulfate predictions by CMAQ-MADRID at K-Bar, BBNP during the individual months and overall 4-month BRAVO period.[2]

Statistic	July	August	September	October	July - October
Observed Mean SO_4^{2-} ($\mu g/m^3$)	1.38	2.79	3.10	2.31	2.49
Predicted Mean SO_4^{2-} ($\mu g/m^3$)	1.07	2.50	3.03	3.38	2.61
Ratio of Predicted Mean / Observed Mean	0.78	0.90	0.98	1.47	1.05
Normalized Bias	7%	-1%	13%	61%	20%

[2] Statistics reflect valid data for the Jul 2-Oct 28 timeframe above a concentration threshold of 0.1 $\mu g/m^3$.

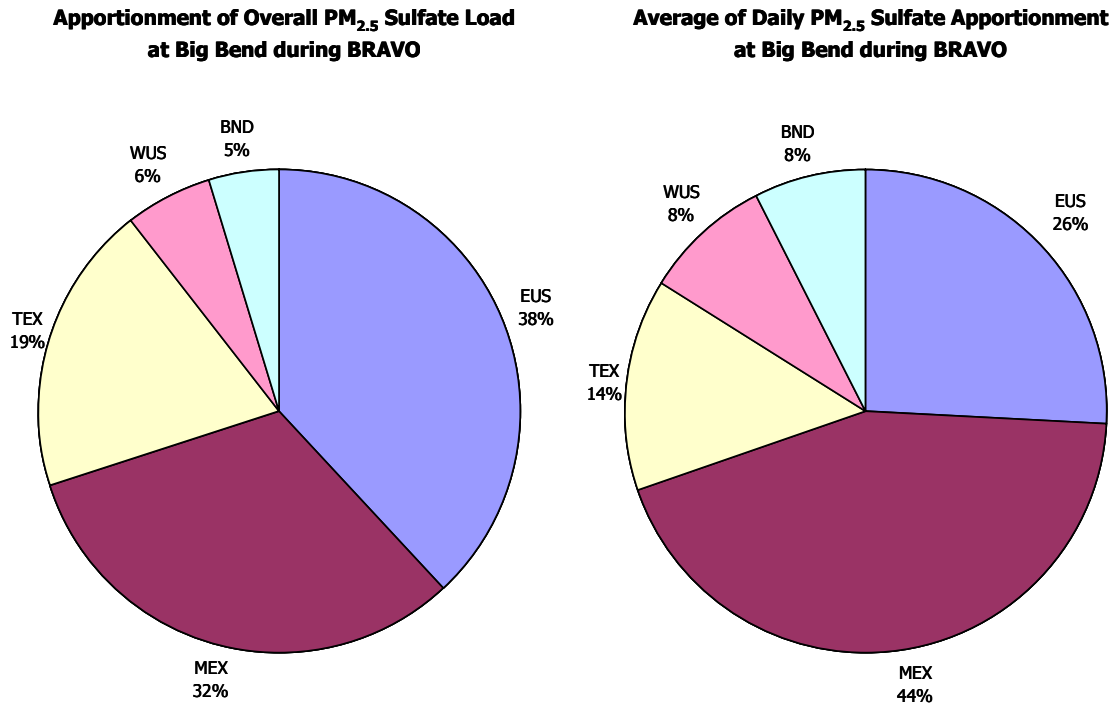

Figure 5-4
Source region attribution of $PM_{2.5}$ sulfate as predicted by CMAQ-MADRID at K-Bar, BBNP, for the duration of BRAVO (July-October, 1999). Source regions are Mexico (MEX); Texas (TEX); eastern U.S. (EUS); western U.S. (WUS), excluding Texas; and boundary conditions (BND) provided by the GOCART model to REMSAD.

6
CONCLUSIONS AND RECOMMENDATIONS

A comprehensive modeling study was conducted using the Community Multiscale Air Quality (CMAQ) model augmented with the Model of Aerosol Dynamics, Reaction, Ionization and Dissolution (MADRID) to simulate regional haze formation at Big Bend National Park during the Big Bend Regional Aerosols and Visibility Observational (BRAVO) study. The BRAVO study included simulations of inert tracers conducted with CMAQ and simulations of transport, chemistry and deposition of ambient gases and particulate matter (PM) conducted with CMAQ-MADRID.

6.1 Tracer Simulations

Tracer simulations were used to evaluate the meteorological inputs and transport components of CMAQ. The transport components of Eulerian models have seldom been evaluated independently of the chemistry modules. BRAVO provided a rare opportunity to test an Eulerian model's ability to simulate the transport and dispersion of pollutants from a point source to a receptor. Tracers were released from four locations: Northeast Texas, Eagle Pass (at the Texas/Mexico border), Houston, and San Antonio. Overall, CMAQ frequently predicted the arrival of tracers at Big Bend National Park (BBNP). However, the model missed several sharp peaks, and occasionally predicted high tracer mixing ratios when they were not observed. The magnitude of the predicted peak mixing ratios (unpaired in time) was too low for the Eagle Pass, Houston, and San Antonio tracers and was too high for the northeast Texas tracer, when compared to the observations at BBNP.

Observed tracer time series were characterized by significant short time-scale fluctuations when tracers arrived at a receptor and low background mixing ratios when the tracer plumes missed the receptor. The low and frequently observed background values tended to distort several of the statistics, e.g., normalized error and bias, customarily used to evaluate 3-D Eulerian models. Hence, the statistical evaluation for BRAVO focused on the overall distribution characteristics of the observed vs. predicted mixing ratios rather than on individual pairs of observed and predicted values. Performance statistics and guidelines should be developed to assess the relationship between the accuracy of the transport modules and the overall accuracy of the modeling system. Without performance criteria for tracers, model performance statistics could not be used to grade the models on an absolute scale (e.g., pass/fail), but provided instead a means to quantitatively compare different model configurations.

In the initial simulations, fine (12-km and 4-km) grids resulted in infrequent transport of tracers to the receptor sites compared to the observations. Several reasons were explored: (1) the accuracy of the meteorological inputs, (2) insufficient amount of dilution, and (3) inefficient horizontal diffusion. While an in-depth investigation of the accuracy of meteorological data at

different resolutions was outside the scope of the current project, a divergence in the predicted plume location may result from small differences in the average resultant wind direction between meteorological simulations with different spatial resolutions. The accuracy requirements for meteorological fields is more stringent for the simulation of primary species such as tracers compared to secondary pollutants (e.g., ozone, sulfate) that are formed over time in the atmosphere and are, consequently, more regionally distributed. The use of larger grid cells, which results in the dilution of pollutants over a larger area once it is injected into or transported to a grid cell, improved the model performance for tracers. Horizontal diffusion schemes also impacted the dispersion characteristics, with the more diffusive Smagorinsky scheme providing better model performance than the original module available in CMAQ. Numerical schemes for solving the advection component of the mass continuity equation in a 3-D model lead to numerical diffusion. Because different levels of numerical diffusion are associated with different advection schemes, the level of simulated diffusion may need to be adjusted with the choice of advection schemes and grid sizes. Thus, the optimal transport characteristics may require careful selection of the grid size, horizontal and vertical diffusion algorithms, and numerical schemes for advection. The best performance was obtained with a horizontal resolution of 36 km and the Smagorinsky horizontal diffusion scheme. The coefficients of correlation between predicted and observed tracer concentrations at BBNP (K-Bar site) were 0.36, 0.31, 0.33, and 0.63 for the Northeast Texas, Eagle Pass, Houston, and San Antonio tracers, respectively.

The seminal conclusion from this tracer performance evaluation is that transport processes should not be undervalued in 3-D modeling. Better characterization of the uncertainties associated with transport processes and their effect on the overall model performance are needed and improvements are required before 3-D models can be used reliably to attribute pollution to individual sources. With their current formulation and inputs, 3-D models are not suitable for simulating the potential impacts of individual sources at specific receptors located hundreds of miles away.

6.2 Particulate Matter Simulations

The model configuration that produced the best results for tracers was then used for the simulations of regional haze conducted with CMAQ-MADRID. The observed concentrations of PM and SO_2 within the BRAVO network were used to evaluate the performance of CMAQ-MADRID. Because sulfate was the dominant component in observed and predicted $PM_{2.5}$, the performance evaluation focused mostly on sulfate and sulfur species. The first round of modeling used boundary conditions from the output of another model, REMSAD, that covered a larger modeling domain (approximately the contiguous United States and northern and central Mexico). An overprediction of sulfur species concentrations from REMSAD was identified that propagated into the CMAQ domain, resulting in a positive bias (overprediction) for sulfate concentrations throughout eastern Texas. Using ambient data to calibrate the boundary conditions resulted in improved performance in the eastern part of the domain, and decreased the domain mean bias of sulfate from 1.6 to 0.9 $\mu g/m^3$. The performance of sulfate at K-Bar, BBNP is as follows: normalized mean gross error of 55%, normalized mean bias of 20%, and coefficient of determination (r^2) of 0.52. If all three BBNP sites are considered together, the normalized mean gross error is 48% and the normalized mean bias is 13%. All three BBNP area sites showed coefficients of determination of 0.5 or above, indicating that CMAQ explained more than 50% of the variance of sulfate at BBNP.

The performance for sulfate concentrations is commensurate with current expectations of PM models (Seigneur, 2001; Seigneur and Moran, 2003). However, some areas of concern are apparent in the simulation. A significant overprediction of sulfate was observed in the eastern part of the modeling domain and in particular along the Gulf coast, calling into question the accuracy of the representation of clouds and aqueous sulfate production processes in that region. By dividing the BRAVO four-month study period into four periods defined by observed concentrations at BBNP, CMAQ-MADRID underestimated sulfate concentrations for the periods extending from July 12 to August 27 and from September 20 to 30, and it overestimated sulfate concentrations for the periods extending from August 28 to September 19 and from October 1 to 28. The periods of overprediction were characterized by flows coming from the East over Texas and are likely due to the overpredictions in sulfate concentrations in eastern Texas mentioned above. The periods of underprediction were characterized by flows that resided largely over Mexico before reaching BBNP. Errors in emissions, meteorological inputs, boundary conditions (e.g., southern sulfur boundary conditions were not calibrated due to a lack of observational data) or model formulation could contribute to divergent model performance.

On average, CMAQ-MADRID satisfactorily predicted the distribution of total sulfur between the gas phase and the particulate phase. However, the low bias was due to compensating over- and underpredictions on individual days. In fact, model predictions of the total sulfur and SO_2 were less satisfactory than those of sulfate. While a primary species such as SO_2 is expected to exhibit a higher degree of fluctuations, reasons for a consistent overprediction of SO_2 at some eastern Texas sites need to be investigated, including possible inaccuracies in the emission inventories of SO_2 and other oxidant and/or particulate-matter precursors such as VOC, NO_x and NH_3.

The second largest PM component, organic material (OM), was underpredicted at all six sites where it was measured. The mean predicted particulate organic material concentration was approximately one-third of the observed OM concentration, and it contributed significantly to the overall underprediction of $PM_{2.5}$ concentrations. There is a need to improve the emission inventories of primary OM and SOA precursors as well as the theoretical understanding of the formation of secondary organic PM.

Particulate nitrate concentrations were low at K-Bar, BBNP during the BRAVO period, with a mean observed concentration of 0.2 $\mu g/m^3$. Although CMAQ-MADRID underestimated nitrate concentrations, the effect on $PM_{2.5}$ concentrations and visibility estimates was negligible.

Concentrations of particulate compounds broadly categorized as “other” compounds (including crustal material, metal oxides and sea salt) accounted for a mean observed concentration of 1.6 $\mu g/m^3$ at K-Bar, BBNP. CMAQ-MADRID underestimated these “other” compounds, which may include PM originating from both regional and global emission sources. Better chemical characterization of this component is needed to allow focused improvements to PM inventories.

6.3 Source Attribution

CMAQ-MADRID was applied to study the attribution of sulfate at K-Bar, BBNP. The CMAQ-MADRID modeling domain was divided into four areas including northern Mexico, Texas and eastern U.S. and western U.S. In addition, information on the influence of a REMSAD source attribution on the CMAQ-MADRID boundary conditions was used to conduct source attribution for regions outside the CMAQ-MADRID domain, i.e., other states of the U.S. Sensitivity simulations were conducted where emissions from a specific source area were removed, and the difference between the base and sensitivity simulations was defined as the contribution from that source area.

For the four-month BRAVO period, the contributions to the average loading of sulfate from Mexico, Texas, eastern U.S., western U.S. and the boundary conditions were respectively 32%, 19%, 38%, 6%, and 5%, respectively. On a monthly basis, the contribution from Mexico was as high as 63% in July and the contribution from eastern U.S. was as high as 52% in September. Contributions from all source areas were important in October.

These results need to be interpreted with caution because of model performance issues. For example, ten out of the 20 days with the most significant underpredictions occurred in October. Therefore, the processes leading to poor model performance were not random and this type of systematic errors will affect source attribution results, especially for individual days or episodes. Some inferences could be made regarding the effects of model performance issues on source attribution results. However, additional diagnostic analyses of the causes of poor performance on specific days need to be conducted before such inferences can be confirmed. Such diagnostic analyses should be used to guide model and data development efforts, resulting in better model performance and, consequently, more reliable source attribution.

7
REFERENCES

Anthes, R.A. and T.T. Warner, 1978. Development of hydrodynamic models suitable for air pollution and other mesometeorological studies, *Mon. Wea. Rev*., **106**, 1045-1078.

Barna, M., B. Schichtel, D. Fox, K. Gebhart, W. Malm, 2003. Assessing the impact of regional pollution sources on air quality and visibility at Big Bend National Park with REMSAD, paper number 69839, A&WMA's 96th Annual Conference and Exhibition, June 2003, San Diego, CA

Byun, D. and J. Ching, 1999. Science Algorithms of the EPA Models-3 Community Multiscale Air Quality (CMAQ) Modeling System EPA/600/R-99/030, United States Environmental Protection Agency, Office of Research and Development, Washington, DC 20460.

Byun, D.W., J. Pleim, R.T. Tang and A. Bourgeois, 1999. Meteorology-Chemistry Interface Processor (MCIP) for Models-3 Community Multiscale Air Quality (CMAQ) modeling system, Chapter 12, *in* Byun and Ching, 1999, *Op. Cit.*

Chin, M., R. B. Rood, S.-J. Lin, J. F. Muller, and A. M. Thomspon, 2000a. Atmospheric sulfur cycle in the global model GOCART: Model description and global properties, *J. Geophys. Res.,* **105,** 24,671-24,687.

Chin, M., D. Savoie, D. Thornton, A. Bandy, and B. Huebert, 2000b. Atmospheric sulfur cycle in the global model GOCART: Comparison with observations, *J. Geophys. Res.,* **105,** 24,698-24,712.

Dudhia, J., 1993. A nonhydrostatic version of the Penn State/NCAR mesoscale model: Validation tests and simulation of an Atlantic Cyclone and Cold Front, *Mon. Wea. Rev*., **121**, 1493-1513.

EPRI, 2002. Community Multiscale Air Quality – Model of Aerosol Dynamics, Reaction, Ionization, and dissolution (CMAQ-MADRID): Technical Documentation, EPRI, Palo Alto, CA: 2002. 1005239

Gebhart, K., B. Schichtel, M. Barna, 2003. Comparison of results of back-trajectory modeling using several combinations of models and input wind fields during the BRAVO study, paper number 69929, A&WMA's 96th Annual Conference and Exhibition, June 2003, San Diego, CA.

Houyoux, M.R., J.M. Vukovich, C.J. Coats, N.J.M. Wheeler and P.S. Kasibhalta, 2000. *J. Geophys. Res*., **105**, 9079-9090.

Nenes, A., C. Pilinis and S.N. Panmdis, 1999. Continued development and testing of a new thermodynamic aerosol module for urban and regional air quality models, *Atmos. Environ.*, **33**, 1553-1560.

Pitchford, M.L., M.C.Green, H.D. Kuhns, V. Etyemezian, R. Dietz, T. Watson, 2001. Perfluorocarbon Tracers Used to Study Transport and Dispersion During the BRAVO Study, Proceedings of the Regional Haze and Global Radiation Balance- Aerosol Measurements and Models: Closure, Reconciliation, and Evaluation, October 2-5, 2001, Bend, OR.

Pun, B.K., C. Seigneur, S.-Y. Wu, N. Kumar, 2003a. Simulating inert tracers in the BRAVO project using CMAQ, paper number 69802, A&WMA's 96th Annual Conference and Exhibition, June 2003, San Diego, CA

Pun, B.K., S.-Y. Wu, C. Seigneur, J.H. Seinfeld, R.J. Griffin, S.N. Pandis, 2003b. Uncertainties in modeling secondary organic aerosols: three-dimensional modeling studies in Nashville/western Tennessee, *Environ. Sci. Technol.*, **37**, 3647-3661.

Schichtel, B., K. Gebhart, W. Malm, M. Barna, 2003. Assessment of the source receptor relations at Big Bend using forward airmass histories, paper number 69918, A&WMA's 96th Annual Conference and Exhibition, June 2003, San Diego, CA.

Seaman, N.L. and D.R. Stauffer, 2003. MM5 Modeling in support of the Big Bend Regional Aerosol and Visibility Observation Study (BRAVO), EPRI, Palo Alto, CA.

Seigneur, C., 2001. Current status of air quality models for particulate matter, *J. Air Waste Manage. Assoc.*, **51**, 1508-1521.

Seigneur, C. and M. Moran, 2003. Chapter 8: Chemical transport models, *in* Particulate Matter Science for Policy Makers: A NARSTO Assessment, EPRI 1007735, P.H. McMurry, M. Shepherd and J. Vickery, eds.

Stauffer, D.R. and N.L. Seaman, 1994. Multiscale four-dimensional data assimilation, *J. Appl. Meteor.*, **33**, 416-434.

Turpin, B.J. and H.-J. Lim, 2001. Species contribution to $PM_{2.5}$ mass concentrations: revisiting common assumptions for estimating organic mass, **35**, 602-610.

Vukovich, J., H. Kuhns, 2003. The emissions inventories and SMOKE modeling efforts used to support the BRAVO study, paper number 69865, A&WMA's 96th Annual Conference and Exhibition, June 2003, San Diego, CA

Vukovich, J., 2002. Technical report: emissions processing for the Big Bend Regional Aerosol and Visibility Observation (BRAVO) study.

Zhang, Y., B. Pun, K. Vijayaraghavan, S.-Y. Wu, C. Seigneur, S. Pandis, M. Jacobson, A. Nenes and J.H. Seinfeld, 2004. Development and application of the Model of Aerosol Dynamics, Reaction, Ionization and Dissolution, *J. Geophys. Res*, in press.

A
PERSPECTIVES ON THE TRAJECTORY MASS BALANCE METHOD FOR SULFATE SOURCE APPORTIONMENT

MEMORANDUM

TO: Naresh Kumar

FROM: Betty Pun and Christian Seigneur

RE: Perspectives on the Trajectory Mass Balance Method for Sulfate Source Apportionment

DATE: 18 April 2003

---

1. Introduction

The use of both source and receptor models is recommended for particulate matter (PM) source apportionment exercises because currently no single model can be considered accurate enough for the purpose (NARSTO, 2003). The insufficiency of models stems from incomplete knowledge regarding the processes that contribute to the formation of some PM components, as well as imperfect data used in the modeling exercises. While corroboration between source and receptor models may increase our confidence regarding source attribution results, we also need to be aware of limitations of both types of models in order to assimilate results wisely.

In the Big Bend Regional Aerosol and Visibility Observational (BRAVO) study, both source modeling and receptor modeling are applied to apportion PM to different source regions. Two source models are applied, CMAQ-MADRID and REMSAD. The uncertainties associated with source models and their input data are documented elsewhere (NARSTO, 2003). Here, we provide an introduction and some review on one of the receptor models applied in BRAVO, the Trajectory Mass Balance (TrMB) method, which has been used to apportion sulfate in various studies (Gebhart and Malm, 1989, 1994; Gebhart et al., 1988, 1993; Iyer 1986; Malm, 1989, 1992; Malm et al., 1989, 1994; Pitchford and Pitchford, 1985), BRAVO being the latest.

2. How Does Trajectory Mass Balance (TrMB) Work?

Traditional receptor modeling methods are considered most accurate for inert pollutants. Some techniques are more restrictive and assume that the source characteristics (e.g., composition) do not change between the source and receptor. Trajectory mass balance (TrMB) was designed to circumvent the limitations of traditional receptor modeling methods, because it takes into account long range transport and some chemistry, deposition, and entrainment processes.

The basic equation governing TrMB is as follows (Iyer, 1986):

$$C_{it} = \sum_{j=1}^{J} Q_{ijt}\, T_{ijt}\, N_{jt}\, E_{ijt} \qquad \textbf{Equation 1}$$

where:

- i is the subscript for a specific species
- t is the subscript for a time period
- j is the subscript for a source area
- C is the concentration at the receptor site of species i at time t
- Q is the total emission for species i (or its precursor) at source area j that corresponds to the measurement at time t
- T is the factor representing transformation, diffusion and deposition of species i between the source area j and the receptor for the sample at time t
- N is the number of trajector end points per unit volume in source area j for the sample at time t
- E is an entrainment factor to account for the coupling between the transport layer and the layer in which pollutant i is emitted.

In practice, many of the terms in Equation 1 are unknown. For applications to sulfate, let's consider two special cases. We shall drop the subscript i in the following discussion. In case 1,

the only know quantities are the concentrations C_t, the source strength Q_{jt}, and the number of end points N_{jt}. Let

$$K_{jt} = Q_{jt} N_{jt} \qquad \textbf{Equation 2}$$

$$B_{jt} = T_{jt} E_{jt} \qquad \textbf{Equation 3}$$

The unknown quantity B_{jt} is then averaged temporally as follows:

$$B_{jt} = B_j + \text{error} \qquad \textbf{Equation 4}$$

where B_j is the temporally averaged value of B_{jt}. Therefore, Equation 1 is reformulated as:

$$C_t = C_0 + \sum_{j=1}^{J} B_j K_{jt} + error_t \qquad \textbf{Equation 5}$$

In Equation 5, C_0 represents the average contribution of the sources not considered in source areas 1 through J. The error term in Equation 5 represents not only the error associated with Equation 4, but also measurement errors. As long as the errors involved in Equation 4 and Equation 5 are random and not systematic, Equation 5 is simply a multiple linear regression problem. The values of B_j can be determined using standard linear programming packages. In some applications, constraints that C_0 and B_j are non-negative may need to be imposed in the solution process.

Once the coefficients B_j and intercept C_0 are estimated, say to have values of β_j and β_0, the estimated concentration at time t can be calculated from the regression model such that

$$\chi_t = \beta_0 + \sum_{j=1}^{J} \beta_j K_{jt} \qquad \textbf{Equation 6}$$

A statistical comparison (e.g., r^2 value) between χ_t and C_t provides some indication of the performance of the regression model. The fractional contribution of source area j to the sample at time t is then defined as

$$F_{jt} = \beta_j K_{jt} / \chi_t \qquad \textbf{Equation 7}$$

The average fractional source contribution of source area j over the entire sampling campaign is then calculated as

$$F_j = \sum_{t=1}^{T} \beta_j K_{jt} \Big/ \sum_{t=1}^{T} \chi_t \qquad \textbf{Equation 8}$$

In the second special case, C_t and N_{jt} are the only known quantities. The formulation of the multiple linear regression problem is quite similar to the first case above. Equation 5 can be rewritten as:

$$C_t = C_0 + \sum_{j=1}^{J} B_j N_{jt} + error_t \qquad \textbf{Equation 9}$$

where in this case, B_j is the temporal average of B_{jt}, which is defined as the product of three quantities: T_{jt}, E_{jt}, and Q_{it}. Analogous to Equation 8, after obtaining the coefficients B_j from regression, the fractional contribution of each source area can be determined as:

$$F_j = \sum_{t=1}^{T} \beta_j N_{jt} \Big/ \sum_{t=1}^{T} \chi_t \qquad \textbf{Equation 10}$$

So far, emission information has not been used in the TrMB analysis for BRAVO. Therefore, Equation 10 represents the source apportionment model used.

3. Assumptions in TrMB

To understand the assumptions that are involved in the derivation of the TrMB equations, especially for secondary sulfate PM, let's first look at individual terms in the right hand side of Equation 1. Given the assumption that primary emissions of sulfate are small compared to atmospheric formation, Q represents the emission of SO_2 from a source area or more appropriately, a source "volume," since elevated point source emissions areconsidered in many cases.

T_{jt} is an unknown that represents the transformation, diffusion, and deposition of air originating from the source area and reaching the receptor at time t. All sources of SO_2 within one source area are treated the same way and the methodology cannot segregate between different source types. For a given area, an implicit assumption is that all sources within that area share the same chemistry and dispersion characteristics at that given time. This assumption may be questionable in some cases. First, the sulfur chemistry in large point source plumes differs significantly from the chemistry in the ambient atmosphere (Richards et al. 1981; Gillani et al., 1998; Karamchandani et al., 1998, 2002), and if more than one major point source reside within one source area, the chemistry within distinct plumes may not be identical. Second, since sulfur chemistry is affected by the presence of clouds, a difference in cloud characteristics within the source region may result in inhomogeneous T factors. Third, the characterization of non-linear sulfur chemistry using a single factor cannot be considered accurate. Using the results of TrMB properly to analyze temporally averaged source contributions will remove some uncertainties associated with temporal variability. Uncertainties due to spatial variability are intrinsic in TrMB applications.

N_{ij}, the number of back trajectory end points in each source region, is assumed to be proportional to the probability that air from that source region is included in the sample measured at time t.

E_{jt} is another "fitted" parameter for a source region, which should in theory be defined for each individual source within the source region. As such, similar model assumptions involved in the determination of T_{jt} also affect E_{jt}.

One limitation of Equation 1 is that linear independence between source areas is necessary for the estimate of individual source area contribution. For example, if all trajectories that pass through one area also pass through another, it will be impossible to distinguish between the contribution from those two areas. This co-linearity problem can be avoided (e.g., by combining source areas), but the solutions are not always acceptable (e.g., due to political boundaries).

A second source of model uncertainties is the approximation shown in Equation 4, where a time-dependent quantity is approximated by its temporal average. This approximation is acceptable if errors are random. However, this is not always the case, especially because T_{jk} is a function of meteorological parameters, such as mixing height, precipitation, temperature, and relative humidity, which are sources of systematic errors (Gebhart and Malm, 1990).

Finally, to solve a set of equations in the form of Equation 5 by regression, there needs to be sufficient independent equations (for C_t) for the designated number of regressed variables, which correspond to the number of source areas. The accuracy of the known term in Equation 5 ($Q_{jt}N_{jt}$ or N_{jt}) for each individual equation for C_t depends on the quality of data on Q and N. Background and sources unaccounted for are estimated from C_0, the intercept. However, errors and uncertainties in N (discussed below) sometimes result in a larger than reasonable intercept term C_0 (Gebhart et al., 1998). Therefore, in the BRAVO application the intercept is fixed at zero, a procedure that is equivalent to assuming that all sources are accounted for. Background sulfate that enters through the boundary is not considered. In general, this procedure tends to provide an upper limit estimate for the contribution of source areas considered in the study, especially source regions close to the edge of the domain. In BRAVO, the boundary contributions may be small (say, less than 10%) because the continental U.S. and Mexico are included as source areas.

4. Uncertainties in the Input Data

For sulfate apportionment, the key input data include concentration, back trajectory end points, and in some cases precursor emissions. Both concentration and emission data are subject to measurement uncertainties. The determination of "end points" requires a back trajectory model to interpolate between modeled or measured wind data. Many previous studies were conducted using the Air Resources Laboratory Atmospheric Transport and Diffusion (ARL-ATAD) model, which is also used in the BRAVO study. Some have argued that uncertainties in the back trajectories may be as large as several hundred kilometers after 5 days of travel time (Gebhart and Malm, 1990). Unless there are systematic errors in the back trajectories, the effect of their uncertainties on the average source contributions should be less significant than on individual days. In addition, stagnant conditions present a challenge for ARL-ATAD. Wind components predicted by prognostic models such as MM5 are likely to be less accurate under stagnant conditions.

In BRAVO, several combinations of model and data have been used by Gebhart in the calculation of trajectory end points to test the sensitivity of the TrMB results. Analyses of these results as a set may provide higher confidence to the source apportionment despite the uncertainties of individual back trajectories. The models include ATAD, Hysplit, and CAPITA Monte Carlo. Meteorology data tested include raw soundings (with and without BRAVO profiles), EDAS, FNL (EDAS and FNL are both observation analysis models) and MM5. Both 3-day and 5-day trajectories are used in BRAVO. Gebhart (2002) shows that on some days, the trajectories may be very different, while they can be quite similar on other days. It is worth noting that ATAD gives 160 end points over a 24-hour sampling period (4 starts x 40 end points per 5-day trajectory), Hysplit provides 2880 end points (24 starts x 120 end points per 5-day trajectory). The level of confidence for N_{jt} may be higher when more end points are used. With the Hysplit model, the maximum trajectory length can also be extended to 10 days, which may be more commensurate with the life time of fine PM. For example, trajectories that end over the Gulf of Mexico after 3 or 5 days may have originated from the Ohio River Valley if more days are tracked.

As shown in Gebhart (2002), some trajectory end points reside over the open ocean. In these cases, the end points that do not correspond to source areas are excluded from the source apportionment calculation. However, end points over parts of Gulf of Mexico that are close to shore are included because marine emissions are considered in the SE Texas source area.

5. Other Issues that Arise During the Application of TrMB

The selection of a set of "source areas" suitable for the BRAVO study involved several intense discussions. From a modeler's perspective, several concerns were mentioned above and summarized here. The set of source areas must be comprehensive enough such that all important sources are considered. Each source area should be relatively large so that errors in the determination of trajectory end points have relatively smaller effect on the source attribution, especially for source areas farther away from the receptor. Each source area also need to contain sources that are homogeneous in terms of their chemical and transport behavior. Co-linearity in transport patterns may prevent source areas from being distinguished by the regression techniques (e.g., West Texas and SE New Mexico). These antagonistic needs make the definition of source areas a complex optimization problem. The consideration of political boundaries, which is also necessary from a practical standpoint, introduces another layer of complexity.

When source strength information was used in TrMB in the past, monthly information represents the highest level of temporal resolution at key sources. If more detailed information (e.g., daily) is available for BRAVO, care needs to be taken to match concentrations at the receptor site at time t to the emissions at t-t_{jt}' where t_{jt}' represents the transport time between the source area j at time t. In theory, the use of emission data in the TrMB model should improve its apportionment results. In practice, uncertainties in emission data may limit the benefit of incorporating emission data in TrMB analyses. Therefore, emissions data have so far not been utilized in TrMB analyses for BRAVO.

6. Conclusions and Recommendations

There are some intrinsic uncertainties associated with the formulation and application of TrMB, as discussed above. In conclusion, we would like to raise two areas that may be problematic.

Is there an intrinsic difficulty for estimating source contributions from far away sources? We have previously discussed issues relating to accuracy of back trajectories, whose uncertainties tend to grow with time. Therefore, the number of end points connecting a far away area to the receptor tends to be more uncertain relative to a close by source area. In addition, on a per unit area basis, the probability of end point per area is lower for a far away source compared to a close by source area. For example, consider a trajectory of fixed wind speed and fixed wind direction that goes a distance of Δr between two end points. Let's consider two source areas, both with an area of 1, distance R and R' from the receptor, where R' >> R. The probability of the trajectory passing through these areas are approximately $1/2\pi R\Delta r$ and $1/2\pi R'\Delta r$, respectively (provided that $2\pi R\Delta r > 1$). The method breaks down for source areas very close to the receptor because there are end points in these areas for every measured sample. Therefore, areas very close to the receptor are excluded in the source attribution analysis. For the areas that are considered, if a certain number of trajectory end points are required to be in each source area to resolve different source areas properly, the farther a source area is from the receptor, the larger its area needs to be for the same number of end points in a probabilistic sense. However, a larger source area is subject to larger variabilities in other parameters, such as T_{it} and E_{it}. Therefore, source apportionment to areas farther away may be less accurate than to areas closer to the receptor site. This may partly explain why when applied to simulate tracers, TrMB performs better for the close by Eagle Pass tracer than for the far away NE Texas tracer. (The NE Texas tracer measurements were low and also quite noisy, and the near zero average concentrations present a high degree of challenge for observation-based techniques such as TrMB.)

Are there performance issues in terms of extreme days? The current level of performance of TrMB over the entire BRAVO period (r^2 ~ 0.5 to 0.7) is commensurate with previous studies. As shown in Equations 5 and 9, a temporal average transport characteristic is applied to each source area. Therefore, the model may be less accurate for days with high and low sulfate concentrations, which are of concern in the regulatory standpoint. Given longer term monitoring, days with high and low concentrations could be analyzed separately. However, the data base may be insufficient for those specific analysis for BRAVO.

TrMB is quite a powerful tool that has been applied with some success for several locations. Like all models, it contains assumptions and is subject to uncertainties in input data, summarized as follows:

- All sources within one defined source area are assumed to share the same chemistry, dispersion, and entrainment characteristics; and it is assumed that these effects can be represented by a single factor.
- Contributions from different source areas are assumed to be linearly independent in the mathematical sense.
- Time-dependent quantities, such as chemistry, are approximated by their averages and associated errors, which are assumed to be random.

- Background contributions are ignored; i.e., only contributions from the source areas included in the analysis are considered.
- TrMB is affected by uncertainties in back trajectories, and it needs sufficient trajectory end points (product of the number of trajectories per sample, length of each trajectory, and frequency of end points) to resolve each source area.

These assumptions and uncertainties need to be taken into account when comparing TrMB results to those of other models and drawing conclusions for source apportionment. Several tests are recommended to provide better confidence on the TrMB results, and provide valuable information when comparing results with those of Eulerian models:

1. Define source areas corresponding to the modeler's best judgement for the application of TrMB, and compare the results with the current source area set used for BRAVO

2. Test the sensitivity of the TrMB results to the length of trajectories and number of endpoints. For example, longer back trajectories may be used, because the atmospheric lifetime of PM2.5 may be more than 5 days without precipitation.

3. Include end points over the ocean as a "background" source area, where applicable. For cases where the back trajectory originates on land, passes over the ocean, and returns to land, the earlier land portion of trajectory should also be included.

4. If sufficient data exist, segregate between high sulfate days and low sulfate days to evaluate the effect of systematic variations (e.g., of meteorology effects) around the average value.

References:

Gebhart, 2002. Trajectory/Wind Field Comparisons and Initial Trajectory Mass Balance Results. Presentation at the BRAVO meeting in Lakewood, CO, October 10-11, 2002. (This presentation contained preliminary results and was not distributed.)

Gebhart, K.A. and W.C. Malm, 1989. Source Apportionment of Particulate Sulfate Concentrations at Three National Parks in the Eastern United States. Transactions of the A&WMA/EPA Specialty Conference-Visibility and Fine Particles, Estes Park, CO, Oct. 15-19, 1989, pp. 898-913, C.V. Mathai, Ed.

Gebhart, K. A. and W.C. Malm, 1994. Source Attribution and Statistical Summary of Data Measured at Grand Canyon National Park during 1989-1991, Proceedings of "Aerosols and Atmospheric Optics", Snowbird, UT, Sept 1994, pp. 1098-1124

Gebhart, K.A., R.A. Alhbrandt, W.C. Malm, and H.K. Iyer, 1988. Estimating the Fractional Contribution of Secondary Aerosols from Different Source Areas on a Regional Scale, Preprints of the 81st Annual APCA Meeting, Dallas, TX, June 1988, Paper No. 88-054.06

Gebhart, K.A., W.C. Malm, and H.K. Iyer, 1993. Comparison of Two Back Trajectory Techniques for Source Apportionment, Preprints of the 86th Annual A&WMA Meeting, Denver, CO, June 13-18, 1993

Gillani, N. V., J. F. Meagher, R. J. Valente, R. E. Imhoff, R. L. Tanner, and M. Luria, 1998. Relative production of ozone and nitrates in urban and rural power plant plumes 1. Composite results based on data from 10 field measurements days, J. Geophys. Res., 103, 22593–22615.

Iyer, H. K., 1986. A Mass Balance Method for Estimating the Fractional Contributions of Pollutants from Various Sources to a Receptor Site, Visibility Protection-Research & Policy Aspects, pp 861-871, Grand Teton NP, APCA Conf. Sept. 1986.

Karamchandani, P., A. Koo, C. Seigneur, 1998. A reduced gas-phase kinetic mechanism for atmopsheric plume chemistry, Environ. Sci. Technol., 32 , 1709-1720.

Karamchandani, P., C. Seigneur, K. Vijayaraghavan, S.Y. Wu, 2002. Development and application of a state-of-the-science plume-in-grid model, J. Geophys. Res. (October 2002)

Malm, W.C., K.A. Gebhart, J. Molenar, T. Cahill, R. Eldred, and D. Huffman, 1994. Examining the Relationship between Atmospheric Aerosols and Light Extinction at Mount Rainier and North Cascades National Parks, Atmos. Environ., 28, 347-360.

Malm, W.C., 1989. Atmospheric Haze: Its Sources and Effects on Visibility in Rural Areas of the Continental United States, Environ. Monitoring and Assess., 12, 203-225.

Malm, W.C., 1992. Characteristics and Origins of Haze in the Continental United States, Earth Sci. Rev., 33, 1-36.

Malm, W.C., H.K. Iyer, J. Watson, and D.A. Latimer, 1989. Survey of a Variety of Receptor Modeling Techniques, Transactions of the A&WMA/EPA Specialty Conference-Visibility & Fine Particles, Estes Park, CO, Oct. 15-19, 1989, pp. 781-805, C.V. Mathai, Ed.

NARSTO 2003. Particulate Matter Science for Policy Makers: A NARSTO Assessment, February, 2003, document number EPRI 1007735.

Pitchford, M., and A. Pitchford, 1985. Analysis of Regional Visibility in the Southwest using Principal Component and Back Trajectory Techniques, Atmos. Environ., 19, 1301 1316.

Richards, L. W., J. A. Anderson, D. L. Blumenthal, A. Brandt, J. A. McDonald, N. Waters, E. S. Macias, and P. S. Bhardwaja, 1981. The chemistry, aerosol physics and optical properties of a western coal-fired power plant plume, Atmos. Environ., 15, 2111 2134.

B
THE BRAVO EMISSIONS INVENTORY: INSIGHTS AND OVERSIGHTS

B.1 GCTVC and Information Secretariat of Energy of Mexico

Initial analysis of REMSAD and preliminary CMAQ-MADRID modeling results suggested that there could be a potential underestimation of SO_2 emissions in the Mexican regions of the *1999 BRAVO Emissions Inventory (BRAVO EI)*. This suggestion echoed observations from modeling studies by the Grand Canyon Visibility Transport Commission, where researchers reached a similar conclusion by observing that predicted sulfate concentrations differed from measurements in the Southern California desert most greatly near the Mexican border, with the discrepancy diminishing with distance north of the border. As part of modeling studies in Project VARED (Visibility Assessment of Regional Emissions Distributions), investigators assumed that the differences between predictions made using a transport-coefficient model and measurements at three desert receptors were caused by the underestimation of Mexican area source emissions (from three regions: Ensenada, Mexicali and Nogales) by an unknown constant factor and the omission of a fixed, unknown amount of offshore emissions (assumed emitted from a single region off the coast of Southern California). Linear model analysis indicated that Mexican emissions may have been underestimated by a factor of 7.4. When original estimates of SO_2 emissions in the GCVTC studies were multiplied by this factor, Mexican SO_2 emissions became commensurate with the range of SO_2 emissions estimated by receptor-modeling studies for regions of Mexico near the U.S. border. As part of the BRAVO Study, the final SO_2 emissions used in the GCVTC analysis were compared to SO_2 emissions in common areas within the *1999 BRAVO EI.* (The contribution from the *Carbon* power plants was excluded from the comparison of these two inventories.) The GCVTC values exceeded the *1999 BRAVO EI* in those regions by a factor of 4.2.

The comparison with the GCVTC values supported the theory that the *1999 BRAVO EI* may underestimate SO_2 emissions. However, the basis of the GCVTC SO_2 emissions was built on a plethora of assumptions and inferences. SO_2 emissions estimates from a presentation imparted by the Secretariat of Energy of Mexico (*Secretaría de Energía – SENER*) to members of the BRAVO Technical Committee were compared for the *Carbon* power plants and for three BRAVO states contained within the smaller BRAVO modeling domain (the CMAQ-MADRID domain). The *1999 BRAVO EI* used estimates for SO_2 emissions at the *Carbon* power plants provided by Southern California Edison/U.S. EPA of ~241,000 tons per year. These were used in all CMAQ-MADRID simulations. However, the REMSAD simulations applied an SO_2 emissions rate at the *Carbon* as found the SENER presentation of ~152,000 tons per year.

The *Carbon* power plants are the largest SO_2 source in the state of Coahuila. It follows that the uncertainty of the SO_2 emissions in that state is different in nature to the broader uncertainty of SO_2 emissions across the rest of Mexico. Therefore, ensuing discussion on SO_2 emissions in Mexico focuses attention to SO_2 emissions apart from the *Carbon* power plant facility. When comparing the SO_2 emissions in the three Mexican states within the smaller BRAVO domain, SO_2 emissions provided by SENER exceeded those contained in the *1999 BRAVO EI* by a factor of 1.8, again excluding the contribution from the *Carbon* power plants from both inventories. As a result of this analysis, emissions of SO_2 and sulfate within the Mexican portion of the CMAQ-MADRID domain were increased by a factor of two, with the exception of emissions from the *Carbon* power plants.

Doubling non-*Carbón* Mexican emissions in the CMAQ-MADRID simulations resulted in an increase of total Mexican SO_2 emissions – including the *Carbón* facilities – within the smaller BRAVO domain by a factor of 1.54, i.e. an increase of 54%. REMSAD simulations with increases to the Mexican emissions were not performed and, therefore, the Mexican boundary conditions provided by REMSAD to the CMAQ-MADRID simulations were not altered in any fashion. Thereby, anthropogenic Mexican emissions of SO_2 in the larger BRAVO domain as a result of CMAQ-MADRID simulations were increased by only 22%. (If the Popocatépetl volcano emissions were included in the analysis, overall Mexican SO_2 emissions were increased by 10%.)

B.2 Mexican National Emissions Inventory, 1999

The first draft of the *Mexican National Emissions Inventory, 1999* was released for public review on July 21, 2003. The emissions inventory is being developed for the Mexican Secretariat of the Environment and Natural Resources (*Secretaría de Medio Ambiente y Recursos Naturales – SEMARNAT*) and National Institute of Ecology (*Instituto Nacional de Ecología – INE*), with funding support from the United States Environmental Protection Agency (U.S. EPA), Western Governors' Association (WGA), and the North American Commission for Environmental Cooperation (CEC). The first draft of the inventory contains emissions estimates for point, area and on-road mobile sources during 1999 for the six northernmost states of Mexico: Baja California Norte, Sonora, Chihuahua, Coahuila, Nuevo León, and Tamaulipas. Non-road mobile source emissions, such as emissions from agricultural and construction equipment, are not included in the draft document. The first draft of the inventory contains state-level estimates for nitrogen oxides (NO_x), sulfur oxides (SO_x), total (unspeciated) volatile organic compounds (VOC), carbon monoxide (CO), ammonia (NH_3), total (unspeciated) particulate matter less than 10 μm in aerodynamic diameter (PM_{10}), and total (unspeciated) particulate matter less than 2.5 μm in aerodynamic diameter ($PM_{2.5}$). A second draft of the inventory, planned for release in February 2004, will contain emissions estimates for the entire country, i.e. the six northern states, the remaining 25 Mexican states and the Federal District. The final report, planned for release in June 2004, will provide emissions estimates for the entire country down to the municipality level.

The release of the first draft of *Mexican National Emissions Inventory, 1999* – henceforth abbreviated as the *1999 N MX NEI* – coincided with the analysis of the results from the REMSAD and CMAQ-MADRID air quality model simulations. Information from the *1999 N MX NEI* could not be incorporated into model simulations for several reasons, including (but not limited to):

- the draft inventory estimates emissions only in the six northernmost states,
- the draft inventory contains no non-road mobile source emissions, and
- the draft inventory currently provides only state-level summaries thus precluding allocation of emissions data to the REMSAD or CMAQ-MADRID model grids.

However, the BRAVO Technical Committee agreed that a comparison of the *1999 BRAVO EI* with the *1999 N MX NEI* could provide additional insights to the nature of the uncertainty in emissions beyond the United States used by the air quality models. Notwithstanding, it is important to note that the *1999 N MX NEI* emission estimates are under technical review and thereby subject to change.

Tables B-1 and B-2 shows display the differences between the *1999 BRAVO EI* and the *1999 N MX NEI* for the six common states. For the state of Coahuila, it is evident that the *1999 N MX NEI* applies a value for Carbon power plant emissions lower than 241,000 tons per year assumed in the *BRAVO EI.* The values for SO_2 emissions in the state of Sonora in the 1999 *N MX NEI* have been lowered from the value found in the July 2003 draft document according to recommendations by Acosta y Asociados (Gildardo Acosta, e-mail communication to the BRAVO Technical Committee). Nonetheless, SO_2 emissions are a factor of 1.4 lower in the *1999 BRAVO EI* in comparison to the *1999 N MX NEI* for regions outside of Coahuila.

Table B-1. Aggregate on-road mobile, non-road mobile, area and point sources – *1999 BRAVO EI* (tpy)

State Name	CO	NO_x	SO_2	VOC	NH_3	$PM_{2.5}$	PM_{10}
Baja California N.	854,940	73,402	67,635	185,676	13,323	42,012	152,716
Coahuila	498,262	110,632	278,970	106,945	13,067	24,419	76,650
Chihuahua	1,177,308	77,672	56,685	211,737	42,596	37,632	111,982
Nuevo Leon	1,495,953	91,396	88,221	215,350	17,082	70,810	172,426
Sonora	514,906	42,888	90,520	141,949	27,156	23,105	64,167
Tamaulipas	974,112	62,963	120,122	178,449	67,014	45,589	122,713
Total	5,515,479	458,951	702,151	1,040,104	180,237	243,565	700,654

Table B-2. Aggregate on-road mobile, area and point sources – *1999 N MX NEI* (w/o non-road mobile sources, tpy)

State Name	CO	NO_x	SO_2	VOC	NH_3	$PM_{2.5}$	PM_{10}
Baja California N.	309,907	31,001	54,885	93,721	9,290	24,856	81,174
Coahuila	185,953	132,991	180,586	67,110	24,336	165,575	230,623
Chihuahua	355,777	51,289	101,450	100,971	57,622	42,369	135,539
Nuevo Leon	410,587	62,473	93,573	110,374	31,854	77,844	258,496
Sonora	157,663	46,685	176,396	64,354	70,464	35,169	112,951
Tamaulipas	208,530	33,507	158,112	68,552	51,385	25,324	86,100
Total	1,628,416	357,946	765,002	505,081	244,951	371,137	904,883

Emissions of NH_3, $PM_{2.5}$ and PM_{10} are all lower in the *1999 BRAVO EI* by factors of 1.4, 1.5 and 1.3, respectively. Assuming that the draft *1999 N MX NEI* better represents the reality of Mexican emissions, underprediction of emissions of primary particles and two important precursors to secondary particulate matter, NH_3 and SO_2, may compromise the ability of the air quality models to accurately represent particulate matter derived from activities in Mexico. However, the most notable discrepancy is observed for the estimates of CO and VOC emissions, where the *1999 BRAVO EI* exceeds the *1999 N MX NEI* by factors of 3.4 and 2.1, respectively. Without further analysis, it is uncertain how the increased levels of CO, VOC and NO_x emissions may have influenced the oxidative capacity of the region in model simulations.

Table B-3. Comparison of SO_2 Emissions in the *1999 BRAVO EI* and *1999 N MX NEI (tpy)

State Name	BRAVO EI Point	N MX NEI Point	N MX NEI/ BRAVO	BRAVO EI Area + Mobile	N MX NEI* Area + Mobile	N MX NEI*/ BRAVO EI Area + Mobile	BRAVO EI Sum	N MX NEI* Sum	N MX NEI*/ BRAVO Sum
Baja California N.	24,090	26,605	1.1	43,545	28,280	0.6	67,635	54,885	0.8
Coahuila	260,975	157,762	0.6	17,995	22,824	1.3	278,970	180,586	0.6
Chihuahua	37,267	65,187	1.7	19,418	36,263	1.9	56,685	101,450	1.8
Nuevo Leon	46,684	49,003	1.0	41,537	44,570	1.1	88,221	93,573	1.1
Sonora	73,584	157,000	2.1	16,936	19,396	1.1	90,520	176,396	1.9
Tamaulipas	98,331	133,568	1.4	21,791	24,544	1.1	120,122	158,112	1.3
Total	540,930	589,126	1.1	161,221	175,877	1.1	702,151	765,002	1.1
Total – Coahuila	279,955	431,364	1.5	143,226	153,052	1.1	423,181	584,416	1.4

*Does not include off-road mobile source emissions

Table B-3 compares Mexican SO_2 emissions at the state level as estimated by *BRAVO EI* and the *1999 N MX NEI* segregated by point and area source categories. (The *BRAVO EI* summarizes area and mobile sources collectively.) The only state where SO_2 emissions from point sources in the *1999 N MX EI* were lower than in the *BRAVO EI* is Coahuila, where SO_2 emissions are dominated by the two different estimates for *Carbón* power plant emissions. Overall, point source SO_2 emissions in northern Mexico, beyond the state of Coahuila, are a factor of 1.5 higher in the *1999 N MX NEI* than in the *1999 BRAVO EI*.

In the case of area and mobile source emissions, a complete comparison among the *1999 BRAVO EI* and the *1999 N MX NEI* cannot be made as the latter does not include non-road mobile source emissions as of the July 2003 draft. However, it is instructive to note that 77% of SO_x emissions from on-road mobile sources are estimated to originate from heavy-duty vehicles. Non-road emissions from agricultural and construction equipment are likely to have a non-negligible impact to the SO_2 emissions therefore, assuming that the other estimates do not alter significantly during the review process, the value of 1.1 may be a lower limit to the factor of exceedance between the *1999 N MX NEI* and the *1999 BRAVO EI*.

As a draft document of an evolving study, no specific level of confidence can be ascribed *1999 N MX EI*. However, *1999 N MX NEI* estimates indicate that SO_2 emissions in northern Mexico, beyond the state of Coahuila, may be at least a factor of 1.4 higher than recorded in the *1999 BRAVO EI*. This factor will increase by an unknown amount with the addition of non-road mobile emissions. No statement can be made regarding the applicability of this, or a similar, factor to the rest of the Mexican territory. However, it is unlikely that the causes for the differences in SO_2 emissions between the two inventories are limited only to the northernmost states of Mexico.

A potential source of uncertainty in the *1999 N MX NEI* is the treatment of petroleum processing emissions. Although "petroleum extraction and petroleum/petrochemical manufacturing" is stated as a point source emission category, SO_x emissions are not given for this category in the point source summary tables. According to the Mexican federal petroleum agency, PEMEX, the states of Nuevo León and Tamaulipas contain two petroleum refineries in the cities of Ciudad Madero and Cadereyta, respectively, processing a combined 465,000 barrels of crude oil per day.

B.3 Oversights in the BRAVO EI

Although the larger BRAVO modeling domain (the REMSAD domain) included most of the continental United States, the entirety of the Mexican federation, the western Caribbean (Cuba and Jamaica), and a small portion of eastern Canada, the *BRAVO EI* estimated emissions only in the United States and portions of Mexico. The Mexican component of the *BRAVO EI* included emissions in the ten northernmost states (Baja California Norte, Sonora, Chihuahua, Coahuila, Nuevo León, Tamaulipas, San Luís Potosí, Sinaloa, Durango, and Zacatecas), Mexico City in the Federal District (*Distrito Federal*), the Tula Industrial Park in the state of Hidalgo, and the Popocatépetl volcano in the state of Puebla. (Minor emissions from maritime vessels over the various bodies of water were not considered in the *BRAVO EI*.) The oversight of these emissions cannot be corrected by boundary conditions; the concentrations prescribed at the boundary only affect the transport of species into the modeling domain from outward regions. (Boundary conditions may represent in-domain emissions only in the special case where in-domain-emitted species circulate from outside the domain back into the domain.)

In order to qualitatively gauge the impact of the oversight of the above-mentioned emissions to the sulfate attribution studies, non-U.S. emissions of SO_2 within the *BRAVO EI* are compared to *EDGAR 3: Emission Database for Global Atmospheric Research*, an anthropogenic emissions inventory generated for global atmospheric and global climate modeling. *EDGAR* datasets, which represent emissions in 1995, form part of the *Global Emissions Inventory Activity (GEIA)* and have been used in IPCC (Intergovernmental Panel on Climate Change) Assessments. Although the *BRAVO EI* and *EDGAR* correspond to different years, the *EDGAR* dataset provides a reasonable estimate of the magnitude of emissions omitted during the BRAVO simulations. As no emissions in the United States were omitted, comparison between the two datasets is not necessary in U.S. regions. (Note that 1999 SO_2 emissions in the United States were generated in the *BRAVO EI* from the 1999 National Emissions Inventory, incorporating continuous emissions monitoring, CEM, data when available; *EDGAR* datasets for 1995 SO_2 emissions in the United States were provided by the National Acid Precipitation Assessment Program, NAPAP.)

A global emissions inventory estimate of non-U.S. emissions is created by combining the 1995 *EDGAR* dataset with the 1995 volcanic emissions inventory from *GEIA*. To focus the comparison on the appropriate regions, the emissions in the three grid cells have been set equal to the BRAVO EI: the *Carbón* power plants, the Popocatépetl volcano, and the Ciudad Madero refinery region. The resulting inventory is referred to as the *GLOBAL EI* in the ensuing discussion. In Table B-4, SO_2 emissions in the *GLOBAL EI* for the six northern Mexican states are compared to values from the *BRAVO EI* and *1999 N MX NEI.* When compared to the *1999 N MX NEI,* the main difference of the *GLOBAL EI* lies in the state of Coahuila, where the grid cell for the Carbon plant has been set to match the BRAVO EI. However, the values of the *BRAVO EI* and *1999 N MX NEI* are relatively consistent over the five other states. This comparison shows that the *GLOBAL EI* values can be instructive in gauging the potential magnitude of underestimation in SO_2 emissions within Mexican regions of the *BRAVO EI*.

Table B-4. Comparison of SO_2 Emissions in the *1999 BRAVO EI* and *GLOBAL EI* (tonnes/year)[†]

State Name	*1999 BRAVO EI*	*1999 N MX NEI*	*GLOBAL EI*
Baja California N.	67,635	54,885	100,505
Coahuila	278,970	180,586	327,261
Chihuahua	56,685	101,450	93,683
Nuevo Leon	88,221	93,573	132,710
Sonora	90,520	176,396	144,238
Tamaulipas	120,122	158,112	157,832
Total	702,151	765,002	966,958
Total – Coahuila	423,181	584,416	628,968

[†]Using higher estimate of Carbón emissions; 1999 N MX NEI does not include off-road mobile source emissions.

Figure B-1 illustrates the extent of the SO_2 emissions missing from the larger BRAVO modeling domain and potential underestimation within Mexico. Table B-5 provides a quantitative assessment of the information in Figure B-1. Overall, the *GLOBAL EI* indicates that SO_2 emissions in the ten northernmost Mexico states within the *BRAVO EI* may have been underestimated by as much as a factor of 1.9. Note that any bias in this comparison due to emissions from the Carbon power plant and the Ciudad Madero refinery effectively has been canceled due to their equalization, thereby focusing emphasis on the remainder of the regions in the inventories. (A similar ratio is obtained if the anthropogenic portion of 4 additional states is included.)

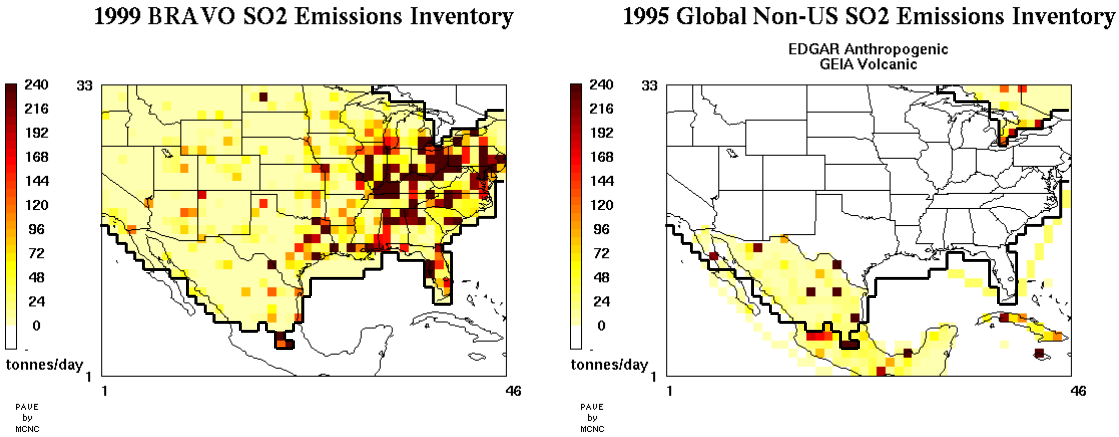

Figure B-1. (Left) SO_2 emissions based on the *1999 BRAVO EI* used in air quality modeling. No emissions were included beyond the black outline shown in the figure. (Right) SO_2 emissions outside of the United States based on modified *EDGAR/GEIA* datasets used in global atmospheric and global climate models.

Table B-5. Comparison of SO_2 Emissions in the *1999 BRAVO EI* and *GLOBAL EI* (ktonnes/year)[†]

REGION	*1999 BRAVO EI*	*GLOBAL EI*	*GLOBAL/BRAVO*
Western U.S.	1,582		
Texas	1,020		
Eastern U.S.	13,899		
Total U.S.	16,501		
Northern Mexico (10 States)	689	1,342	1.9
Federal District, Mexico, Hidalgo, and Puebla*	338	572	1.7
Subtotal 14 Mexican States*	1,027	1,914	1.9
Popocatépetl Volcano	1544	1544	
Southern Mexico (18 Mexican States)**	0	881	
Total Mexico**	2,571	4,340	
Western Caribbean	0	370	
Ship Lanes	0	189	
Canada	0	437	
Total Other	0	996	
Total Non-U.S.	2,571	5,336	

* Anthropogenic emissions only
** Anthropogenic and volcanic emissions
[†]Using lower estimate of Carbón emissions

Using the *GLOBAL EI* as an approximate benchmark, the *BRAVO EI* fails to include 881 tonnes per year of SO_2 emissions contained within the southern Mexican states. Furthermore, the *BRAVO EI* does not contain 996 tonnes per year of SO_2 emitted in non-U.S. and non-Mexico areas of the domain, i.e. a small region of eastern Canada, the west Caribbean islands and ship lanes.

Finally, the effect of uncertainties in the SO_2 emissions from the Popocatépetl volcano was explored by BRAVO researchers using trajectory-based regression models. The results of these analyses indicates that during the four-month BRAVO period, emissions from the Popocatépetl volcano were unlikely to have impacted Big Bend National Park in any significant fashion (Mark Green and Bret Schichtel, personal communication). It is uncertain how the Popocatépetl volcano may impact Big Bend NP during other periods or during specific eruption events. For example, a worthwhile study could investigate whether uncharacteristic increases in particulate sulfate concentrations at Big Bend NP in late 2000 and early 2001 were impacted by a large, extended eruption episode of Popocatépetl during the same time frame.

B.4 Discussion

Four different analyses, of variable complexity and assumptions, yielded corroborating evidence that SO_2 emissions may have been underestimated in the *1999 BRAVO EI.* Three of these analyses gave underestimation factors within a similar range for regions beyond the *Carbón* power plant or beyond the state of Coahuila, location of the *Carbón* power plant:

- Comparison of emissions in three Mexican states (excluding the *Carbón* power plant) with estimates from the Mexican Secretariat of Energy (SENER): 1.8
- Comparison of emissions in six Mexican states (excluding Coahuila) with the draft *1999 Mexican National Emissions Inventory*: lower limit of 1.4 (due to incomplete mobile source inventory)
- Comparison of emissions in ten Mexican states with a modified 1995 global emissions inventory (canceling any bias due to the *Carbón* power plant and the Ciudad Madero refinery): 1.9

In addition to the evidence of underestimation of SO_2 emissions in northern Mexico, global inventory estimates suggest that on the order of 1,877 tonnes per year of SO_2 were not calculated in the *BRAVO EI* from emissions in southern Mexico, the Caribbean, Canada, and maritime regions contained within the BRAVO domain. The combined effect of underestimation in northern Mexico and omissions in other regions has the potential of not considering on the order of 2,765 tonnes per year of SO_2 emissions in the BRAVO domain. This value is roughly equal to the amount of non-U.S. emissions that was estimated by the *BRAVO EI*, and roughly 2.5 times larger than the anthropogenic portion of that value. However, to place in full perspective, 2,765 tonnes per year is roughly 17% of the United States portion of SO_2 emissions in the *BRAVO EI*, although consideration of these emissions would have increased to the ratio of non-U.S. emissions to U.S. emissions from 0.15 to 0.32.

It should be noted that uncertainties in emissions inventories are not the only source of uncertainty in depicting the evolution of particulate matter over Mexico in air quality models. Errors in the simulation of meteorological fields over Mexico may also affect the capacity of the air quality models to accurately represent atmospheric chemistry over Mexican regions. This is particularly true of clouds, which serve as efficient chemical reactors for the conversion of SO_2 to sulfate, and precipitation, which can effectively remove particles and particulate precursors from the atmosphere. Finally, errors in wind fields can preclude the model from faithfully represent the transport of species, both to receptor sites or to regions where they can be affected by distinct chemical or physical processes. Notwithstanding biases detected in the meteorological model resulting in increased precipitation events near the U.S.-Mexico border region, the analysis above provides strong evidence that Mexican SO_2 emissions were underestimated in the *BRAVO EI*. In addition, the analysis above also demonstrates the need to include the best-available estimates for SO_2 emissions within the entirety of a modeling domain in regional haze studies. The absence of SO_2 emissions over particular regions of the larger BRAVO domain adds unwarranted, albeit moderate, uncertainty to the modeling analysis.

References

ERG, Acosta y Asociados, TransEngineering, Alejandro Villegas-López (2003) *Mexico Emissions Inventory, 1999–Draft, Prepared for:* Secretariat of the Environment and Natural Resources and the

National Institute of Ecology of Mexico, United States Environmental Protection Agency, Western Governors' Association and North American Commission for Environmental Cooperation, ERG, Sacramento, CA.

Olivier, J.G.J. and J.J.M. Berdowski (2001a) Global emissions sources and sinks. *In*: Berdowski, J., Guicherit, R. and B.J. Heij (eds.) *The Climate System*, pp. 33-78. A.A. Balkema Publishers/Swets & Zeitlinger Publishers, Lisse, The Netherlands.

Olivier, J.G.J., J.J.M. Berdowski, J.A.H.W. Peters, J. Bakker, A.J.H. Visschedijk and J.-P.J. Bloos (2001b) *Applications of EDGAR. Including a description of EDGAR 3.0: reference database with trend data for 1970-1995.* RIVM, Bilthoven. RIVM report no. 773301 001/ NOP report no. 410200 051.

Tombach, I., Karamchandani, P. and P. Pai (1996) Development Evaluation, and Application of Transfer Coefficients for Predicting Colorado Plateau Air Quality, ENSR, Camarillo, CA, Report 96-TP46.03.

Joint UNDP/World Bank Energy Sector Management Assistance Programme (ESMAP) (2001) *Mexico Energy Environment Review*.

Leal Santa Ana, A. (2001) *Opportunities & Challenges for Challenges for Refiners in Latin Refiners: Mexico's Case (PEMEX Refinacion)*. Hart 2001 World Fuel's Conference: Latin America & Caribbean, Rio De Janeiro, Brazil. August, 2001.

Favela, R. (2001) *PEMEX Perspective on Fuel Quality Improvement (PEMEX Refinacion)*. Hart 2001 World Fuel's Conference: Latin America & Caribbean, Rio De Janeiro, Brazil. August, 2001.

Gilbreath, Jan (2002) Economic Integration's Effects on Air Emissions in Mexico's Refining and Electricity Generating Sectors, Prepared for the World Bank. Center for Strategic & International Studies.

Sasaki, T., Hayashi, K. and T. Takagi (2001) *The Mexico City Sulfur Dioxide Emission Reduction Project*, Mitsubishi Research Institute, Ltd.

Program:

Assessment Tools for Ozone, Particulate Matter, and Haze

About EPRI

EPRI creates science and technology solutions for the global energy and energy services industry. U.S. electric utilities established the Electric Power Research Institute in 1973 as a nonprofit research consortium for the benefit of utility members, their customers, and society. Now known simply as EPRI, the company provides a wide range of innovative products and services to more than 1000 energy-related organizations in 40 countries. EPRI's multidisciplinary team of scientists and engineers draws on a worldwide network of technical and business expertise to help solve today's toughest energy and environmental problems.

EPRI. Electrify the World

Printed on recycled paper in the United States of America

1009283

EPRI • 3412 Hillview Avenue, Palo Alto, California 94304 • PO Box 10412, Palo Alto, California 94303 • USA
800.313.3774 • 650.855.2121 • askepri@epri.com • www.epri.com